HIGH PRECISION GEOID FOR MODERNIZATION OF HEIGHT SYSTEMS IN INDONESIA

By

Adolfientje Kasenda

M.Surv.Sc, University of New South Wales, Australia, 1992

A thesis submitted to the University of New South Wales
in partial fulfilment of the requirement for the degree of
Doctor of Philosophy

School of Surveying and Spatial Information Systems
The University of New South wales
Sydney NSW, 2052, Australia

July 2009

ABSTRACT

To establish a nationwide consistent height system for an archipelago country like Indonesia is exceptionally challenging. Yet, it needs to be resolved in order to provide infrastructure for mapping and the cadastre, planning and the development in natural resources or hydrocarbon exploration, monitoring sea level rise or flood control and other civil works. The height system generated from the precise leveling measurement has been inconsistent between islands datum. In this investigation, the height datum misfits between separated islands are assessed using various geoid models (i.e., EGM96, INDGED, GRACE and EGM08) and the results show different scales of distortions depending on which geoid model is used. The datum distortion between Sumatra and Jawa is 0.78m using INDGED, 0.80 m using the EGM96 and 0.48 m using the EGM08 geoids.

Replacing the tedious terrestrial leveling observations by the more rapid technique which uses Global Navigation Satellite System (GNSS) will certainly accelerate the establishment of the height system and give a more consistent height datum. However, adopting the GNSS observation techniques to determine the modern height system requires a high precision gravimetric geoid model. This is the main problem that is addressed in this work.

Various methods of geoid computation applied in the RINT and the GRAVSOFT program packages are tested for the gravimetric geoid solution. The comparison between the gravimetric and the geometric geoid using the Ring integration method computed with smaller capsize (0.2 degrees) shows similar results to those obtained using the FFT method applying Wong-Gore kernel modification up to degrees 360. Similar trends are also given by using the Collocation method. The result confirms that a high precision geoid model is achievable for the test area and with improved

gravity data coverage as demonstrated in the error propagation study by simulating ‘fill-in airborne data’. The analysis shows that it should be possible to produce a geoid to better than 10 cm.

A combination of the newly released EGM08 model, a high resolution DEM (e.g., 3 arc second SRTM) and the proposed airborne gravity measurements, (especially) in the coastal zone will provide the desired geoid. It is therefore, highly recommended that such measurements are implemented and (hopefully), that the high precision geoid for modernization of the Indonesian Height System can be realized in less than 5 years from now.

ORIGINALITY STATEMENT

'I hereby declare that this submission is my work and to the best of my knowledge it contains no materials previously published or written by another person, or substantial proportions of material which have been accepted for the award or any other degree or diploma at UNSW or any other educational institution, except where due acknowledgement is made in the thesis. Any contribution made to the research by others, with whom I have worked at UNSW or elsewhere, is explicitly acknowledged in the thesis. I also declare that the intellectual content of this thesis is the product of my own work, except to the extent that assistance from others in the project's design and conception or in style, presentation and linguistic expression is acknowledged.'

Signed ……

Date ……..

TABLE OF CONTENTS

ACKNOWLEDGEMENTS

I would like to express my gratitude to many people who has given their time, advice and support me through many years of this study. Above all I am most grateful to my supervisor Prof. Bill Kearsley for his guidance and assistance in helping me with both the theoretical and practical aspects of the work. His constant support and encouragement has given me confidence and motivation to finish this work.

I would like to extend my gratitude to friends and colleagues at Geodesy and Geodynamic Departments, DNSC (previously in KMS), Denmark, for allowing me to use their in-house geoid software and altimetry model. In particular thank to Rene Forsberg for his invaluable input.

I would also like to thank The Australian Government as its AusAid program has given the financial support and a chance for me to undertake this study. My gratitude goes also to The Indonesian Coordinating Agency for Surveys and Mapping (BAKOSURTANAL) for releasing from offices duty during my study time.

I am thankful to postgraduate friends and staffs at The School of Surveying and Spatial Information System, UNSW for their comments, friendship and supports has broaden my horizon and provided me enjoyable research environment. Lastly, I should also thank my husband for his in-sights and suggestions to improve the work.

CHAPTER 1

INTRODUCTION

1.1 General background and motivation for the investigation

The orthometric and the normal heights are height systems that have been used world wide for more than a century to define the vertical position for points on or near the earth surface. A reference surface for which the datum is assumed to be zero is historically the mean sea level determined from tide gauge observations over a period (18.6 years) of time. Due to oceanic variability and the effect of sea surface topography, mean sea levels as defined from tide gauge observations at various locations will not necessarily lie on a common equipotential surface. As a result, height distortions exist between different zones or regions.

The use of mean sea level as the reference surface causes some problems in the definition of vertical datum for a wide area. Fixing tide gauge estimates from mean sea level to "zero" in a leveling network adjustment over a large region causes discrepancies through out and beyond the region and the resultant height values have significant differences from those obtained from a free adjustment. For example, the height differences between constrained and free adjustments of the National Geodetic Vertical Datum (NGVD) 1929 in the United State exceeds more than 50 cm with a very large relative height difference of 86 cm occurring in a specific area (Zilkoski et al., 1992). Similarly, the Australian Height Datum, AHD 1971, the difference between constrained and free adjustment suggested a rise of Mean Sea Level up the east coast of about 1.5 m (Roelse et al., 1971, Morgan, P., 1992), although subsequent re-leveling tended to lessen this difference.

The other problem caused by the use of mean sea level as a reference surface for height determination is that the deviation of the mean sea level from the equipotential surface defined as the geoid is quite significant, and in some parts may reach the order of ± 2 m (Rapp and Balasubramania, 1992). These facts will affect the

definition and the unification of vertical datum separated by oceans if the mean sea level is to be used as height reference.

To reduce the problem resulting from the use of mean sea level as a reference surface, we may adopt the geoid, the equipotential surface of the earth gravity field that best fits mean sea level, as a better definition of the "zero height" reference surface. In addition to that, in precise leveling measurements the geometric height difference which is measured along the local plumb line is everywhere orthogonal to this equipotential surface of the earth gravity field. Therefore, from a number of theoretical and practical view points, the geoid is considered more appropriate for the geodetic vertical reference surface.

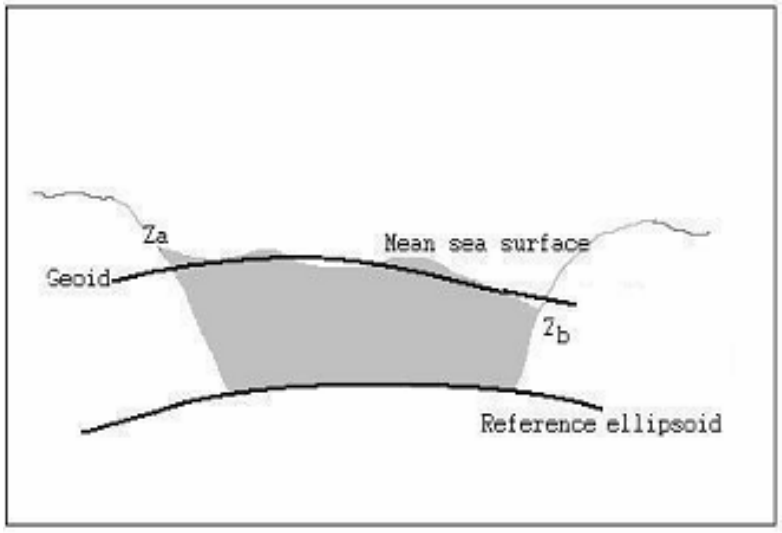

Figure 1.1 The deviation of mean sea level from the geoid (Z_a and Z_b are MSL zero points of local datums A and B)

A properly defined geodetic reference system is not only essential for the definition and the unification of the vertical datum but also for other purposes, including an understanding of environmental issues such as sea-level change, integrated spatial data infrastructure as well as the monitoring of seismic, volcanic and tectonic activities and for engineering and cadastral applications.

This thesis work attempts to establish a national unified geodetic vertical reference system for the Indonesian archipelago. A consistent national vertical datum is necessary for this country made up of thousands of islands in order to enable a proper connection of the many local height systems. Such a height system connection would be beneficial for many practical applications such as civil constructions or flood control monitoring. Moreover, for a broader application a unified national vertical datum will allow the connection of the Indonesian height system to the regional and the global one. The unification of height systems has become a major problem, above all through the growing demands for height determination by the combination of precise point positioning from Global Positioning Satellite measurements and a geoid model, also known as GNSS surveying (GPS, GLONASS and GALILEO). In line with the Cartagena Statement on Vertical Reference Systems declared in 2001, the International Association of Geodesy (IAG) agrees that there is an urgent need for the establishment of an integrated national and regional geodetic vertical reference system, with the longer term aim of establishing a unified global vertical reference system. For those reasons this investigation is highly relevant. The background for the Indonesian vertical datum is outlined in Section 1.2 of this chapter.

In Chapter 2 the theoretical basis of height systems, their fundamental relationships and the mathematical model are presented. Also the role of the regional/global geoid in the solution for the unification of vertical datum is described in this chapter. In Chapter 3 a preliminary investigation of vertical datum distortions between different islands in western part of Indonesia is performed. The height datum comparisons are carried out by using the GPS (ellipsoidal) heights, leveling heights and the gravimetric geoid computed from a combination of EGM96 geopotential model and the regional gravity dataset. The EGM96 model was used in the geoid computation since the latter EGM08 model was not yet available at the time when this preliminary part of the work was undertaken. The results and the problems encountered are also discussed in this chapter. The geoid plays the most important role in the vertical datum unification and its accuracy is critical. Having

evaluated the results and analyzed the problems appearing in the datum comparison, it was necessary to search for a more precise gravimetric geoid model.

In Chapters 4 and 5 the geoid computation work are emphasized. The main objective of the investigation presented in Chapter 4 is to search for the best geoid computation technique to be applied for the test area with typical gravity data coverage. The geoid model was computed based on the remove-restore method with various applications. Different techniques namely Ring Integration, Collocation and FFT techniques are applied in the practical computation for a selected test area where local observed gravity data are available. In order to examine their accuracy the computed gravimetric geoid were compared to the geometric geoid at control points. The results of this comparison are also presented and discussed in Chapter 4. The results implied that the situation of the precise geoid model for the Indonesian region may only be improved once the gravity data coverage is improved. As data gaps are mainly in inaccessible remote areas and areas of difficult terrain and using conventional techniques such as terrestrial gravimetry for land data measurement will be very difficult. Also, it is difficult to use shipborne measurements in the transition zone between land and open sea, which is an area with a pronounced lack of reliable data, since it is mainly characterized by shallow waters.

An alternative way to improve the gravity data situation in such areas is by using airborne or spaceborne techniques. In Chapter 5 an error-simulation study is performed by fill-in data gaps with airborne gravimetry of different line spacing. The error propagation from gravity data to geoid is analyzed by the use of collocation for two scenarios. One scenario is the existing data coverage the other is a simulated situation with airborne fill-in data in the near coastal zone. Chapter 6 is devoted to the analysis of global gravity and geoid models. Geopotential models from the CHAMP and GRACE satellites are compared to other datasets. There is also a look towards the future where data from the GOCE gravity satellite will be available. Later on, after being released, the most recent earth gravitational potential model (the EGM08) is used for computing the Indonesian geoid and the height datums comparison is re-assessed. The impact of using the new constant gravity potential of

the geoid (W_0) upon the geoid values is also explored. Their results are presented and discussed in the last section of Chapter 6. Finally, conclusions and the recommendation are written in Chapter 7.

1.2 Background for the Indonesian Vertical Datum

The geodetic control network in Indonesia was initiated during the colonial era in 1862. The intention of this network was to provide control for mapping as well as for hydrographic surveying and charting. The measurements were undertaken mainly in Jawa Island and resulted in a triangulation network with an average spacing of approximately 60 km throughout the island. Later on, between 1925 until the late

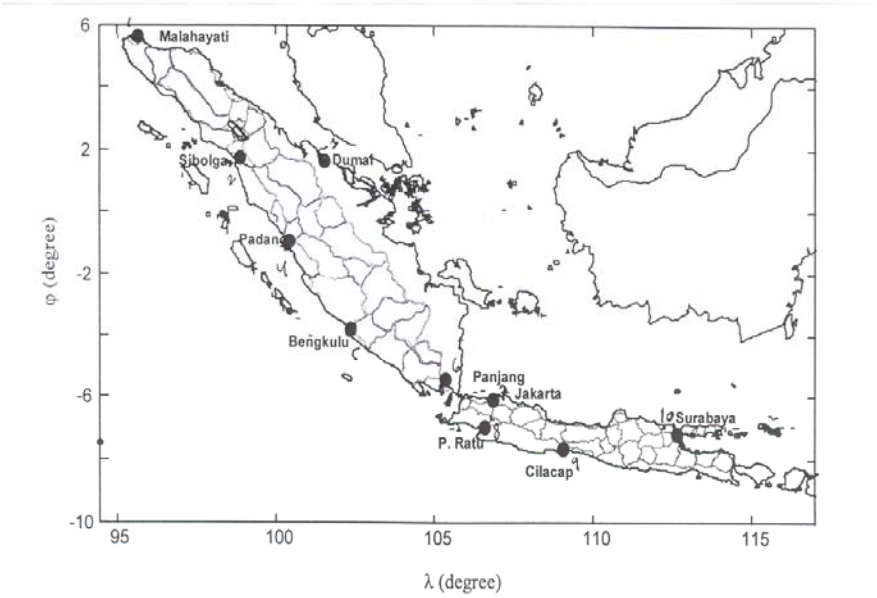

Figure 1.2 Leveling Network in Jawa and Sumatera

1930's the first vertical control network in Indonesia was established under the Dutch administration. The network specified as first order precise leveling was measured in west Jawa and in part of central Jawa, while second order precise leveling network were established in some parts of north and south Sulawesi and Bangka islands. The definition of the datum point for Jawa network (NWP-3 Jakarta) was based on mean sea level (MSL) derived from tide gauge observation in 1926.

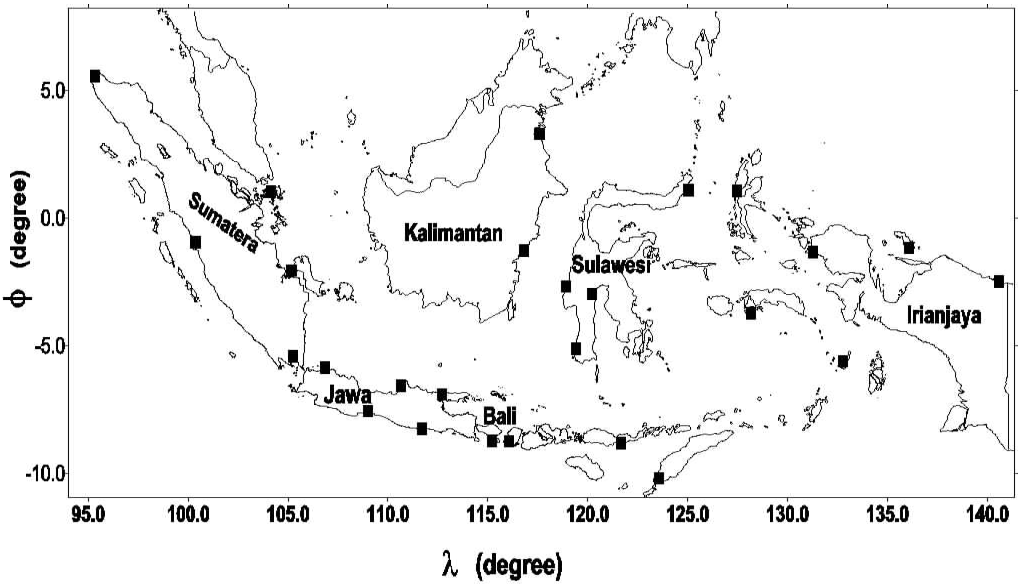

Figure 1.3 Distribution of tide gauge stations

Unfortunately, these initial networks were not well documented, and only a few of the vertical control points in Jawa were recovered. Most of the old benchmarks were either destroyed or disappeared; only 420 benchmarks from about 2083 in Jawa remain and of these, a mere 280 benchmarks were in good condition.

Because of the fundamental importance of height data for mapping, engineering, and other physical planning applications, a new national vertical control network in Indonesia was re-started in 1980 by the Indonesian Coordinating Agency for Surveys and Mapping (BAKOSURTANAL) as part of the government's long-term development programs for infrastructures. As a result a systematic first order geodetic leveling network started in 1980 in Jawa Island and was completed in 1987. These leveling measurements were continued to the island of Bali (from 1987 until 1991), then Lombok and Madura islands (from 1991 until 1994). The total length of the classified First Order Leveling lines is approximately 22 273 km and a total of 5503 benchmarks were established. Second Order Leveling Networks were carried out in Sumatra Island (from 1988 until 1993), the western part of Kalimantan Island (from 1988 until 1993) and in northern and southern part of Sulawesi Island (from 1988 until 1995). The orthometric height systems were used by applying the gravity

correction obtained from gravity observations at leveling benchmarks. The height references for these geodetic leveling networks were defined separately per island partition based on tide gauges observation of mean sea level at each island. There are about 28 tide gauge stations operating between 5 to 15 years distributed across the country. Five of these stations (two located in Jawa, one each in Sumatera, Bali, and Sulawesi islands) are part of the world Permanent Service for the Mean Sea Level (PSMLS). In addition to that there are 25 new stations mounted recently and monitored for less than five years. The variability of these tide gauges records may consequently vary and the accuracy of the mean sea level at the tide gauge and the tide gauge estimates of height (H) will depart from the orthometric height above the datum.

The first attempt to connect the local heights datum in this region was undertaken by using an oceanographic approach (Khafid et.al., 1994). The solution concentrated on the ocean-related component using the mean sea surface determined from satellite altimetry and the oceanographic leveling derived from hydrographic data. The preliminary results suggested that the sea surface topography in the Southwest coast of Sumatera is about – 16 cm, while in South coast of Jawa it increased from –14 cm in the west to –8 cm in the east (Khafid, 1998). The results also showed that altimetry can provide a reliable component for vertical datum connections. However its accuracy in this region was limited by the lack of accurate regional tide models.

The spirit leveling used in the determination of the vertical datum is very precise. The networks in Jawa is classified as the National 1st Order Leveling Network and the precision of the heights is around ±2 cm, while the leveling networks in Sumatra has a lower order with average height accuracy of ± 4 cm (Sutisna , 2001). On the other hand the inaccurate definition of zero level at tide gauges causes height inconsistencies between the regions and hence height datum unification becomes a major problem. The spirit leveling technique also has the disadvantage when used for the vertical control network for vast areas with rough terrain like Indonesia. This technique is very time consuming and therefore very expensive.

CHAPTER 2

THEORETICAL BASIS AND HEIGHT SYSTEM

2.1 Height system

The height of a point located on the earth's surface is defined as the vertical distance between this point and a specified reference surface. The classical technique of height determination using spirit leveling technique in principle is to measure the difference in height between two points, obtained as the difference between backward and forward readings on a level rod. This conventional way of height determination by spirit leveling introduces misclosure in the closed line measurements if the gravity field is ignored. This is due to the fact that leveled height differences do not only reflect the topographical variations but they also include the effects of the earth's gravity disturbances. Theoretically the potential differences which are derived from the height differences measured vertically by spirit leveling in combination with gravity observations are adopted as basic in height systems (Heiskanen and Moritz, 1967).

Basically, the heights used in geodesy are categorized according to the way they were determined, i.e., the application or the mathematical or physical models used in their definition. In principle there are two types of heights, namely the geometric and the physical heights. The geometric types include leveled and ellipsoidal heights, while the physical types include dynamic height, normal height and orthometric height.

2.1.1 Geometric height

The **leveled height** (H) is commonly obtained by spirit leveling. It measures the vertical distance between points located on the earth surface to a defined local mean sea level. The observed height differences fluctuate in response to the local gravity field variations. Therefore, in practice the algebraic sum of all measured height

differences in a closed network will not in general be zero as maybe expected intuitively. If the gravity field is ignored in the observations (i.e., the gravity component not applied), this height system can only be applied in a local network of approximately 10 km extension (see Section 2.1.2 below).

The **ellipsoidal height** (h) is the distance between the topographical surface of the earth and the mathematical model of the reference ellipsoid surface. It is measured by, for example, the global satellite positioning techniques (GPS). The vertical distance is defined along the straight line perpendicular to the ellipsoidal surface. This type of height is only practical if the information of the geoid undulation is available.

2.1.2 Physical height

Theoretically, the way to determine actual height differences is through their potential differences. This is due to the fact that the potential differences measured along the closed loop line give zero misclosure regardless the chosen path of the loop. The potential difference between an observed point and the equipotential surface of the earth's gravity field (geoid) is known as the geopotential number (C) and can be determined through classical leveling procedures along with gravity measurements or their estimates along the level line. The equation is written as (Heiskanen and Moritz, 1967)

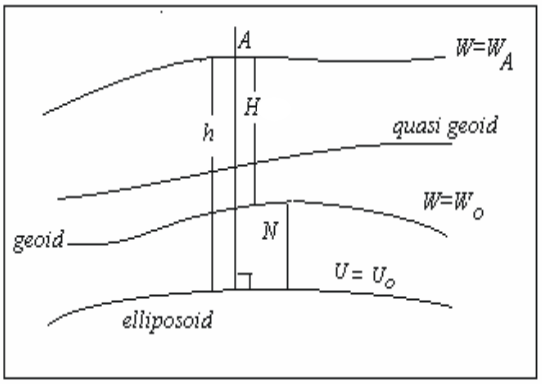

Figure 2.1 The geopotential differences

$$W_o - W_A = C = \int_o^A g\, dn \tag{2.1}$$

where,

W_o is the potential of the geoid

W_A is the potential of the surface that passes the measured point.

g is the observed point gravity

dn is the leveled height differences

The unit dimension of the geopotential numbers is in (m^2/s^2). Practically this is inconvenient, as height dimension is commonly given in metric length (m). The geopotential numbers can be converted into unit length by dividing them by gravity values as follows,

$$H = \frac{C}{G}$$

H is the obtained height in meter, *C* is the geopotential number and *G* is the "gravity" values. The **type of** the calculated ***H*** depends on the **type of** the **gravity** used in the conversion. If *G* is a constant value of a theoretical gravity for an arbitrary point (e.g. γ_e), then *H* is known as a dynamic height. The advantage of this dynamic height is that it is the same for all identical height values located on an equipotential surface. However, by ignoring the gravity variations between points, the calculated height distance may differ slightly from its **actual** geometric distance. For that reason some prefer to use the **actual** gravity values for G instead. If the gravity value used is the mean normal gravity between the reference surface and the measured point, then the obtained height is called normal height and the formula can be written as,

$$H_{normal} = \frac{C}{\gamma} \tag{2.2}$$

The gravity value (γ) is computed by using the formula for the earth's normal gravity field (Heiskanen and Moritz, ibid),

$$\gamma = \gamma_e \left(1 + \beta_1 \sin^2 \varphi - \beta_2 \sin^2 2\varphi\right) \tag{2.3}$$

which is a function only of the geographical latitude (φ) of the measured point. The γ_e is the normal gravity at equator and its value based on the geodetic reference system 1980 (GRS-80) is 9.780 327 ms^{-2}, while β_1 and β_2 are constants to account for the ellipsoidal flattening and their values are 0.0053024 and 0.0000058 respectively.

This normal height can be derived as well from the combination of GPS ellipsoidal height (*h)* and the quasi-geoid undulation (also called height anomaly) as shown in the following equation,

$$H_{normal} = h - \zeta \tag{2.4}$$

The height anomaly ζ can be computed by gravimetric or satellite methods.

The other type of the physical height system is known as the "orthometric height", where the geopotential numbers are divided by the mean value of the true or actual gravity ($\bar{g}$ *)* between the measured point and the respective reference surface as given in the equation below,

$$H_{ort\,\mathrm{hom}\,etric} = \frac{C}{\bar{g}} \tag{2.5}$$

This type of height can be determined if the subsurface density is known. Since the actual gravity values (g) are measured on the topographic surface the density distribution of the terrestrial masses is required for the downward continuation along the plumb line between the surface point and the geoid. The mean gravity is written as (e.g., in Heiskanen and Moritz, 1967, p.167),

$$\bar{g} = g - \left(\frac{1}{2} \frac{\partial \gamma}{\partial h} + 2\pi k\rho \right) H \tag{2.6}$$

where ρ is the assumed constant density and k = 66.7 x 10^{-9} c.g.s unit is the gravitational constant. $\frac{\partial \gamma}{\partial h}$ is the normal free-air gradient, can be computed from the following formula,

$$\frac{\partial \gamma}{\partial h} = -\frac{2\gamma}{a}\left(1 + f + m - 2f\sin^2\varphi\right) \tag{2.7}$$

where a and f are geometric parameters of semi-major axis and the flattening of the respective ellipsoid and m is a constant value related to the centrifugal force and gravity at the equator. The corresponding orthometric height obtained from equations 2.5, 2.5 and 2.7 is called Helmert height and can be expressed as,

$$H_{Helmert} = \frac{C}{g - 2\pi k\rho H + \frac{1}{2}\frac{\partial \gamma}{\partial h}H} \tag{2.8}$$

The reduction in the approximated mean gravity in Helmert height is derived from a model of an infinite Bouguer plate of constant density down to the geoid. If a terrain correction was also considered, then, the orthometric height is known as Niethammer height and the mean gravity is written as,

$$\bar{g} = g - \left(\frac{1}{2}\frac{\partial \gamma}{\partial h} + 2\pi k\rho\right)H + \Delta g_T \tag{2.9}$$

where Δg_T is the terrain correction.

A simplified mean gravity can also be obtained by assuming that gravity g measured at the topographic surface varies linearly along the plumb line, hence

$$\bar{g} = \frac{1}{2}\left(g + g_0\right) \tag{2.10}$$

where g_0 is the computed gravity value at the geoid.

The orthometric height can be estimated as well from the ellipsoidal height *h*, by applying the geoid undulation (*N*) to *h* as follows,

$$H_{orth} = h - N \tag{2.11}$$

The geoid undulation is determined from gravity taking into account the indirect effect, hence in this evaluation density distribution of the masses inside the earth is also required.

Having seen various types of physical heights, it is a matter of preference which type of height systems to use because the dependency of both orthometric and normal heights on geopotential numbers. Therefore it is possible to transform from one to the other system, given the gravity information is adequate. So, we have,

$$C = \gamma_c H^{dynamic} = \gamma H^{normal} = \bar{g} H^{orthometric} \tag{2.12}$$

If the geopotential numbers are not available and only the orthometric heights are given, then the normal heights can be converted from the simplified equation given as follows,

$$H_{normal} \approx H_{orth} + \frac{\Delta g_B}{982000(mgal)} H_{orth} \tag{2.13}$$

where Δg_B is the Bouguer anomaly.

2.2 The fundamental relationships

The reference surface for which the height is zero corresponds with the chosen height system. Figure 2.2 shows various reference surfaces and their relationships. The measured heights datum commonly refers to the local mean sea level as a zero point. The reference surface for orthometric heights is an equipotential surface of the

earth's gravity field that is closely associated with mean sea level on a global basis, the geoid, which in fact deviates relatively from the datum reference surface by up to

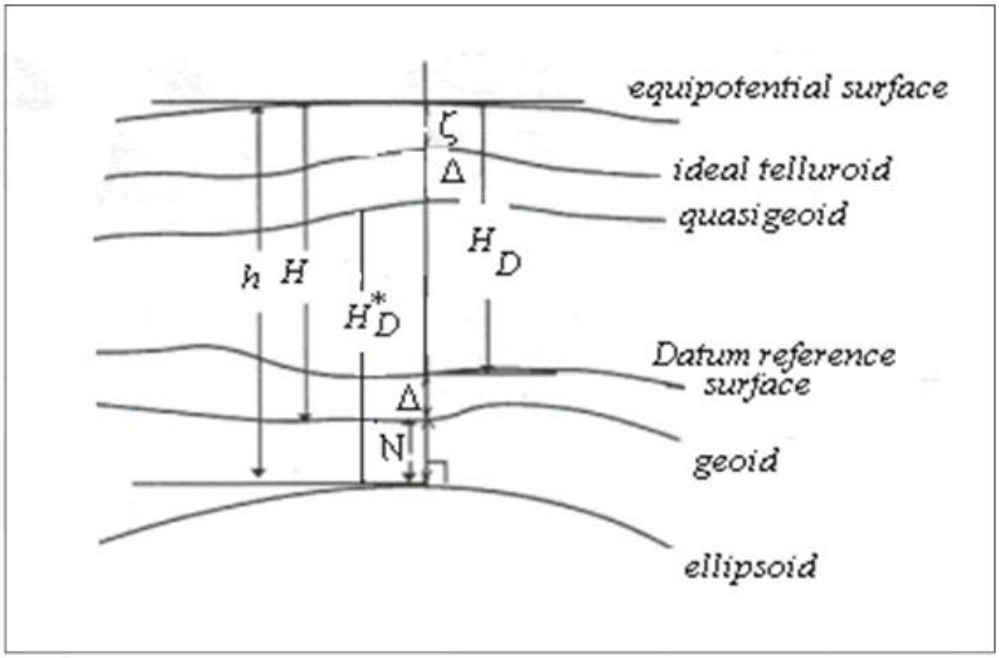

Figure 2.2 Relationships between different reference surfaces

± 2 m. The reference surface for normal heights is the 'geoid-like' surface called the quasi-geoid, which is neither a physically defined level surface nor a geoid, and has no physical meaning. However, it is more practical to compute than the geoid since no mass density distribution between the measurement point and the geoid is required. In general there is only a small difference between orthometric and normal height systems, and at the coastline the geoid and the quasi geoid are at the same level. Another reference surface is the ellipsoid, which is a simple mathematical model for the earths shape and is an ellipsoid of revolution about its minor axis defined by an equatorial radius and flattening. This is the reference surface for heights derived from e.g. the global satellite positioning or satellite altimetry.

Combining equations (2.4) and (2.11), and following (Rapp, 1995), the fundamental relationships between various height systems can be written:

$$h = N + H_D + \Delta = \zeta + H_D^* + \Delta \tag{2.14}$$

where Δ is the deviation between the vertical datum reference surface and the geoid surface. If the geoid is the reference surface, then the Δ value will be zero. In terms of potential numbers, the deviation can be expressed as,

$$\Delta = h - N - \frac{C}{\overline{g}} = h - N - \frac{\Delta W_0}{\overline{g}} = h - \zeta - \frac{\Delta W_0}{\overline{\gamma}} \tag{2.15}$$

where ΔW_0 is the geopotential difference between the geopotential value at the observed point and the geoid.

2.3 The role of the Geoid

The term "geoid" has been in common use for more than hundred years since first introduced by C.F.Gauss in 1828. However, the problem of what is the definition of geoid remains an open question. To answer the question of "what is the geoid ?", (Grafarend, 1994) following the Gauss and Listing proposal, adopted the geoid as a specified reference equipotential surface for the geodetic heights. In addition, according to the US National Geodetic Survey, the geoid is defined as the equipotential surface of the earth gravity field which best fits, in a least squares sense, global mean sea level. Since height differences which are measured along the local plumb line, are everywhere orthogonal to this equipotential surface of the earth gravity field, this equipotential surface (geoid) is considered better for the height reference surface.

On the other hand, the mean sea surface appears to be a "natural" reference for heights. The "traditional" way to define national height systems was also to refer it to mean sea level where the long records of a tide gauge were averaged and the height of a nearby marker was defined relative to this realization of mean sea level. This local mean sea level defined at different tide gauges has the real advantage that it is physically defined and measurable, but it may deviate from the geoid due to the

oceanic variability. The difference between the local mean sea level and the geoid is called sea surface topography (SST). The SST depends on both oceanographic and meteorological factors such as salinity, temperature, pressure, etc. Its magnitude is about ± 2m. The SST also shows temporal variations with long and short period and in different spatial scales due to changes in water density and meteorological conditions. In the definition of the conventional vertical datum the SST is usually not considered because the mean sea level is assumed to coincide with the geoid. Excluding SST may introduce a systematic displacement of height datum relative to the geoid and distortions in the height reference with respect to the equipotential surface. As a result, height unification becomes more complicated in particular when points are separated by sea, if the mean sea level is used as the reference for local or national height datums.

The unification of height systems has become a major problem, above all through the growing demands to determine physical heights by the combination of precise satellite-based point positioning measurements in combination with the evaluation of the geoid

2.4 Regional and global height datum references

The development of a world height system has been discussed for the last two decades by various authors. Mather, et, al., (1978) considered the role of satellite altimetry in a global unified vertical datum determination. Another approach by Colombo (1980) described the development of a world vertical network of fundamental stations with all data referring to them, emphasizing the determination of the potential differences between vertical datums. Rummel and Teunissen (1988) considered the height datum definition and connection problem emphasizing the role of the geodetic boundary value problem. Rapp (1995) described a simplified approach to define a world height system based on a world vertical datum reference surface and Kearsley (1999) proposed the geoid to serve as a regional and global reference for height systems. In addition, Bursa (1999) introduced the geopotential value at the geoid surface (W_o) as global datum where the local vertical datum shift can be defined.

2.5 The unification of height systems

In line with the rapid increase of space techniques for positioning determinations, studies on the solution of height datum unification has been in focus for the last two decades. The method for vertical datum unification has been discussed and written by numerous authors. For example Rummel and Teunnissen (1988) proposed the integrated approach based on the solution of the Geodetic Boundary Value Problem (GBVP), and the so-called indirect method is proposed in order to connect datum separated by ocean (Rummel and Ilk, 1995). Other discussions on the solution for vertical datum unification can be found as well in Rapp and Balasubramania (1992), Rapp (1995) and Kearsley (1999). In this section, the solution strategy is reviewed for the regional vertical datum unification, applicable for Indonesian region. The geoid surface is adopted as the fundamental surface, therefore this requires the determination of the geoid height.

The geoid heights can be determined geometrically, i.e., by combining the GPS ellipsoidal height and the leveling measurements at chosen benchmark stations. At the same sites geoid computations can also be performed by solving the geodetic boundary value problem using the local gravity anomaly field and the global geopotential model. From these two independent estimates of the geoid heights the datum connection parameters can be solved by a least-squares adjustment.

2.5.1 Solution strategy

Theoretically, the potential numbers (C), which are determined from leveling and gravity observations (see section 2.1.2), are the parameters used for datum comparisons. Let C_d be a potential numbers with respect to the local vertical datum d and C_w is the potential numbers with respect to the global vertical datum (geoid). By comparing the two geopotential numbers at all common points, following Rapp (1995), the mean potential off-set is written as,

$$\overline{\Delta C} = \overline{C_d - C_w} \tag{2.16}$$

and the datum connections can be written as,

$$C_d = C_w + \Delta C \qquad (2.17)$$

In practice, a simple way to determine the datum off-sets for which the orthometric height H, ellipsoidal h and geoid N are known, is written as,

$$\Delta_{D(i)} = h_i - N_i - H_i \qquad (2.18)$$

However, this approach has limitations since it does not convert the geometric heights into a potential system. Various techniques can be applied to compute the $\Delta_{D(i)}$ based on a set of points. In this case, the least-squares adjustment is proposed, since this method allows the verification of the precision of the derived datum connection parameters and the reliability of the measured parameters.

A rigorous method based on Heiskanen and Moritz (1967), following Rummel and Teunnissen (1988) and Xu and Rummel (1991) and re-written in Onselen (2001), the datum connection parameter is expressed as,

$$Y_k = \frac{-\Delta W_0}{\gamma} + \frac{C_{Q_i 0}}{\gamma}\left(1 + 2J(\psi)\right) \qquad (2.19)$$

where ΔW_0 and $C_{Q_i 0}$ are unknown quantities and the parameters to be determined. $J(\psi)$ is the Stoke integral and can be derived according to Lambert and Darling (1936), and is given as,

$$J(\psi) = \frac{1}{2}\left\{1 + 4\sin\frac{\psi}{2} - \cos\psi - 6\sin^3\frac{\psi}{2} - \frac{7}{4}\sin^2 - \frac{3}{2}\sin^2\psi.\log_e\left(\sin\frac{\psi}{2} + \sin^2\frac{\psi}{2}\right)\right\} \qquad (2.20)$$

By defining the radius of integration up to a known cap size ψ, the $J(\psi)$ can be evaluated and hence the parameters ΔW_0 and $C_{Q_i 0}$ can be determined through a

rigorous adjustment process. For the adjustment purposes the misclosure vector in the observation equation is formed as,

$$Y = AX + \Delta \tag{2.21}$$

where,

A is the design matrix

X is parameters of the model ΔW_0 and the potential differences $C_{Q_i 0}$

Δ is the observation residual vector

From (eq. 2.20) the coefficient for ΔW_0 and $C_{Q_i 0}$ are $-\frac{1}{\gamma}$ and $\frac{(1+2J(\psi))}{\gamma}$ respectively. By assuming Δ =0, and the three observation types (h, H and N) are independently determined, then $Y = AX$ and the solution of the observation equation by least square adjustment gives the estimated parameter vector of,

$$\hat{X} = \left(A^T \sum_y^{-1} A\right)^{-1} A^T \sum_y^{-1} Y \tag{2.22}$$

where,

$$\Sigma_y = \Sigma_h + \Sigma_H + \Sigma_N$$

and,

$$D\{Y\} = \Sigma_y$$

is the variance-covariance matrix of Y , and the error variance-covariance matrix can be written as follows,

$$D = \Sigma_x = \left(A^T \sum_y^{-1} A\right)^{-1} \tag{2.23}$$

2.5.2 Practical Implementation

The vertical datum connection can be solved according to the equation model given in (Section 2.5.1), provided following conditions are fulfilled. First, precise geocentric coordinates derived by space methods and orthometric heights measured at co-located benchmark sites. Second, an accurate geopotential model and sufficient terrestrial gravity anomalies around the benchmark sites. However, in practice some aspects need to be examined. Kearsley (1999), identified that the main barriers to a practical implementation are being the accuracy of each of the parameters N, h and H for the areas, and the reliability and the stability of the selected benchmark sites at which the datum comparisons are made.

The accuracy of the parameters h and H depends on the observation procedure and the precision of the measurements, while the accuracy of the N component depend on several factors. Such factors are errors associated with the gravity data in the vicinity of benchmarks site, errors associated with the geopotential coefficients model used as the reference field and errors in handling the topography corrections.

There are advantages and disadvantages in choosing the co-located sites at tide gauges versus benchmark sites located inland as fundamental stations for datum comparison. The computed geoid undulation suffers from gravity deficiencies in near off-shore field while inland the benchmark sites can be chosen in stable areas where gravity data are well supplied. In addition to the disadvantages related with tide gauges station is that the ellipsoidal height (h) measured from GPS technique may suffer from multipath. Given the weaknesses of using the tide gauge station for the datum comparison, for a practical approach it is proposed to make the comparisons at selected sites located inland, where h and H observations are available and the gravimetric geoid (N) values can be computed from a reasonable coverage of local gravity data.

CHAPTER 3

VERTICAL DATUM COMPARISON

In general, a connection of various local heights datum located on one island or continent is made directly by comparing the potential numbers with respect to the local vertical datum (C_d) and the potential numbers with respect to the reference surface or global vertical datum (C_w) at all common points, and the connection can be performed according to the (eq. 2.17). The potential numbers differences can be established provided that levelled heights referring to each local datum are known and the gravity information is available. The differences in the geopotential numbers at common points can be considered a reasonable first approximation to the relationship between local heights datum. These values need to be heavily qualified when distortions in the local height datum from an equipotential surface are known to exist.

In order to connect points separated by oceans an **indirect** comparison can be applied. In this case, a simple practical way to determine the datum offsets is based on eq. (2.18) provided the orthometric height H, ellipsoidal height h and the gravimetric geoid undulation N are known. Combining the geoid undulation N with the ellipsoidal height h at leveling benchmarks will provide from GPS an orthometric height above the reference equipotential surface (geoid) at co-located points. The mean differences between the leveling heights and the GPS-geoid heights is interpreted (as a first approximation) as the local vertical datum offset, and written as

$$\Delta_i = \frac{1}{n}\sum_{\kappa=1}^{n} h_k - N_k - H_{ki} \tag{3.1}$$

where,

Δ_i is the vertical offset of local datum *i*,

h_k is the GPS derived ellipsoidal height

N_k is the gravimetric geoid at point *k*

H_{ki} is the leveling height at point *k* which refer to the local datum *i*,

n is the number of comparison points.

The differences between various local datum offsets to a common regional (or global) datum are considered as the distortion of the local vertical datum, and is written as,

$$\delta_{ij} = \Delta_i - \Delta_j \tag{3.2}$$

where Δ_j is the vertical offset of local datum *j.*

This approach admittedly has many shortcomings. For example, systematic errors in GPS heights, in the gravimetric geoid and in the leveling data are likely to exist. Nonetheless, this value should give a reasonable 'first estimate' of the magnitudes of the local datum offsets. A more rigorous comparison would be achieved by using geopotential numbers instead of orthometric heights (Rapp, 1994; 1995). For that purpose, measured gravity values are required at GPS/Leveling common points. Unfortunately, most of the GPS/leveling points in our test area did not have measured gravity, so the geopotential number option was not yet available. However, it is hoped that measured gravity will be available for the future, and the comparison then refined.

3.1 Data requirements and datasets

It is important in performing vertical datum comparisons that the reliability and stability of the chosen benchmark sites at which the comparisons are made, are considered. However, the accuracy of each parameters N, h and H are the most critical elements. The expected standard deviation of the datum comparison depends on the accuracy of those parameters in the dataset used for the comparison. In the following section accuracies of each component are investigated and the expected accuracy of the datum connection is assessed.

3.1.1 GPS Heights.

The accuracy of the coordinates determined from GPS measurements depend on many factors, such as observation precision and the method of the GPS data processing and the post-processing adjustment. These factors could contribute up to several meters. There are several sources of observation errors such as satellite orbit errors, the ionosphere and troposphere effects, receiver related errors and multipath effects. The major error sources such as satellite orbit and tropospheric refraction effect could degrade the GPS height estimation by 10 cm each. In addition to that, the effect of ocean loading should be considered. For sites near the coast the effect may reach more than 10 cm and even for stations located far from the coast the effect could be at the 1 cm level (Rothacher, 2000). Another major error source is introduced by inaccurate geocentric coordinate of the fixed station height in the network adjustment. This could give up to 10 cm error in the GPS station height estimation.

In order to eliminate, or at least minimize the measurement errors an adequate observation procedure should be followed. For instance, the double-differenced pseudorange method will eliminate the systematic errors originating from the satellites and the receiver clocks, while a proper combination of dual frequency phase data will reduce the ionospheric refraction effect (Hofmann-Wellenhof et, al, 1994). To reduce the satellite orbit errors the IGS precise orbit should be used and the IGS estimation of trophospheric zenith delays should be applied to minimize the tropospheric effect. In order to reduce errors from inaccurate geocentric coordinates of fixed station heights, the ITRF coordinate should be used for the fixed sites. By selecting the benchmark stations which are free from signals reflection such as trees, buildings, vehicles or other reflecting surfaces (including water surfaces), the multipath effect will be reduced. Establishing the GPS stations far from the coast will reduce both multipath due to reflections on the surface and ocean loading effects.

The ideal GPS sites appropriate as fundamental stations for the vertical datum comparison are those measured for GPS-Geodynamic stations where both the quality

of the observations and the stability of the sites are reliable. In addition to that, stations located inland some way (e.g., 50 km) are preferable than those near the tide gauges. The GPS-geodynamic stations in Indonesia are part of a geodynamic network of 42 sites located in the South and South-East Asia region. The observations were conducted simultaneously and periodically from 1994 to 2000 within the frameworks of the Geodynamics in South East Asia (GEODYSSEA) and the Asia Pacific Regional Geodynamics (APRG) projects. The data was computed by several analysis centers and the precision of the coordinates of the GEODYSSEA stations are reported as 4-7 mm for horizontal and 10 mm for the vertical components (Becker, 2000).

3.1.2 The leveling heights

The approximate accuracy of the orthometric height component H cannot be accessed here, as most of the GPS-geodynamic stations are not located at leveling benchmarks. It is therefore proposed that these stations should be tied into the national leveling network. The precision of the leveling height H will be a function of the length of the tie from the benchmark to the GPS station and the accuracy of leveling employed. Xu and Rummel (1991, p.25) consider an acceptable accuracy of leveling to be 1 mm/km excluding systematic effects. However, Rapp (1992, p.23) assigned a standard deviation of 5 cm for the orthometric heights of the fundamental stations used in the first attempt to unify the world vertical datum.

3.1.3 The gravimetric Geoid

The precision of the geoid undulation depends upon the accuracy and coverage of the gravity data used in the geoid computation. The geoid undulation computed from gravity anomalies according to the classical Stokes formula is written as (Heiskanen and Moritz, 1967, p. 94),

$$N = \frac{R}{4\pi\gamma}\iint_{\sigma}\Delta g S(\psi)d\sigma \tag{3.3}$$

where,

Δg is the gravity anomalies which should be known over the entire globe

$S(\psi)$ is the Stokes function

γ is the earth's mean gravity

R is the earth's mean radius

More detailed discussions on the implementation of the Stokes formula for the geoid computation are given in Chapter 4.

In practice, the computation of the geoid undulation is done by a combination of a global geopotential model, local free-air gravity anomalies and topography data and can be expressed as,

$$N = N_l + N_s \tag{3.4}$$

where N_l is the long wavelength geoid component calculated based on the geopotential coefficients model and the N_s is the short wavelength geoid component computed from gravity anomalies and the topographic data. The accuracy of the computed total *N* value depends on the contributions of the long wavelength error ε_{N_l} introduced by the errors in the geopotential coefficients models and the short wavelength error ε_{N_s} coming from the local gravity and topographic data.

The error in the geopotential models is expressed in terms of error degree variances and given as,

$$\varepsilon^2_{Nl_n} = \left(\frac{GM}{\alpha\gamma}\right)^2 \left(\frac{a^2}{R^2}\right)^{n+1} \sum_{m=-n}^{n} \left(\varepsilon\overline{C}_{nm}\right)^2 \tag{3.5}$$

where $\varepsilon\overline{C}_{nm}$ is the standard deviations of the geopotential coefficients model. This is called the commission error. The estimated global RMS value of the commission

error based on the geopotential models OSU91A and EGM96 is shown in Table 3.1 (Lemoine et.al, 1998, p.10-36). However, the actual long wavelength geoid undulation errors may vary geographically and could be considerably larger in areas like South East Asia where there is a lack of gravity data in several places.

Table 3.1 The RMS Geoid Commission Error from Geopotential Models.

To degree (n)	**Errors in cm**	
	OSU91A	**EGM96**
2	0.18	0.05
6	2.2	0.6
10	5.1	1.8
20	10.8	4.9
30	17.2	7.9
50	25.8	14.6
70	32.7	19.0
75	34.0	20.6
100	38.8	26.0
120	41.7	29.0
180	47.3	34.7
360	54.7	42.1

The error in the short wavelength component depends on the coverage, density and the accuracy of local gravity data. In addition to that, errors are also introduced by the inaccurate topography data used in the reduction of the gravity anomalies. Kearsley (1986) suggested that the short wavelength contribution is achievable to better than ± 5 cm over 100 km providing the mean error of 10 km grid gravity data used in the computation does not exceed ± 3 mgal. Errors are also introduced by inaccurate topography data used in the reduction of the gravity anomalies. By using a good elevation model of 1 km by 1 km the relative errors can be reduced to below 2 ppm.

More precise geoid models are expected from the GRACE and GOCE gravity satellite missions. The accuracy could be as good as 1 cm for spatial resolutions from 100 to 20000 km (Rummel, 2002). Such models will help greatly in the unification of vertical datum compared to the present situation.

3.2. The Actual Pilot Test Computation

At present time, the data needed for the vertical datum comparison are not available for the whole Indonesian region that consists of more than 17 000 islands. The GPS-Geodynamic stations are mostly established in major islands (Jawa, Sumatera, Kalimantan, Sulawesi and Irian Jaya) and only a few sites are located in several smaller islands. However, the leveling heights are not available at most of those stations. The leveling measurements were only completed in the two major islands of Jawa and Sumatera and part of Sulawesi.

Due to these data constraints, the pilot test computation is performed only for a subset area in the western part of the Indonesian region. The vertical datum comparison is carried out in an area chosen so as to connect the Sumatera and Jawa islands, where the parameters h, H and N are available. The test area is bounded by 16^0x20^0 ($-10^o<\varphi<6^o$ and $94^o<\lambda<114^o$). There are 8 GPS-Geodynamic stations located within the test area, which are ideal as fundamental stations for the vertical datum comparison. Unfortunately only two of these points coincide with the leveling benchmarks and a connection of the remaining stations to the national leveling network was not possible during this study. As an option, it was decided to employ the documented Bakosurtanal GPS/leveling common points as fundamental stations for the datum comparison, see Figure 3.1.

3.2.1 Data sources and the quality of the datasets

a. The geometric heights

For this test computation 56 GPS points located at leveling Benchmarks in the local networks have been used. These are made up from 47 points in Sumatra and 9 points in Jawa. The distribution of these points is shown in Figure 3.1. In addition to these points, the GPS-geodynamic stations of GEODYSSEA/APRG sites co-located with leveling benchmarks (one each in Jawa and Sumatra) were also used.

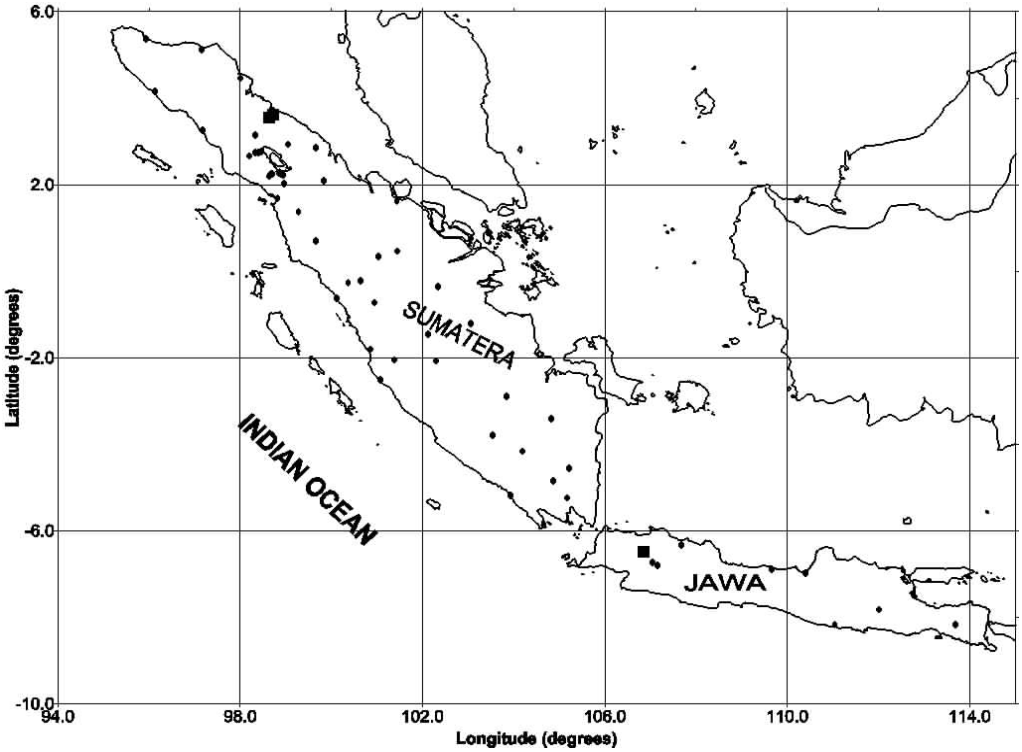

Figure 3.1 Distribution of GPS/Levelling points (●) and the GPS-geodynamic stations (■) for the test area.

The GPS-Geodynamic coordinates were given in the ITRF2000 datum (Morgan, P., 2002, pers. comm.). The local GPS points at leveling Bench Marks in Sumatra and Jawa were measured in several different networks within the period of 1991 to 1993. To avoid any inconsistency in the GPS heights used in this computation, their geodetic coordinate positions have been re-adjusted into ITRF2000 and their new documented coordinates are consistent with the GEODYSSEA/APRG coordinates (Subarya, 2002, pers. comm.). The leveling networks in Jawa is classified as the National 1st Order Leveling Network and the precision of the heights is around ±2

cm, while the leveling networks in Sumatra has a lower order with average height accuracy of ± 4 cm (Sutisna , 2001).

b. The gravimetric Geoid

A high precision regional geoid model for the country has not yet been available. The main impediment to its production is the deficiency of gravity data, especially in mountainous and coastal regions. To date, the existing regional geoid model that covers the whole Indonesian region was computed by either combining the global free-air gravity anomaly data set with the gravity anomalies derived from GEM-8 potential coefficients (Kahar, 1981), or by using the 5' grid Indonesian gravity database with the geopotential coefficients model OSU91A (Kahar J., Kasenda, A., Prijatna, 1996). The accuracy of the first model was relatively low (of the order of 4 to 5 meters). Improvement was made in the latter model (order of 1 to 1.5 m), but still far from the accuracy required for vertical datum comparison. Therefore, these models can't be employed for such purpose and a better geoid is needed.

As mentioned earlier, the accuracy of the gravimetric geoid depends on the computation method and the quality and coverage of the gravity data. The gravity data over the Indonesian region consist of land and marine gravity dataset measured by different groups and institutions, mainly by the National Oil Company and the Geological Survey Department. Since the observations are mostly aimed at geophysical exploration and geological structure interpretations, the spatial density of the data distribution is uneven. It is very dense in some prospecting areas and rather sparse to non-existent in the areas of lesser hydrocarbon potential. There is also a lack of gravity data in rugged terrain or in swamp areas. The distribution of the terrestrial and marine gravity data over the region is given in Figure 3.2. This gravity data situation will influence the accuracy of the computed geoid.

To date, the only regional gravity dataset that covers the whole Indonesian region is from the South East Asia Gravity Project (SEAGP). This project was undertaken by The Geophysical Exploration Technology, The University of Leeds, UK in

collaboration with the Indonesian Gravity Commission. The project ran from 1991 to 1995. All the available land and offshore gravity data on different datum and from various sources were adjusted and standardized into a uniform South East Asia Gravity data set. Offshore data gaps were filled with gravity anomalies derived from satellite altimetry. All observed datasets have been adjusted into the IGSN71 gravity datum, and processed using the WGS84 gravity formula (GETECH, 1995). However, the accuracy of the final 5' grid dataset remains uncertain due to large data gaps in the land areas, especially in the mountains and in the coastal regions.

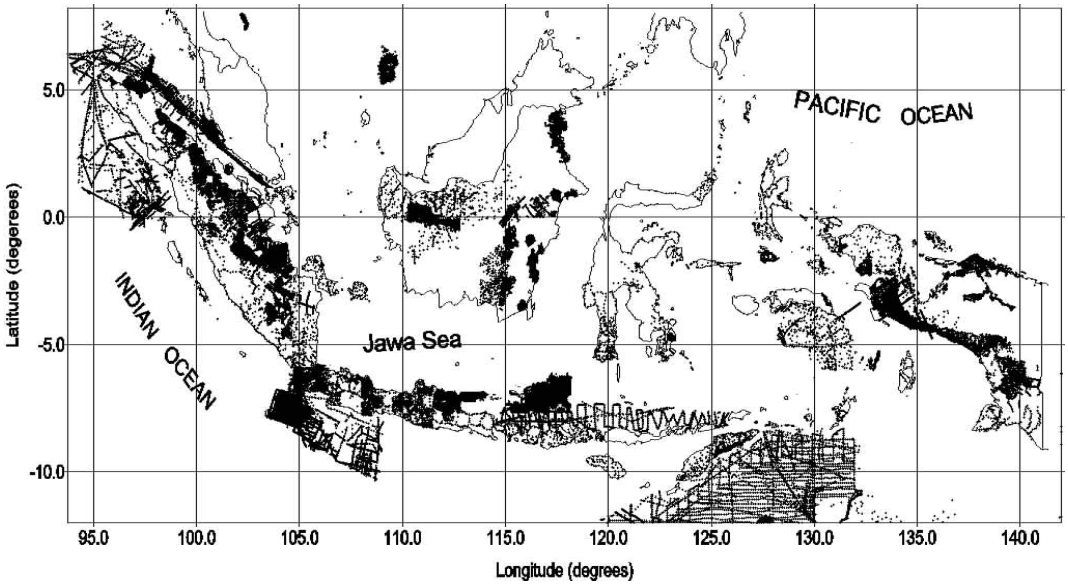

Figure 3.2 The Gravity Data Distribution over The Indonesian region (GETECH/KGN, 1995)

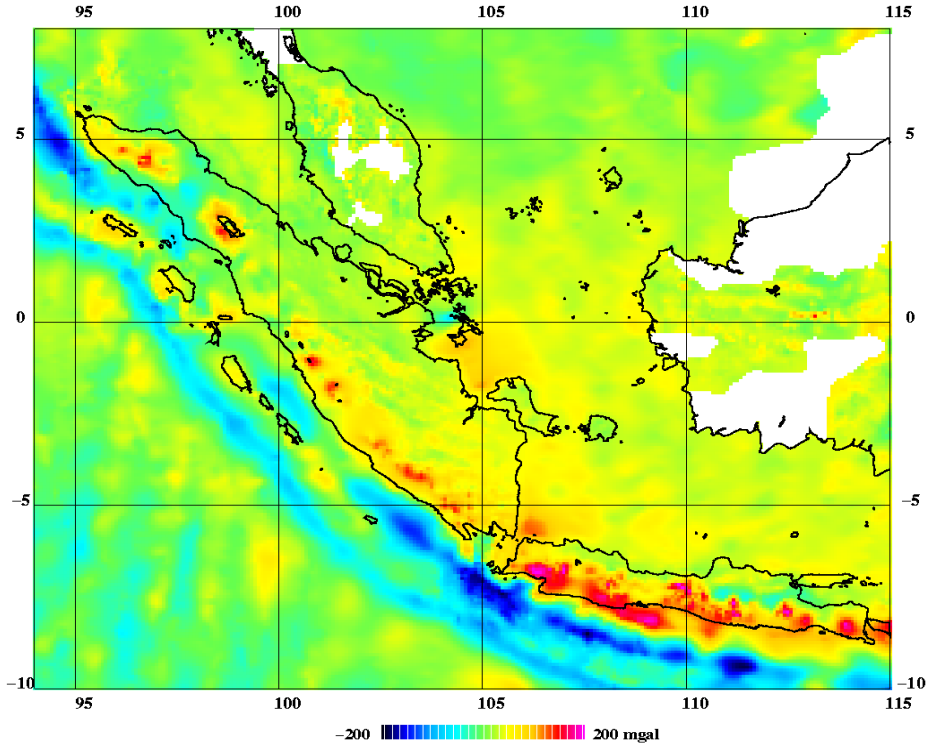

Figure 3.3 The free-air gravity anomalies over the test area

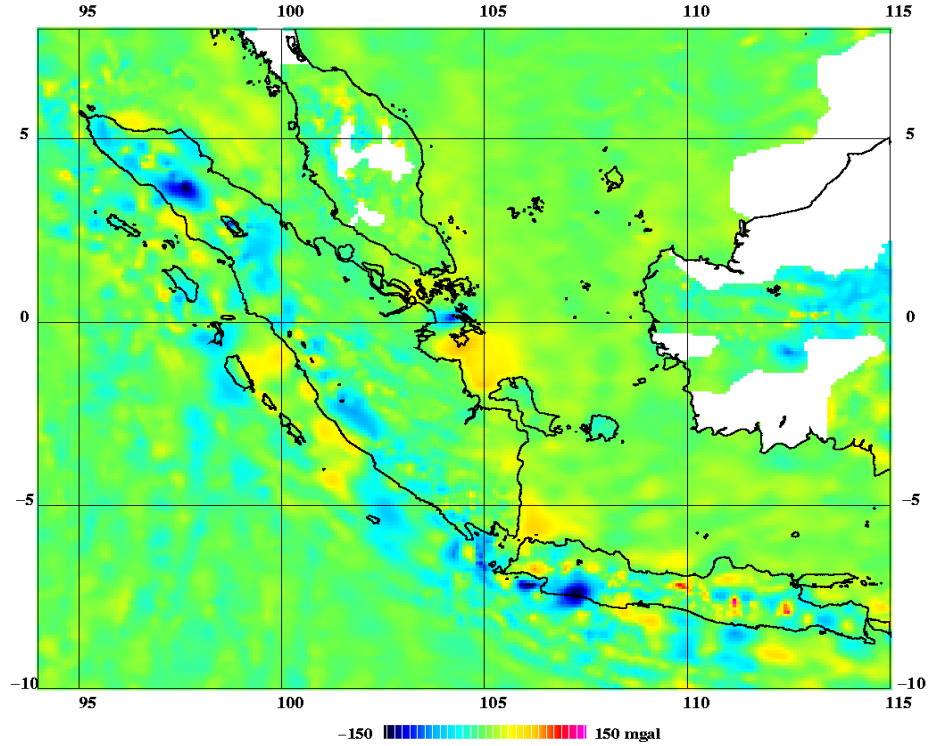

Figure 3.4 The residual anomalies after removing the EGM96

The gravimetric geoid for the test area (namely INDGED02) is computed based on the free-air gravity anomalies from the data mentioned above, combined with the geopotential model EGM96 as the reference field. The gravity features over the test area are quite dynamic, the free-air anomalies varies from –190 mgal over the ocean areas in west of Sumatera and south of Jawa to more than 250 mgal over the land part of Jawa island. After removing the long wavelength components from the 'observed' data, the residual gravity field becomes smoother (compare Figure 3.3 and Figure 3.4). The statistics of the data reductions are given in the Table 3.2 below. It is seen from this table that the residual anomalies have an effective zero mean value (- 0.61 mGal) and a much reduced standard deviation (± 18 mGal) and range (around 320 mGal), as would be expected, since much of this gravity data were likely used in the evaluation of the EGM96 coefficients.

Table 3.2 The statistics of the gravity reduction (unit in mGal).

Free-air Anomalies	Mean	Std. Deviation	Min.	Max.
'Observed' data	15.63	40.65	-190.02	272.70
EGM96	16.24	39.13	-159.47	237.13
Residual	-0.61	17.96	-154.68	172.87

The computation is carried out using the FFT technique as implemented in the GRAVSOFT packages. A more detailed discussion on the FFT technique is given in Chapter 4. The geoid height is calculated at a grid spacing of 5' for the larger area before interpolating into the control points. The variation of the geoid within the test area is relatively high, ranging from – 40 m in the west to more than +40 m in the eastern part of the area (see Figure 3.5). The contribution of the residual geoid varies from a minimum of -1.35 to a maximum of +1.84 m over the area. The standard deviation of the residual geoid is about 0.11 m, while the interpolated values at the control points have standard deviation of about 0.24 m.

The global geoid commission error from the EGM96 geopotential models expanded up to 360 degrees is about 42 cm (see Table 3.1). The accuracy of the residual geoid from the geoid computation done here by FFT cannot be assessed directly, since the FFT technique does not propagate errors. So the total geoid error

budget is unknown. To assess the error of the residual geoid Least Squares Collocation should be used. This is done in Chapter 5 for a smaller area (i.e., part of Jawa and southern part of Sumatera). The error estimates here were between 20 and 30 cm for most areas. If we assume the error to be 25 cm for the present residual FFT geoid and that the global commission error is applicable for this specific area, then the total geoid error should be around 50 cm. Although far from the desired precision, this result is considerably better than the previous geoid models for the area. This geoid is therefore adopted as the reference surface and its value at GPS/leveling common points are then used in the vertical datum comparison.

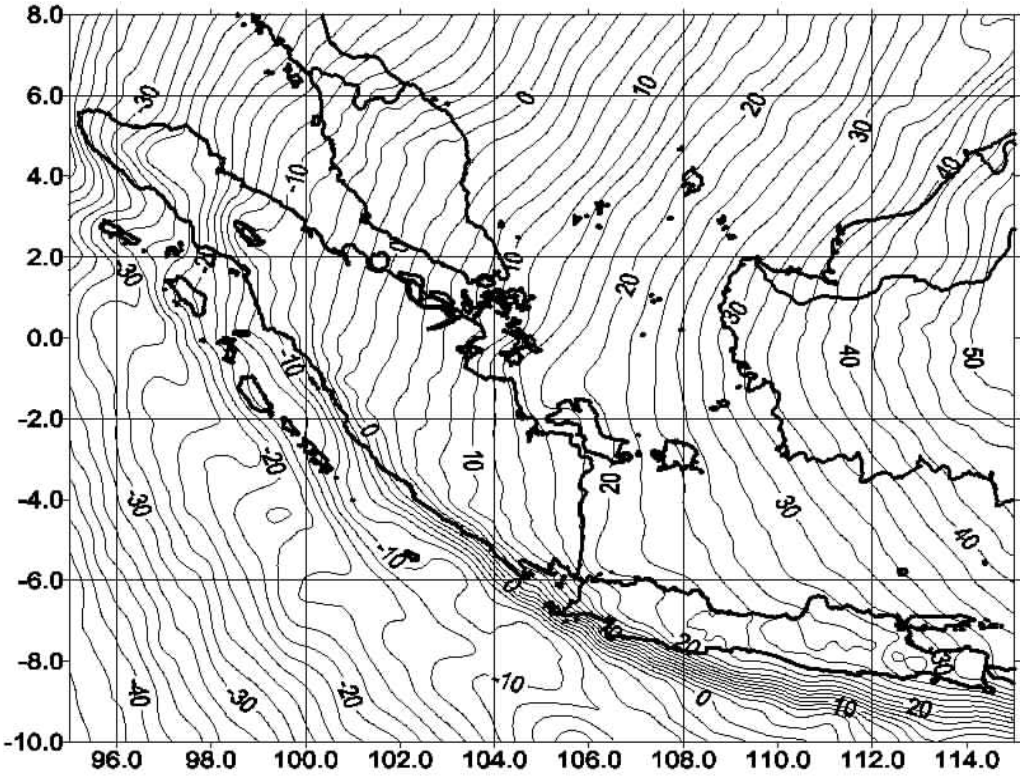

Figure 3.5 The gravimetric geoid (INDGED02) over the test area (contour interval 2 m)

3.2.2 The Comparison at control point

A comparison is carried out using equations (3.1) and (3.2). The ellipsoidal height h, the orthometric height H and the computed geoid undulation N are given in Table 3.3 and Table 3.4 together with the misfit for the control points. The local datum offsets

from the reference surface is given in Table 3.5 in terms of mean and standard deviations of the misfit from Table 3.3 and Table 3.4. It shows that the mean offset of local heights in Sumatera is about 0.38 m from the reference surface with a standard deviation of 0.67 m. In Jawa the local heights deviate more from the reference surface. The mean offset is 1.16 meter with a standard deviation of 1.54 meter. This large standard deviation shows that significant variation from the mean offset is present. This may be partly explained by the small sample size in Jawa. However, for Sumatera, where we have much bigger sample, the standard deviation of 0.67 meter also indicates that there are problems in the data used in the comparisons. Since the geoid was estimated to be accurate at the 50 cm level, the combined error for leveling and GPS must be approximately at the same level in order to give a total misfit of 0.67 m standard deviation (assuming the GPS/leveling error to be uncorrelated with the geoid error). These may both include errors in ellipsoidal height h and leveling height H, but could also point to the presence of distortions in the local height datum, i.e. that the local height datum refer to different tide gauges (see Kasenda and Kearsley, 2002).

Table 3.3 The comparison at Jawa GPS/leveling control points

Pt #	Latitude	Longitude	h (meter)	N (meter)	H (meter)	dH (meter)
1	- 8.168	113.702	119.770	31.641	85.766	2.363
2	-7.826	112.010	94.640	26.302	66.809	1.529
3	-8.177	111.045	411.510	24.814	384.503	2.193
4	-6.984	110.409	31.280	25.905	4.793	0.582
5	-6.889	109.664	28.610	24.776	6.426	-2.592
6	-6.333	107.673	32.150	20.189	10.967	0.994
7	-6.808	107.156	427.490	19.446	405.723	2.321
8	-6.731	107.041	1075.390	19.913	1053.558	1.919
9	-6.491	106.849	158.170	18.629	138.410	1.131

Table 3.4 The comparison at Sumatera GPS/leveling control points

Pt #	Latitude	Longitude	h (meter)	N (meter)	H (meter)	dH (meter)
1	-4.553	105.221	38.620	15.725	22.226	0.669
2	-5.240	105.175	100.380	14.322	85.879	0.179
3	-4.847	104.856	46.090	14.037	31.748	0.305
4	-3.412	104.824	25.910	14.635	10.422	0.853

Pt #	Latitude	Longitude	h (meter)	N (meter)	H (meter)	dH (meter)
5	-4.166	104.197	71.910	12.250	58.907	0.753
6	-5.188	103.934	9.330	4.953	3.758	0.619
7	-2.888	103.839	21.910	11.297	10.192	0.421
8	-3.786	103.533	123.560	9.637	112.816	1.107
9	-1.205	103.066	40.680	7.736	32.324	0.620
10	-0.349	102.333	26.000	3.720	21.746	0.534
11	-2.075	102.288	65.200	5.227	59.806	0.167
12	-1.463	102.123	54.790	4.154	49.701	0.935
13	0.462	101.446	39.070	-0.207	39.503	-0.226
14	-2.054	101.390	808.810	1.292	805.439	2.079
15	1.619	101.436	15.880	-1.281	17.355	-0.194
16	-1.806	100.855	35.100	-3.338	37.366	1.072
17	-2.514	101.068	-0.680	-4.657	3.831	0.146
18	0.346	101.025	35.240	-1.736	36.896	0.080
19	-0.728	100.944	180.240	-0.908	180.314	0.834
20	-0.223	100.633	511.170	-2.339	512.747	0.762
21	-0.271	100.369	910.740	-3.899	913.796	0.843
22	-0.620	100.120	-3.440	-6.977	3.853	-0.316
23	2.095	99.833	29.160	-7.800	37.070	-0.110
24	2.848	99.653	19.160	-9.276	29.364	-0.928
25	3.569	98.677	12.190	-15.539	28.193	-0.464
26	0.693	99.652	391.470	-8.088	398.038	1.520
27	1.369	99.278	286.090	-10.142	295.520	0.712
28	2.936	99.047	422.670	-11.098	434.551	-0.783
29	2.020	98.962	945.320	-10.771	955.779	0.312
30	1.687	98.818	-9.630	-12.907	3.322	-0.045
31	3.145	98.328	1291.910	-15.573	1305.441	2.042
32	2.736	98.328	1084.770	-14.417	1099.377	-0.190
33	4.457	97.999	-19.030	-21.075	2.750	-0.705
34	3.258	97.184	-22.530	-26.577	2.298	1.749
35	4.153	96.132	-27.080	-30.819	3.054	0.685
36	5.366	95.933	-25.290	-31.160	4.619	1.251
37	5.120	97.158	-21.130	-25.180	3.969	0.081
38	2.665	98.198	401.800	-16.395	417.874	0.321
39	2.742	98.399	1008.300	-13.613	1021.839	0.074
40	2.762	98.459	1380.100	-12.987	1392.892	0.195
41	2.192	98.642	1303.100	-11.874	1314.914	0.060
42	2.225	98.656	1409.400	-11.517	1421.008	-0.091
43	2.252	98.678	1465.300	-11.159	1476.592	-0.133
44	2.257	98.712	1393.700	-10.890	1404.726	-0.136
45	2.262	98.859	1402.500	-10.038	1412.740	-0.202
46	2.248	98.902	1394.600	-9.902	1404.513	-0.011
47	2.225	98.939	1309.900	-9.891	1319.374	0.417

Table 3.5 The departure between local height datum and the reference surface (unit in meter)

	Mean	Standard Deviation	Minimum	Maximum
Sumatera	0.380	0.675	-0.928	2.079
Jawa	1.160	1.542	-2.592	2.363

Since documentation for the adjustment of the leveling networks is not available, it is difficult to identify which control points refer to which tide gauge. There is little systematic error in the spatial distribution of the misfit shown in Figure 3.6, eventhough there is some tendency to clustering, e.g. in the northern part and there may also (in some areas) be a correlation between elevation and misfit. A closer look at a possible correlation between elevation and misfit, though, shows that there is little correlation for Sumatera as a whole (see Figure 3.7). Based on these observations, the mean value of 0.38 m for the misfit was adapted as a common datum offset for Sumatera. The mean value of the misfit for Jawa is 1.16 m, which indicates that a local datum distortion of about 78 cm appears between Sumatra and Jawa. In cases where the misfit displays a more systematic pattern it may be better to assess the offset as a correction surface across the area rather than adopt a single value for the offset between the local datum and the equipotential reference surface or global datum.

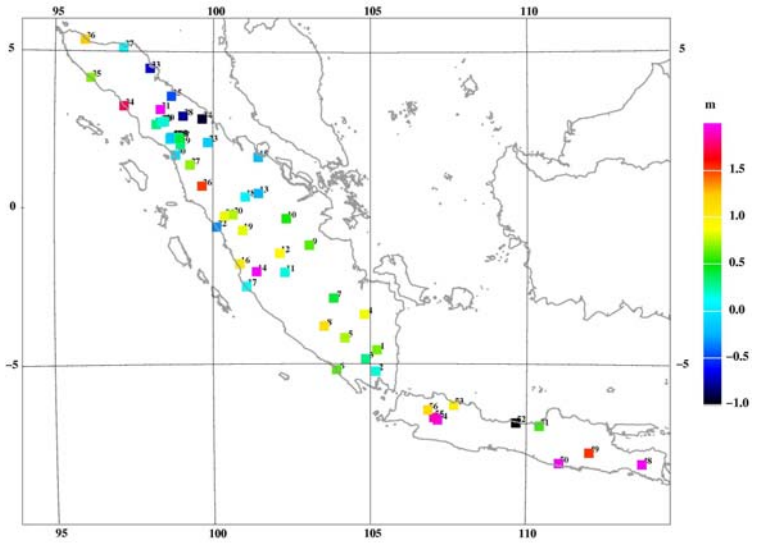

Figure 3.6 Misfit at control points

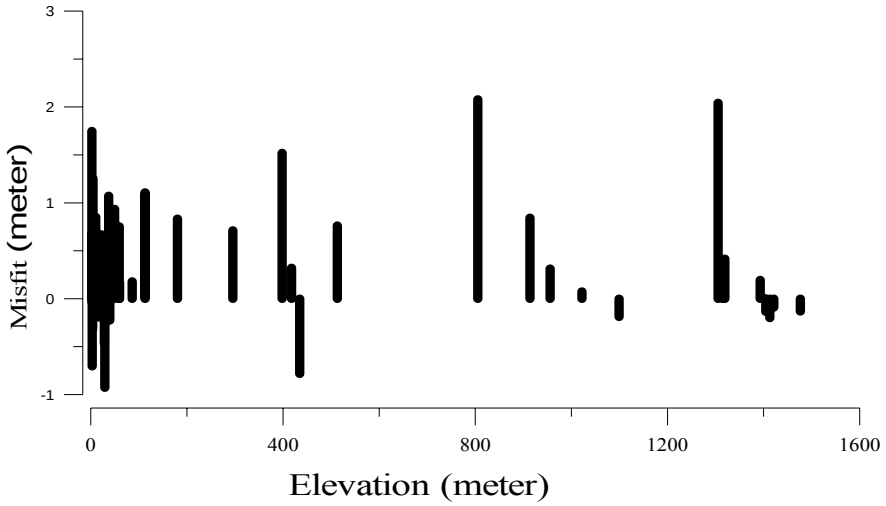

Figure 3.7. Misfit as function of elevation for the control points in Sumatera

CHAPTER 4

THE GEOID SOLUTION

4.1 Implementations of Stokes' integration formulae

Determination of the geoid undulation N is based on Stokes integration formulae which was published in 1849 by G. G. Stokes (Heiskanen and Moritz 1967, p. 94) and given as,

$$N = \frac{R}{4\pi\gamma}\iint_{\sigma} \Delta g S(\psi) d\sigma \tag{4.1}$$

where R is the Earth radius, γ is normal gravity, Δg is the gravity anomaly at the geoid and ψ is the spherical distance between the computation and the data point. The function S is Stokes' function and given by

$$S(\psi) = \frac{1}{\sin(\psi/2)} - 6\sin\frac{\psi}{2} + 1 - 5\cos\psi - 3\cos\psi\ln(\sin\frac{\psi}{2} + \sin^2\frac{\psi}{2}) \tag{4.2}$$

Equation (4.1) gives the solution to a boundary value problem for the disturbing potential T, assuming T to be harmonic, i.e. obeying the Laplace equation, outside the geoidal surface and further assuming that the gravity anomalies are given on the geoid. This means that actual observed gravity has to be reduced to meet these requirements (at least approximately). The reduction will normally consist of two steps. First is a removal or shifting of masses above the geoid and secondly a lowering (or downward continuation) of the actual gravity station from the surface upon which it is measured to the geoid.

The shifting or removal of masses will obviously have an effect on the derived geoid and a correction term to account for this so-called indirect effect on geoid has to be computed. The indirect effect will depend on the actual reduction scheme used. The condensation reduction of Helmert, used here as an example, has the advantage

of a rather small indirect effect, and a first order approximation may suffice in practice. The Helmert reduction corresponds to condensation of the masses above the geoid to a surface layer on the geoidal surface. Helmert reduced gravity anomalies (also called Faye anomalies) are computed as (Heiskanen and Moritz 1967, p. 145)

$$\Delta g_H = \Delta g_{FA} + c \tag{4.3}$$

where Δg_{FA} is the traditional 'free air anomaly', which formally refers to the geoid, and c is the classical terrain correction. A small term called the indirect effect on gravity has been neglected here. The indirect effect on the geoid for the Helmert reduction scheme is in the planar approximation given by (Sideris, 1994) and written as,

$$\delta N_{Helmert} \approx -\frac{\pi G \gamma \rho H}{\gamma} \cdot H \tag{4.4}$$

A more recent formulation of the geodetic boundary value problem was given by Molodenskii, where a "quasi geoid" is determined. Here the solution is computed directly from observations on the topographic surface

$$\zeta = \frac{R}{4\pi\gamma} \iint_{\sigma} (\Delta g_{FA} + g_1) S(\psi) d\sigma \tag{4.5}$$

where the free air anomaly Δg_{FA} now formally refers to the topographic surface. The distinction between free air anomalies referred to the surface and those referred and to the geoid is mainly a conceptual distinction, for practical purposes they can be considered identical (Heiskanen and Moritz 1967, p. 310). The expression g_1 is the first term in the Molodensky series and for practical purposes can be approximated with the classical terrain correction term c (Heiskanen and Moritz 1967, ibid). The integral (4.5) yields the quasi-geoid or the height anomaly, which relates to the definition of normal heights, see also Section 2.1.

The separation between the geoid and the quasi-geoid, $\delta\zeta$, may to a first order approximation be expressed as (Heiskanen and Moritz 1967, p. 327)

$$\delta\zeta = \frac{\bar{g} - \bar{\gamma}}{\bar{\gamma}} \cdot H \approx \frac{\Delta g_B}{981{,}000 mgal} \cdot H \tag{4.6}$$

where $\bar{g}$ is mean value of gravity along the plumbline between the surface of topography and the geoid, $\bar{\gamma}$ is the corresponding mean value of normal gravity, Δg_B the Bouguer anomaly and H the orthometric height.

So despite of the conceptual difference between the original formulation of the geodetic boundary value problem by Stokes and the more recent one by Moledenskii, there is little difference in the computation of a solution to the problem as seen from a practical point of view.

The integration in (4.1) and (4.3) is formally done over the whole globe. For practical implementations the gravity signal and the corresponding geoid signal are split into three terms, reflecting the spectral content of the signals

$$\Delta g = \Delta g_{GM} + \Delta g_{reg} + \Delta g_{topo} \tag{4.7}$$

Similarly, the geoid can be split up into the equivalent components

$$N = N_{GM} + N_{reg} + N_{topo} \tag{4.8}$$

The first term Δg_{GM} or N_{GM} contains the longest wavelengths of the anomalous gravity field and is taken from global geopotential coefficient models such as EGM96 (Lemoine, et. al, 1998), Eigen-2 from the satellite mission CHAMP and GGM01 or GMM02 from the GRACE satellite mission. These models are given as spherical harmonic coefficient sets, $[C_{nm}, S_{nm}]$, to degree and order, for e.g., 360 for the EGM96 model and 120 for GGM01s. The corresponding geoid undulation and gravity anomaly are expressed as

$$N_{GM} = R\sum_{n=2}^{N_{\max}}\sum_{m=0}^{n}\left[C_{nm}\cos m\lambda + S_{nm}\sin m\lambda\right] P_{nm}(\sin\phi) \tag{4.9}$$

and,

$$\Delta g_{GM} = \frac{GM}{R^2}\sum_{n=2}^{N_{\max}}(n-1)\sum_{m=0}^{n}\left[C_{nm}\cos m\lambda + S_{nm}\sin m\lambda\right] P_{nm}(\sin\phi) \tag{4.10}$$

where R is earths radius, G is the gravitation constant, M the mass of the earth and P_{nm} are fully normalized associated Legendre polynomials. The spherical functions $C_{nm}\cos m\lambda\, P_{nm}(\sin\phi)$ and $S_{nm}\sin m\lambda\, P_{nm}(\sin\phi)$ are all solutions to the Laplace equation. The highest degree of the models corresponds to wavelengths of 100 and 300 km respectively. The GRACE model is later on amended to degree 200 in the GMM02C and the EGM06 is updated into a higher degree (see later Chapter 6).

To split the remaining signal into two components Δg_{reg} and Δg_{topo}, N_{reg} and N_{topo} respectively, serves two purposes. First the gravity data coverage may not be adequate and gravity values have to be interpolated from existing data. Second is to account for topographic effects on gravity and geoid. Due to the high correlation between gravity and topography a gravity field reduced for topographic effects will be much smoother and therefore more suitable for interpolation than the original free air anomaly field. The Bouguer anomaly field Δg_B has been widely used for this purpose but it suffers from the fact that even the Bouguer gravity field is rather smooth on shorter scale, there is considerable energy in the field for wavelengths longer than 50 to 100 km due to isostatic compensation. This can lead to large systematic interpolation errors in areas where larger data gaps are present. The use of residual terrain models, RTM's, where the longer wavelengths are absent may serve better for interpolation purposes.

4.1.1 FFT techniques in geoid computation

Stokes integral (eq. 4.1) is basically a convolution integral. Such integrals can be estimated very efficiently by Fast Fourier Transforms (FFT) methods (Forsberg and

Sideris, 1993). The program SPFOUR from the GRAVSOFT package (Tcherning et al, 1992) was used for the FFT-based geoid computations presented here. In this program the Fourier transform is done as a bandwise 2-dimensional FFT, where the underlying coordinate system is the geographical coordinates scaled to mean latitude for each computation band.

Other implementations of the Fast Fourier Transform are the spherical FFT (Strang van Hess, 1990) and multiple 1-dimensional FFT with subsequent interpolation between the computation parallels (Haagmans et al, 1993).

A prerequisite for the use of FFT is that the data are on a grid format. The program GEOGRID (also from the GRAVSOFT package) was used to this purpose. Since the gridded data will be treated with equal weight in the FFT step, it is very important to consider what happens in the gridding process, especially in this test case with rather large data gaps. Both the near coastal offshore zone and the more mountainous parts of Java Island have very little reliable gravity data, see also Figure 4.4. The GEOGRID program offers two ways of interpolation, either by a simple weighting of the data, where data are weighted with the inverse squared distance, or by collocation based interpolation.

The collocation approach will give predicted values close to zero in areas where the nearest data point is further away than the correlation length used in the prediction (see Section 4.1.3). This may lead to systematic interpolation errors if the real (and unknown) mean value for the data gap fails to be close to zero. The correlation length can be chosen arbitrarily, but too long a correlation length will smooth the predicted values too much. So, despite the advantages of collocation based interpolation like the availability of error estimates there are also some drawbacks. Collocation based interpolation is treated in more details in Section 4.1.3.

The weighted mean interpolation method will give values that reflect the mean value of the surrounding data points better. Gridding by weighted mean was used in the geoid computations presented in the sequel.

Systematic or long wavelength errors in the gravity data can produce large geoid errors, which may degrade the geoid derived from the geopotential model instead of improving it. Wong and Gore (1969) proposed a modification of Stokes' function or Stokes' kernel to avoid this problem. With the Stokes' kernel written in terms of Legendre polynomials

$$S(\psi) = \sum_{n=2}^{\infty} \frac{2n+1}{n-1} P_n(\cos\psi) \tag{4.11}$$

Wong and Gore proposed to modify the kernel by removing the low degree harmonics, (4.11) then becomes,

$$S^{\tau}(\psi) = \sum_{n=\tau}^{\infty} \frac{2n+1}{n-1} P_n(\cos\psi) \tag{4.12}$$

where τ is the Wong-Gore cut-off degree. This will make the resulting gravimetric geoid less prone to long wavelength errors in the gravity data. On the other hand choosing too high a cut-off degree could mean that the medium wavelengths of the geoid signal won't benefit enough from the information in the gravity data. The choice of an optimal cut-off degree is based on a judgment, which adds some subjectivity to the geoid determination process.

4.1.2 The RING integration approach

The Stokes' function in equation (4.2) becomes infinity as ψ (the angular distance between the computation point and the surface element $d\sigma$) approaches zero (see Figure 4.1). To avoid the nonlinearity of the $S(\psi)$ as ψ becomes small, the $F(\psi)$ function is used (Kearsley, 1985). It is given in the form of $S(\psi)\sin\psi$,

$$F(\psi) = S(\psi)\sin\psi = 2\cos\frac{\psi}{2} - \sin\psi\left\{6\sin\frac{\psi}{2} - 1 + \cos\psi\left[5 + 3\ln(\sin\frac{\psi}{2} + \sin^2\frac{\psi}{2})\right]\right\} \tag{4.13}$$

This $F(\psi)$ function behaves better (see Figure 4.1 below), having a maximum value of about 2.5 at $\psi \approx 10°$ and moving towards 2 as ψ approaching zero.

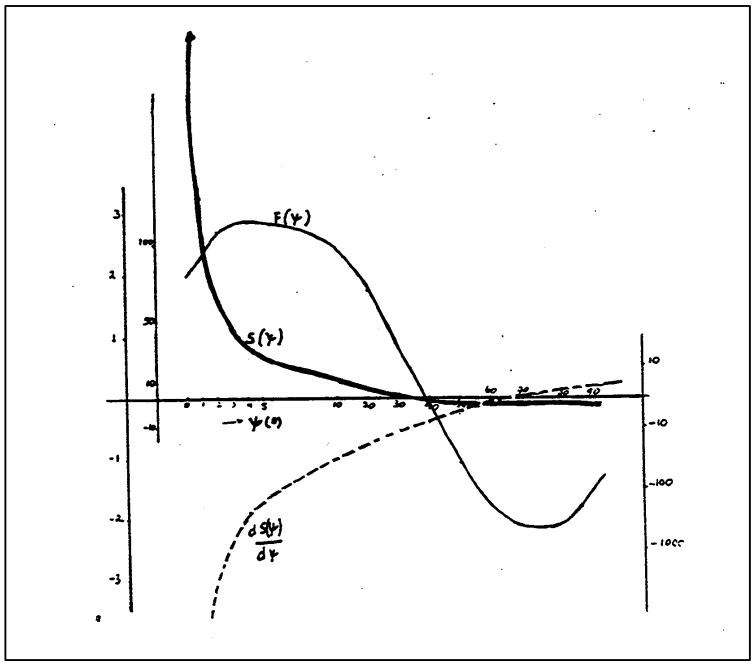

Figure 4.1 The S(ψ) and F(ψ) functions

The solution of the Stokes' integral formula in equation (4.1) is then carried out using this modified Stokes function and the geoid undulation formula and written as,

$$N = \frac{R}{4\pi\gamma} \iint_{\sigma} \Delta g F(\psi) d\psi d\alpha$$

$$= \frac{R}{4\pi\gamma} \int_{\alpha=0}^{2\pi} \int_{\psi=0}^{\pi} \Delta g F(\psi) d\psi d\alpha \qquad (4.14)$$

where $d\psi$ is the increment in the spherical radial distance originating from the computation point, $d\alpha$ is the increment in the direction of the radial line. The practical evaluation of this integration formula is called the Ring Integration method.

It is implemented in the RINT software package and is fully developed in Kearsley (1985). In this method, the surface is subdivided into compartments formed by concentric rings and radial lines centered on the computation point P (see Figure 4.2). The mean gravity anomalies values of each compartments ($\overline{\Delta g}$) are estimated by fitting plane surfaces to the point data and interpolating the value from the plane at the mid point. The contribution in meters to the geoid per mGal of $\overline{\Delta g}$ values from a compartment bounded by ψ_i and ψ_j is written as,

$$C_N = k \int_{\psi_1}^{\psi_j} F(\psi) d\psi \tag{4.15}$$

and the integration is then calculated in terms of summation,

$$N_s = C_N \sum_{h=1}^{H} \sum_{i=1}^{I} \overline{\Delta g_{h,i}} \tag{4.16}$$

where N_s is the short wavelength component of the geoid (the inner zone contribution where $0^o \leq \psi \leq 1.5^o$), h is counter for the azimuth component and i is counter for the radius component. The C_N is set up to 0.3 mm/mGal for this test. The formal error estimate in N_s is simultaneously propagated through the Ring integration solution, based upon its variance estimate in the gravity anomaly (Kearsley, pers. comm.).

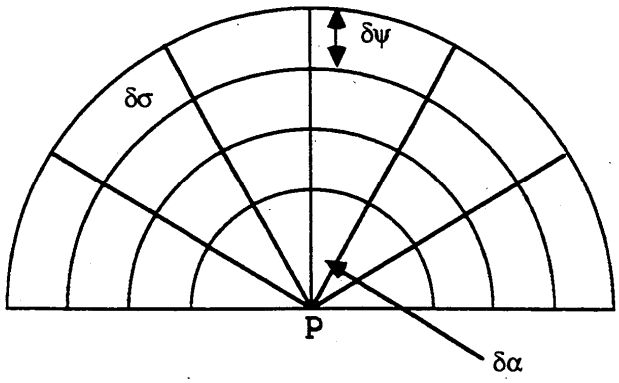

Figure 4.2 The concentric ring compartments

The medium to long wavelength component of the geoid undulation (the remote zone contribution) is determined from the geopotential coefficients model using the formula (4.9) mentioned in Section 4.1.

4.1.3 Least Squares Collocation (LSC)

Estimation or prediction of the gravity field in areas with no data is of major importance for the determination of the geoid. It is obvious that the roughness of the gravity field has an impact on such predictions. It is easier to make good predictions in areas with a benign or gently undulating gravity field than in areas where the field is wildly fluctuating. In the first case neighbouring points are more likely to have similar values than in the latter.

The empirical covariance function, $C(\psi)$, which is a measure of the tendency for neighbouring points to have similar values plays an important role in least squares prediction. It is written as,

$$C(\psi) = \overline{\Delta g_P \cdot \Delta g_Q}\Big|_{dist(P,Q)=\psi} \tag{4.17}$$

where the mean is taken over all pairs of data points P and Q separated by the spherical distance ψ. An example of such a covariance function is shown in Figure 4.3.

The spherical distance where $C(\psi)$ drops off to one half of the maximum value is called the correlation length. The figure shows both the empirical covariance function as determined from (4.17) and an approximate analytical representation.

The optimal prediction of the gravity field in a point P expressed as a linear combination of all observations Δg_i is given by the following matrix form (Moritz 1980, p. 80 and p.102)

$$\Delta\tilde{g}_P = \{C_{P1}, C_{P2}, \cdots, C_{Pn}\}\left(\begin{bmatrix} C_{11} & C_{12} & \cdot & C_{1n} \\ C_{21} & \cdot & \cdot & \cdot \\ \cdot & \cdot & \cdot & \cdot \\ C_{n1} & \cdot & \cdot & C_{nn} \end{bmatrix} + \begin{bmatrix} v_{11} & v_{12} & \cdot & v_{1n} \\ v_{21} & \cdot & \cdot & \cdot \\ \cdot & \cdot & \cdot & \cdot \\ v_{n1} & \cdot & \cdot & v_{nn} \end{bmatrix}\right)^{-1} \cdot \begin{pmatrix} \Delta g_1 \\ \Delta g_2 \\ \cdot \\ \Delta g_n \end{pmatrix} \quad (4.18)$$

where n is the number of observations and $C_{ij} = C(dist(i, j))$ denotes the value of the covariance function with an argument equal to the distance between the data points *i* and *j*. The matrices $[C_{ij}]$ and $[v_{ij}]$ are called the auto covariance and observation error covariance matrices. The observation error covariance matrix will often just be a diagonal matrix assuming the observation error or noise to be uncorrelated from one observation point to another.

The least square prediction method also gives estimates of the prediction errors. The squared standard error in the prediction point P is given as

$$\sigma_P^2 = C(0) - \{C_{P1}, C_{P2}, \cdots, C_{Pn}\}\left(\begin{bmatrix} C_{11} & C_{12} & \cdot & C_{1n} \\ C_{21} & \cdot & \cdot & \cdot \\ \cdot & \cdot & \cdot & \cdot \\ C_{n1} & \cdot & \cdot & C_{nn} \end{bmatrix} + \begin{bmatrix} v_{11} & v_{12} & \cdot & v_{1n} \\ v_{21} & \cdot & \cdot & \cdot \\ \cdot & \cdot & \cdot & \cdot \\ v_{n1} & \cdot & \cdot & v_{nn} \end{bmatrix}\right)^{-1} \cdot \begin{pmatrix} C_{P1} \\ C_{P2} \\ \cdot \\ C_{Pn} \end{pmatrix} \quad (4.19)$$

Geoid heights N can also be estimated from gravity observations if the cross covariance matrix $[C_{ij}^{Ng}]$ between geoid heights and gravity anomalies are known (Moritz 1980, p 102).

$$\tilde{N}_P = \{C_{P1}^{Ng}, C_{P2}^{Ng}, \cdots, C_{Pn}^{Ng}\}\left(\begin{bmatrix} C_{11} & C_{12} & \cdot & C_{1n} \\ C_{21} & \cdot & \cdot & \cdot \\ \cdot & \cdot & \cdot & \cdot \\ C_{n1} & \cdot & \cdot & C_{nn} \end{bmatrix} + \begin{bmatrix} v_{11} & v_{12} & \cdot & v_{1n} \\ v_{21} & \cdot & \cdot & \cdot \\ \cdot & \cdot & \cdot & \cdot \\ v_{n1} & \cdot & \cdot & v_{nn} \end{bmatrix}\right)^{-1} \cdot \begin{pmatrix} \Delta g_1 \\ \Delta g_2 \\ \cdot \\ \Delta g_n \end{pmatrix} \quad (4.20)$$

The method is called least squares collocation, when derived quantities like the geoid undulation are estimated. Also geoid error estimates becomes available in a

manner similar to (4.19). The key point in this approach is that the cross covariance matrix [C_{ij}^{Ng}] between geoid undulation and gravity anomaly can be derived from the analytical representation of the empirical covariance function. This important property is called covariance propagation (Moritz 1980, p. 87). The method is not limited to making predictions based on one type of observations like gravity anomalies. The observation vector in eq. (4.20) can consist of any combination of quantities that can be expressed as a linear functional of the disturbing potential T, e.g. gravity anomalies, geoid heights, deflections of the vertical or the disturbing potential T itself. Also upward/downward continuation of the quantities can be performed in the same collocation step (Moritz 1980, p. 97).

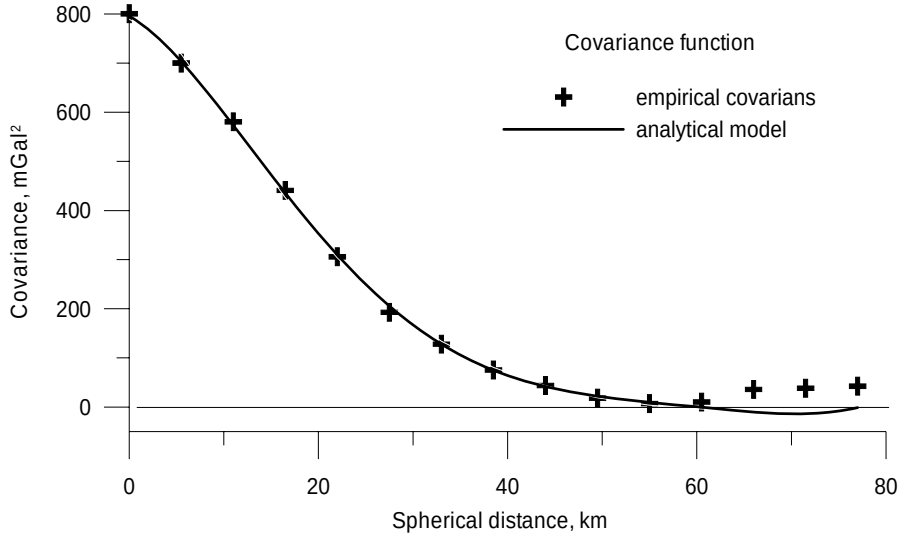

Figure 4.3. The covariance function used for the geoid computation. The function is based on residual land free air anomalies

There are two basic assumptions about the underlying structure of the gravity field that should apply when using collocation. First the mean value of the gravity field is assumed to be zero and secondly the field is assumed to be isotropic, i.e. behaves (statistically) the same in all directions and is independent of azimuth. Both assumptions will be closely approximated even for smaller areas when a good global reference field is subtracted the observed anomalous gravity field. Kearsley (1977)

has shown there needs to be significant anisotropy before the collocation solution breaks down.

In mountainous areas it is however necessary to go a step further and also try to remove regional and local trends in the gravity field before using optimal estimation and/or collocation. The classical Bouguer anomaly is much smoother and exhibits less local features than the Free Air anomaly but suffers from pronounced regional trends in the anomaly field stemming from isostacy. The Residual Terrain Model approach (RTM) take into account both the local topography and the effect of isostacy and thus represents the most sophisticated scheme for the reduction of gravity observations (Forsberg and Tscherning 1981).

4.2 Data sets and Pre-processing

The island of Java was chosen as test area for the geoid computations due to the relatively better surface gravity data coverage as compared to other parts of Indonesia and because of the presence of several control points with geometric geoid values from combined GPS and levelling measurements (see Figure 4.4). Gravity and elevation data within the area bounded by southern latitude -10° to -4° and eastern longitude 103° to 119° were included for the computations.

4.2.1 Gravity Data for the Test Area

Most of the terrestrial gravity data are compiled from exploration surveys for oil, gas and coal and collected by different private companies, or they are data collected for general geological interpretation purposes by the Department of Geology. There is good reason to be somewhat cautious about the geodetic quality of both types of data. Documentation for a proper connection to the Indonesian Gravity Network can in general not be established. In addition to that is the fact that some of the data are interpreted from Bouguer anomaly maps with heights and Bouguer corrections back-substituted from topographic maps.

A small part of the terrestrial gravity data were collected by the Indonesian Mapping Agency (Bakosurtanal) along levelling lines and these data are of course of

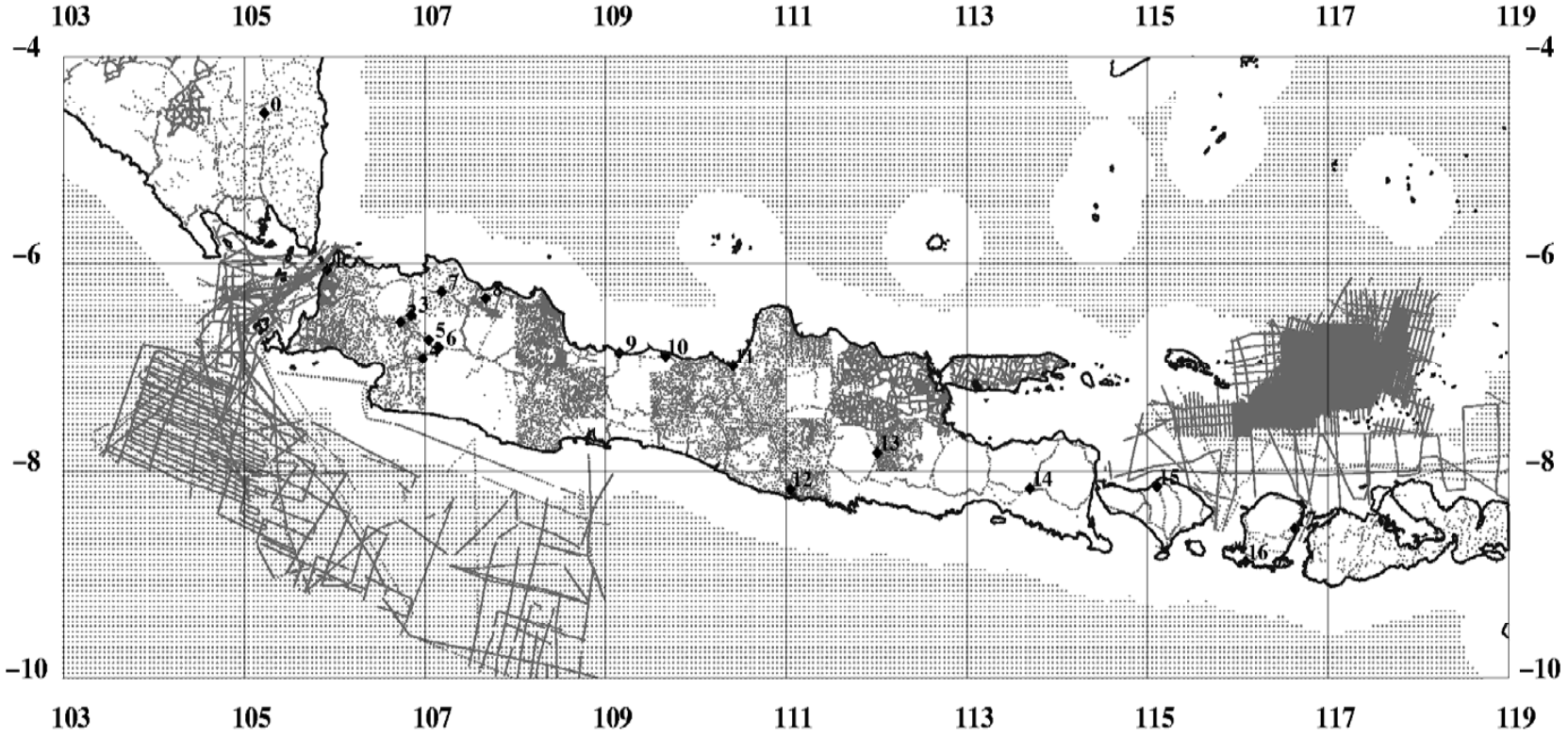

Figure 4.4. Distribution of gravity data and GPS/levelling points.

a very good quality. The total number of terrestrial gravity data points within the test area (10° to 4° S and 103° to 119° E) is 26,483 of which approximately 1,200 data points were collected by Bakosurtanal. Statistics of the data are given in Table 4.1.

The marine data dates back to the 60's and 70's era and were gathered for oil exploration purposes. The total number of data points within the test area are 110972 concentrated in two blocks, one Southwest of Java and the other East of Java (see Figure 4.4). Gravity derived from satellite altimetry was also included to supplement the marine data. The data was extracted from the KMS99 gravity model. This model is based on sea surface height observations from the GEOSAT and ERS-1 geodetic and repeat missions satellite altimetry. Sea surface heights are subsequently inverted to gravity anomalies by the inverse Stoke's method (Andersen and Knudsen, 1998). In near coastal regions, the accuracy of this altimetric gravity field is known to degrade due to the coastal sea state variability (Andersen and Knudsen, 2000).

Comparisons between satellite altimetry and marine data showed rather large discrepancies near the coast; in some places the difference amounts to more than 200

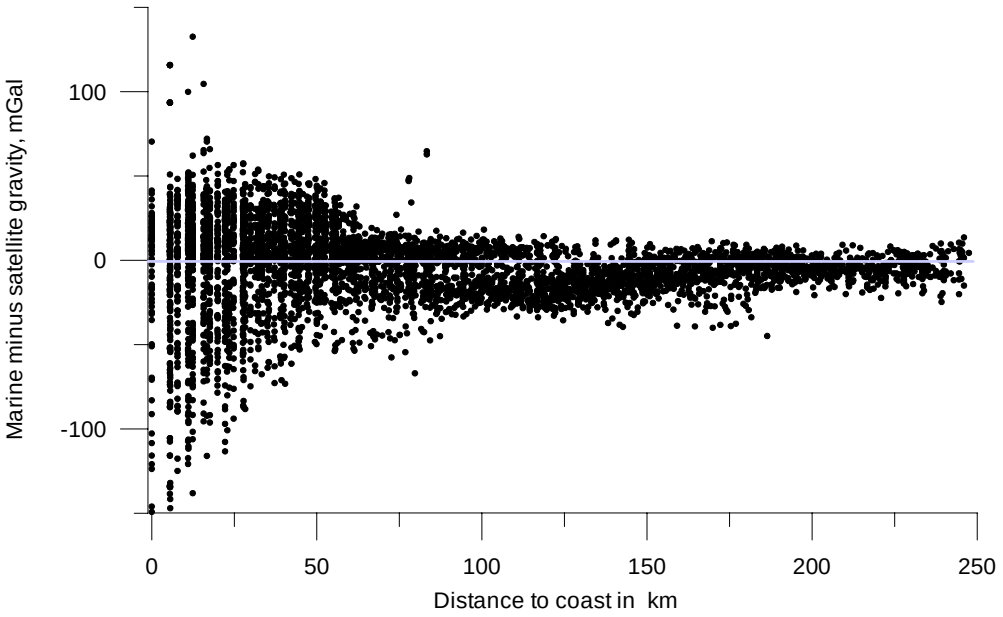

Figure 4.5. Difference between marine and satellite gravity as function of distance to coast.

mGal, see Figure 4.5 and Table 4.1. This is thought to be mainly due to problems with the altimetric gravity model, as the discrepancy shows a close relationship with the distance to the coastline.

If the comparison is limited to data points more than 50 km from the coastline the agreement is seen to be considerably better, see again in Table 4.1 below.

It was therefore decided to discard gravity estimates from the altimetric model that were closer than approximately 50 km from the coastline even though 50 km is much further away from the coastline than the error model associated with the altimetric gravity model would suggest for reliability of the model. The distance of 50 km was therefore chosen as a trade off between reliability and good data coverage. Table 4.1 also indicates that there is a problem with the mean value of the data sets the mean difference between marine and satellite data being –5.7 mGal when the comparison is restricted to points more than 50 km from the coast.

Table 4.1. Comparison between marine and satellite gravity. Marine minus satellite as function of distance to coast [mGal]

Min.dist. to coast	No data*	Mean	Std. Dev.	Minimum	Maximum
0 km	5347	-3.6	26.8	-167.8	417.1
50 km	3162	-5.7	13.3	-67.0	64.7
100 km	1876	-8.3	9.8	-44.9	18.2
*) Comparisons include satellite data points less than 5 km from nearest marine data point					

The marine data refer to IGNS71 system according to the data provider (GETECH, 1995), so it is not likely to be due to some of the marine data referred to a wrong datum, e.g. the old Potsdam datum which is approximately 14 mGal to high.

The processing of the satellite altimetry data is based on the EGM96 geoid (Andersen and Knudsen, 1998), and possible deficiencies in the EGM96 geoid of wavelength longer than 200 km will not be improved from the altimetric observations. This may lead to long wavelength errors in the altimetry derived gravity field (Andersen and Knudsen, ibid).

Table 4.2. Free air anomalies statistics [mGal]

Data set	No data	Mean	Std. Dev.	Minimum	Maximum
Terrestrial	26483	54.0	48.3	-43.8	268.3
Marine	110973	5.8	60.3	-188.8	195.4
Satellite*	20415	-4.5	55.1	-177.8	171.9
*) Satellite data given on 3 arc minutes grid. Only data points more than 50 km from the coastline are included in this table					

It was decided to use all of the marine data and to use altimetric data located more than 50 km from the coast for the geoid processing. This means effectively that in areas with both altimetric and marine data most weight is given to the latter due to the relative high density of marine data in these areas.

4.2.2 The EGM96 reference field

The geopotential model EGM96 (Lemoine et al, 1998) is used to estimate the long wavelength components of the free air gravity field and the corresponding quasi-geoid in the remove/restore geoid computation scheme. The model is based on surface, marine, submarine, airborne and altimetric gravity data, satellite tracking data and digital elevation models. Statistics of the gravity data after removal of the geopotential model (EGM96) contribution up to degree 360 are given in Table 4.3.

Table 4.3. Residual free air residuals relative to EGM96 [mGal]

Data set	**No. data**	**Mean**	**Std. Dev.**	**Minimum**	**Maximum**
Terrestrial – EGM96	26483	3.4	25.0	-108.9	169.2
Marine – EGM96	110973	-5.6	21.1	-188.8	195.4
Satellite – EGM96	20415*	1.0	15.9	-60.4	89.7
*) Satellite data given on 3 arc minutes grid. Only data points more than 50 km from the coast line are included in this table					

Clearly, the residual anomaly field is smoother than the original (i.e., before the model removed). The standard deviation of the terrestrial gravity data for e.g improves by 23.3 mGal (see Table 4.2 and Table 4.3). However, the residual values

shown in Table 4.3 or in Figure 4.7 are still very large and the results of the local geoid analysis are likely to suffer inaccuracy as a result.

The significant positive and negative residual free-air anomalies shown in Figure 4.7 are related to the high topography in-land Jawa and the deep trench in Indian Ocean, south of Jawa. The local dynamic features of the gravity field are not present in the EGM96 model.

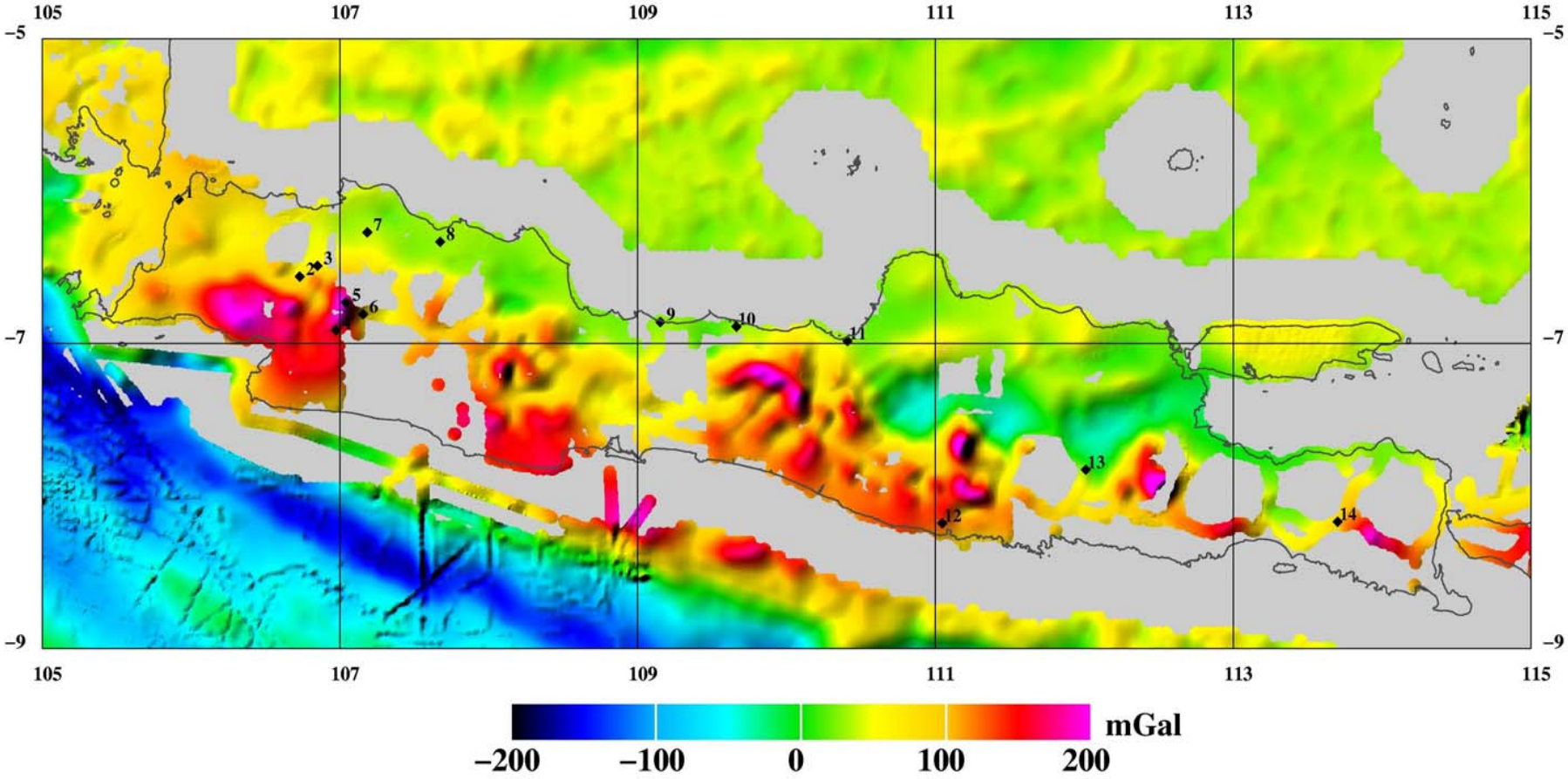

Figure 4.6. The combined terrestrial, marine and altemetric free air anomaly gravity field for the area of investigation. Discrepancies between the marine and the altimetric data show up very clearly in the southeast part of the area. Also shown are the GPS/levelling control points.

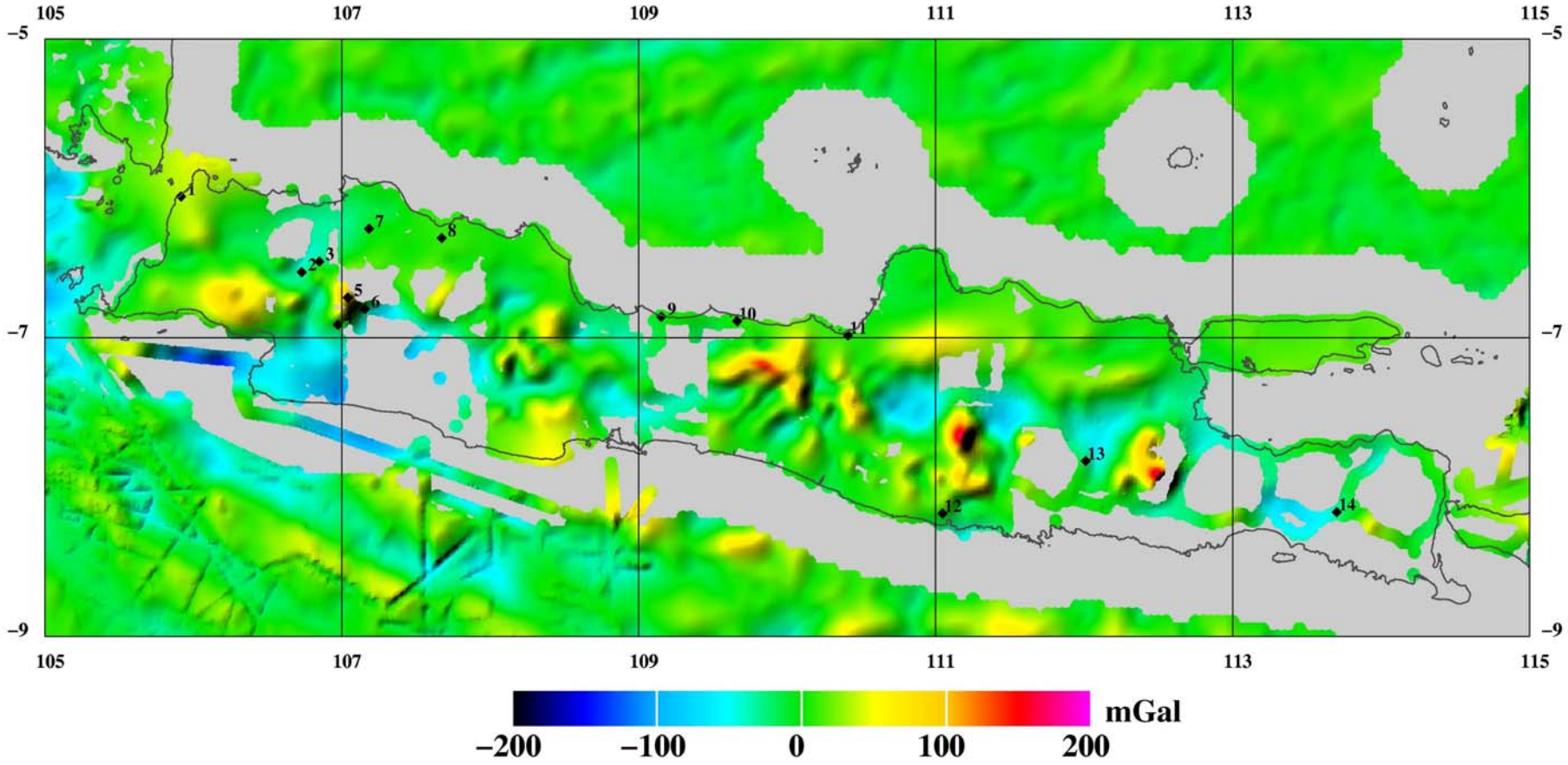

Figure 4.7. The combined terrestrial, marine and altemetric residual free air anomaly field for the area of investigation. Free air anomalies are subtracted the EGM96 reference field to degree 360.

4.2.3 Digital elevation models, DEM's

Due to the high degree of correlation between the gravity free air anomaly and topography, high resolution models of elevation or topography may be used to densify the existing gravity data. Two different elevation models were retrieved and tested for the geoid computations.

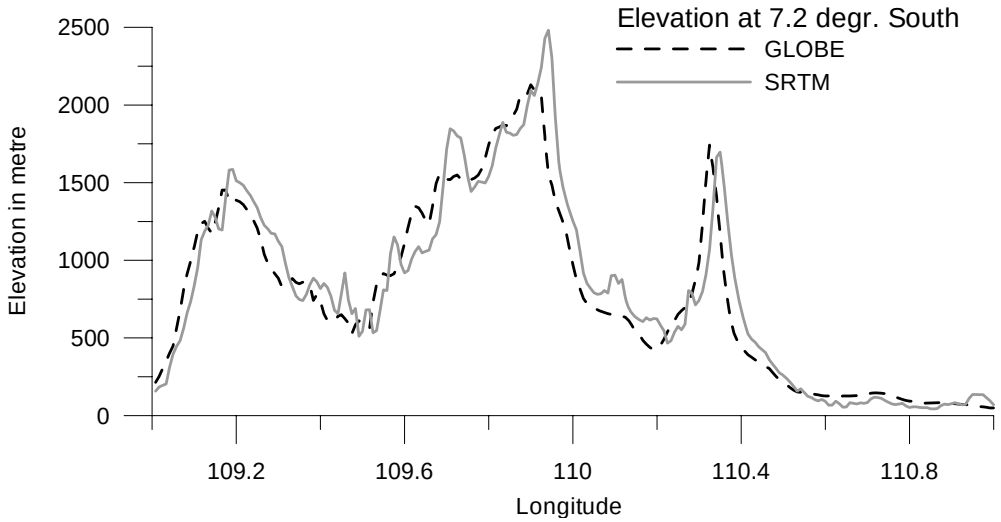

Figure 4.8. DEM results along one grid scan line at 7.2 degrees southern latitude.

The first is The Global Land One-km Base Elevation (GLOBE) model from the US National Oceanic and Atmospheric Administration (see GLOBE Task Team, 1999).

The other elevation model is the Shuttle Radar Topography Mission (SRTM) model from the US National Aeronautics and Space Administration (NASA). It is a preliminary 30 arc seconds model. The final 3 arc seconds model for the test area was not available during this test computation.

The DEM results from both models along one grid scan line over Java Island are shown in Figure 4.8. From this figure the SRTM model appears to be more detailed than in the GLOBE model. It also appears to be a lateral shift between the two models. Elevation comparisons are made at levelling control points. Statistics of the

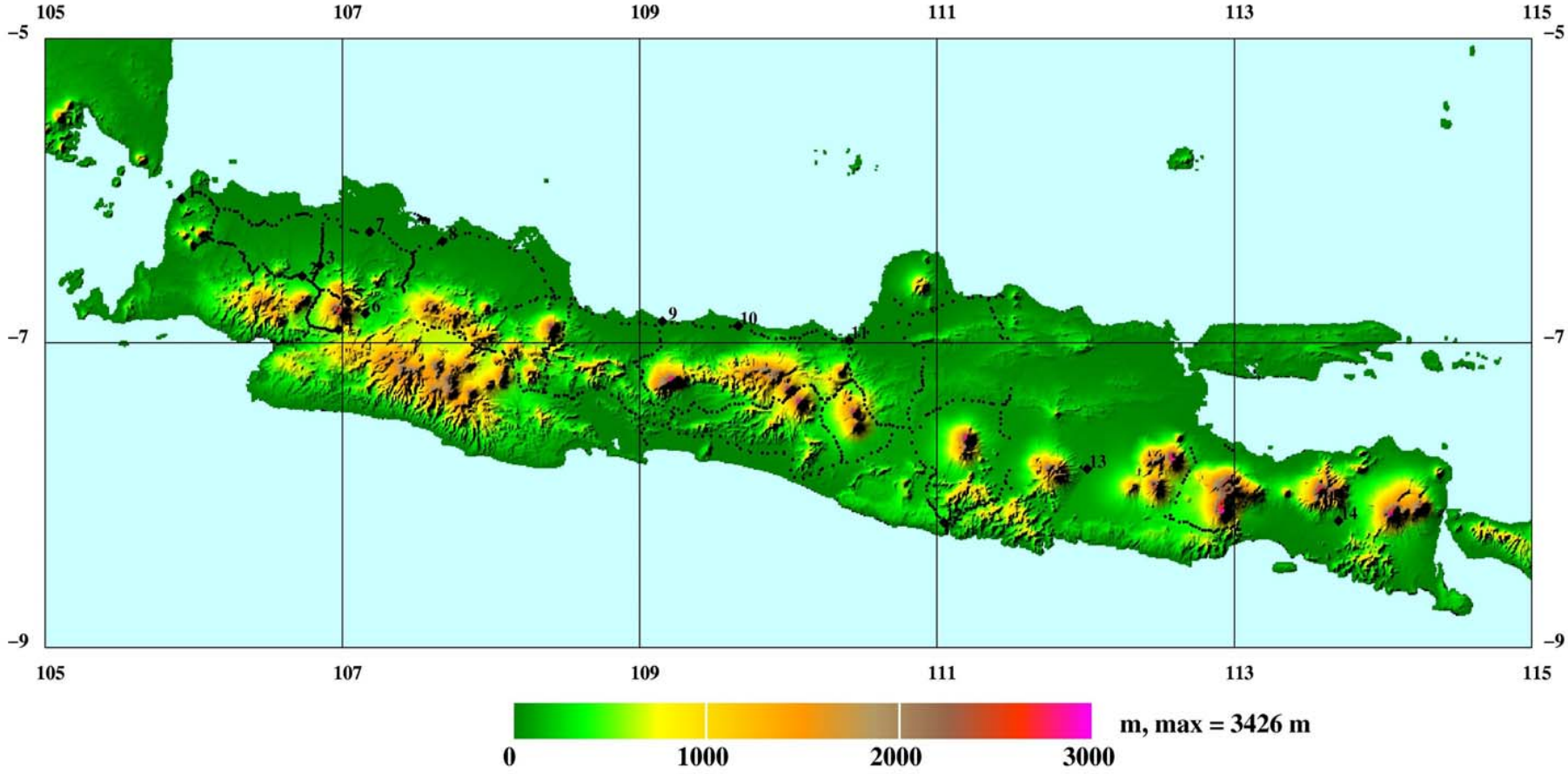

Figure 4.9. The SRTM DEM for Java Island. Also shown, as small dots, are the BAKOSURTANAL gravity points that have been levelled at the time when the gravity data were retrieved. The levelling has later on been extended to include all of the GPS/levelling control points (labelled diamonds).

two models and their comparison to levelling data is given in Table 4.4. Location of the levelling data is shown in Figure 4.9 and Figure 4.10 together with the SRTM model for Java.

Table 4.4. Statistics of the GLOBE and SRTM model over the area bounded by 10 to 4 southern latitude and 103 to 119 eastern longitude and comparisons to levelling data and gravity station heights. Unit is metre.

Data set	No. data	Mean	Std. Dev.	Minimum	Maximum
GLOBE	246736*	328.1	407.4	1	3690
SRTM	246736*	318.9	412.9	1	3426
Levelling heights	774	251.3	258.8	1.2	1386.9
Gravity station heights	26483	158.8	228.9	0	1603
SRTM – GLOBE	246736*	-1.7	35.3	-917	839
Levelling – GLOBE	774	-20.5	55.1	-329	151
Levelling – SRTM	774	-6.8	20.3	-141	87
Station height – GLOBE	26483	-14.7	108.4	-1990	637
Station height – SRTM	26483	-5.9	105.3	-2070	527
*) data given on 30 arc seconds grid. Only data points over land areas included.					

Table 4.4 shows that the SRTM model fits the levelling data much better than the GLOBE model, the mean and standard deviation of the difference between levelling data and DEM's being –6.8 m and 20.3 m range for the SRTM model compared to -20.5 m and 55.1 m for the GLOBE model. The difference between the models is less striking when compared to the gravity station heights for all the land gravity data. The standard deviations of the differences between gravity station heights and DEM's are 108.4 metre and 105.3 metres for the GLOBE and the SRTM respectively. This observation may be explained with noise in the gravity station heights, which to some extent will blur the difference in quality of the two DEM's.

Based on this comparison, it was decided to use the SRTM model for the geoid computations because of the better fit to the levelled heights. The discussion in the following is restricted to the SRTM digital elevation model.

If the levelling points are representative of the roughness of the landscape in areas

with gravity data then the fit of the levelling data to the DEM and the fit of gravity station heights to the DEM may be compared directly. The standard deviation of the levelled heights is 258.8 metre compared to 228.9 for the gravity stations. The poorer fit of the DEM to gravity stations than to levelling points cannot be explained by the gravity points located in a generally rougher terrain than the levelling points. Table 4.4 therefore indicates that the noise of the gravity station heights is at least at the 100 metres level and thereby much poorer than the DEM heights.

The formal error analysis is as follows. The combined noise of DEM and gravity station heights is 105.3 m. The noise on the levelling data can be neglected in this context so the comparison of levelling data with DEM gives an estimate of the noise on the DEM for the actual area and that is 20.3 metre. This leaves approximately 100 metres noise to be attributed to the gravity station heights if this noise is assumed uncorrelated with the noise in the DEM. I tested whether the bad fit between gravity station heights and DEM could be explained by a lateral offsets, but only small insignificant improvements in the fit could be achieved by minimising the misfit as a function of a shift in the two horizontal directions.

An error in the heights of gravity measurement will propagate into the computation of the free air anomaly, which means the free air anomalies could also be as noisy. Since the supplied data is only available as free air anomalies this may be a concern.

An alternative land gravity database was built by substituting the gravity station height with the height from the SRTM elevation model. The free air anomaly was corrected accordingly, i.e. 0.3086 mGal was added for each meter the height was increased. There will for certain be blunders in the DEM as well as in the station heights. So in order not to do more harm than good, only those points whose misfit between DEM and station height were less than twice the estimated noise were included, i.e. points where the difference between DEM and station heights were less than 200 metre.

Table 4.5 Comparison of the effect of topography on the original data set and on the 'improved'-height data set [mGal]

Data set	No. data	Mean	Std. Dev.	Minimum	Maximum
Original land data*	23917	49.8	45.8	-43.8	243.8
Effect of topography removed from do	23917	35.7	38.5	-56.5	184.9
Improved-height data set	23917	49.7	49.3	-65.8	289.2
Effect of topography removed from do	23917	35.6	41.3	-69.4	203.8
*) Only data points where the difference between DEM and station heights is less than 200 m are included in this table					

It is not possible to tell definitively which of the two datasets, the original one or the one with 'improved' heights, is the best, but the smoothness of the field after a reduction for terrain effects may give a lead. Table 4.5 shows that the original data set gives the smoothest gravity field after the effect of topography is removed and thus indicates that it may not be justifiable to replace the station heights with heights from the DEM.

4.3 Geoid computations in the Test area

Several local geoid models were computed using different methods of computations and incorporating the digital elevation model in the gridding step for the FFT approach. All grids produced are essential *Faye* anomaly grids. The simplest is just gridding of the *point residual Faye* anomalies without any information added from the DEM. The residual is relative to the EGM96 gravity model. Next method is gridding of point *residual Bouguer anomalies* with subsequent back substitution of the Bouguer correction term at the grid points. The last method is the *Reduced Terrain Model* approach, where only the shorter wavelengths of the topography are used in the removal of topographic gravity signals in the data before the gridding process. The topographic signal is then back substituted to give the final grid values.

Ring integration and collocation were performed on point residual Faye anomalies. For collocation, the data set was thinned to avoid excessively large equation systems to be solved in this approach. The thinning was done with the help of a grid in the following way: for grid cells containing data points the data point closest to the midpoint of the cell was chosen, and the rest of the data was discarded. This way the thinned data set still reflects the geometry of the original data set, see Figure 4.10. A grid specification of 0.1 times 0.1 degree was used for the terrestrial data, whereas offshore data were selected at a 0.2 times 0.2 degree spacing.

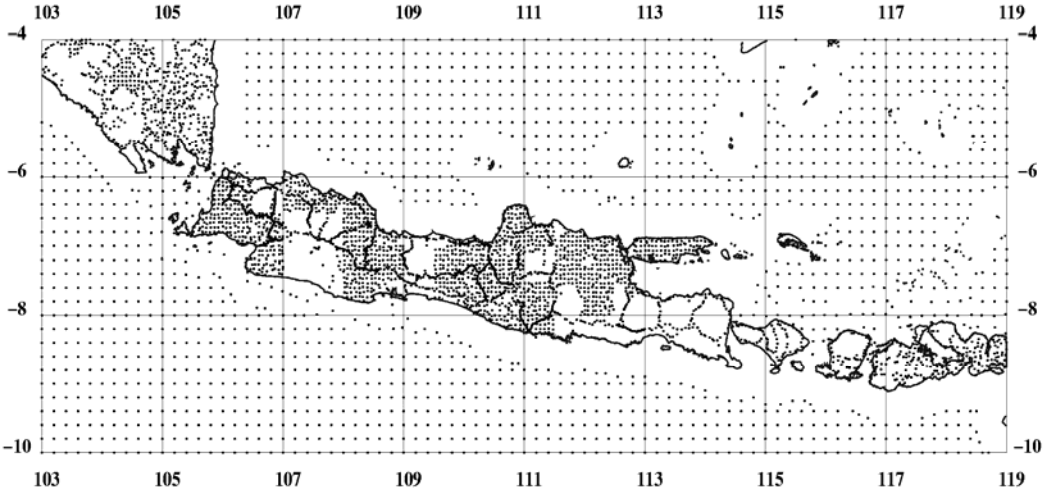

Figure 4.10. The thinned data set used for ring integration and collocation. The thinning was done with the help of a grid in the following way: for grid cells containing data points the data point closest to the midpoint of the cell was chosen the rest of the data was discarded. A grid specification of 0.1 times 0.1 degree was used for the terrestrial data, whereas offshore data were selected at a 0.2 times 0.2 degree spacing.

For the sake of the collocation method a noise of 3 mGal was assigned to the gravity data, apart from the Bakosurtanal data set measured at levelling points. These data were assigned a noise of 0.2 mGal. This thinned data set was used both for the collocation and the ring integration methods.

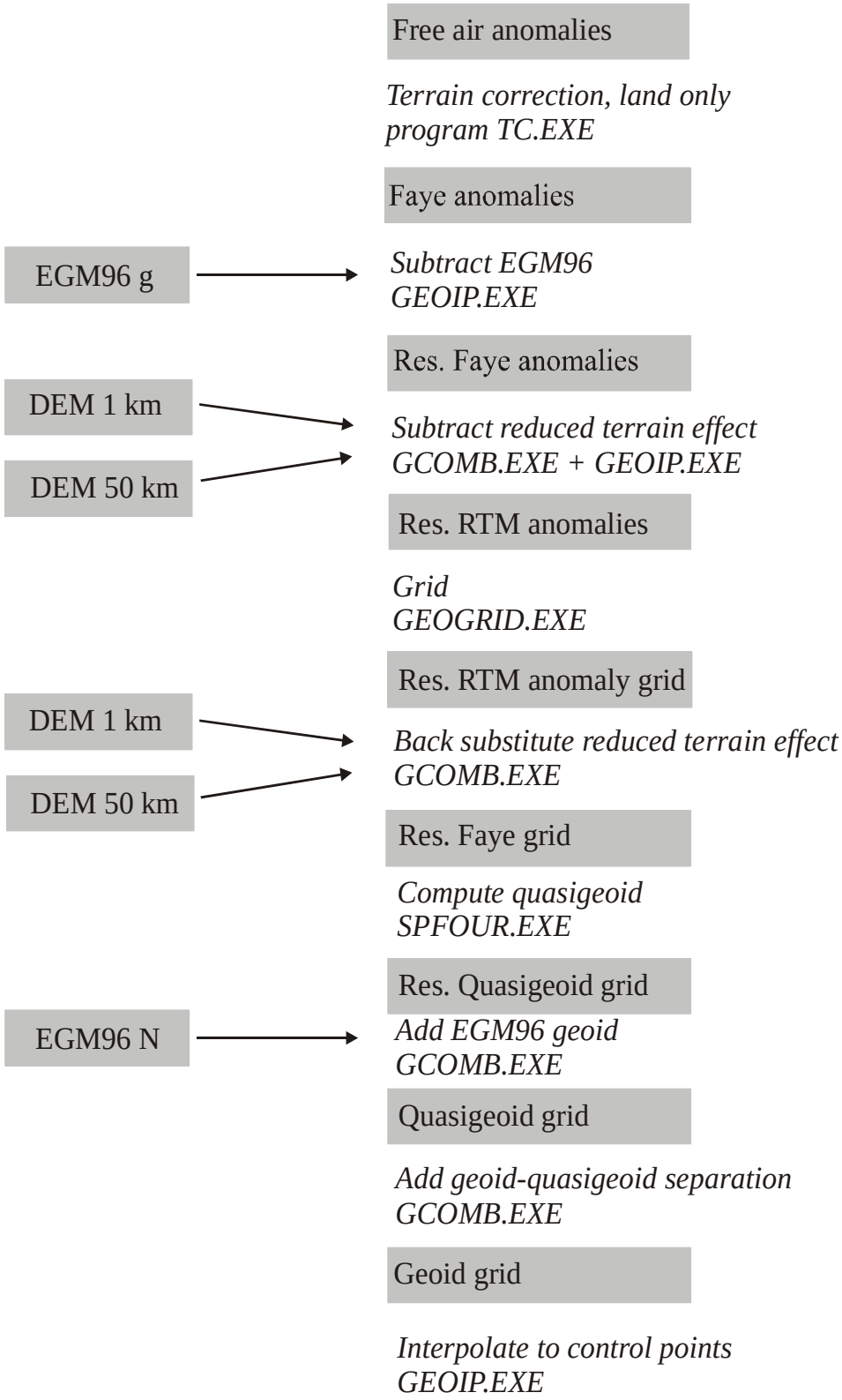

Figure 4.11. Data flow in the FFT approach with reduced terrain model reduction before gridding.

Table 4.6. Comparisons of gravimetric geoids with GPS/levelling results at control points. Figures are standard deviation of the misfit in metres.

Geoid	Points 1 to 14	Points 4 to 14	Points 4 to 11
EGM96	0.59	0.28	0.31
FFT360, grid Faye anomalies	0.45	0.20	0.14
FFT360, grid Bouguer anomalies	0.45	0.17	0.10
FFT360, grid RTM anomalies	0.45	0.19	0.11
FFT60, grid RTM anomalies	0.68	0.59	0.68
Ring integration to ring 1, Faye	0.42	0.14	0.11
Ring integration to ring 2, Faye	0.41	0.26	0.22
Ring integration to ring 3, Faye	0.48	0.35	0.33
Collocation, Faye	0.45	0.23	0.25

Comparison of the different gravimetric geoids to the geometric geoid at the control points is summarized in Table 4.6. The FFT method was applied with a Wong-Gore kernel modification to degree 60 (FFT60) and degree 360 (FFT360). The results for the two different kernel modifications on the same data set (the RTM gridded one) show that the low degree modification perform worse than the EGM96 model itself, with a 0.68 m standard deviation for the misfit in the control points compared to 0.59 m for EGM96. The higher degree modification (FFT360) fits better, 0.45 m standard deviation. These are the numbers when all the control points are included in the comparison. The difference becomes more striking if we exclude the three westernmost points in the comparison (see below), now the standard deviation of the misfit are 0.28 m, 0.59 m and 0.19 m for EGM96, FFT60 and FFT360 respectively. So it seems like including the lower degrees of Stokes' kernel degrade the longer wavelengths of the geoid. The results obtained with ring integration shows similar trend, i.e., the best fit is obtained with the smaller capsize.

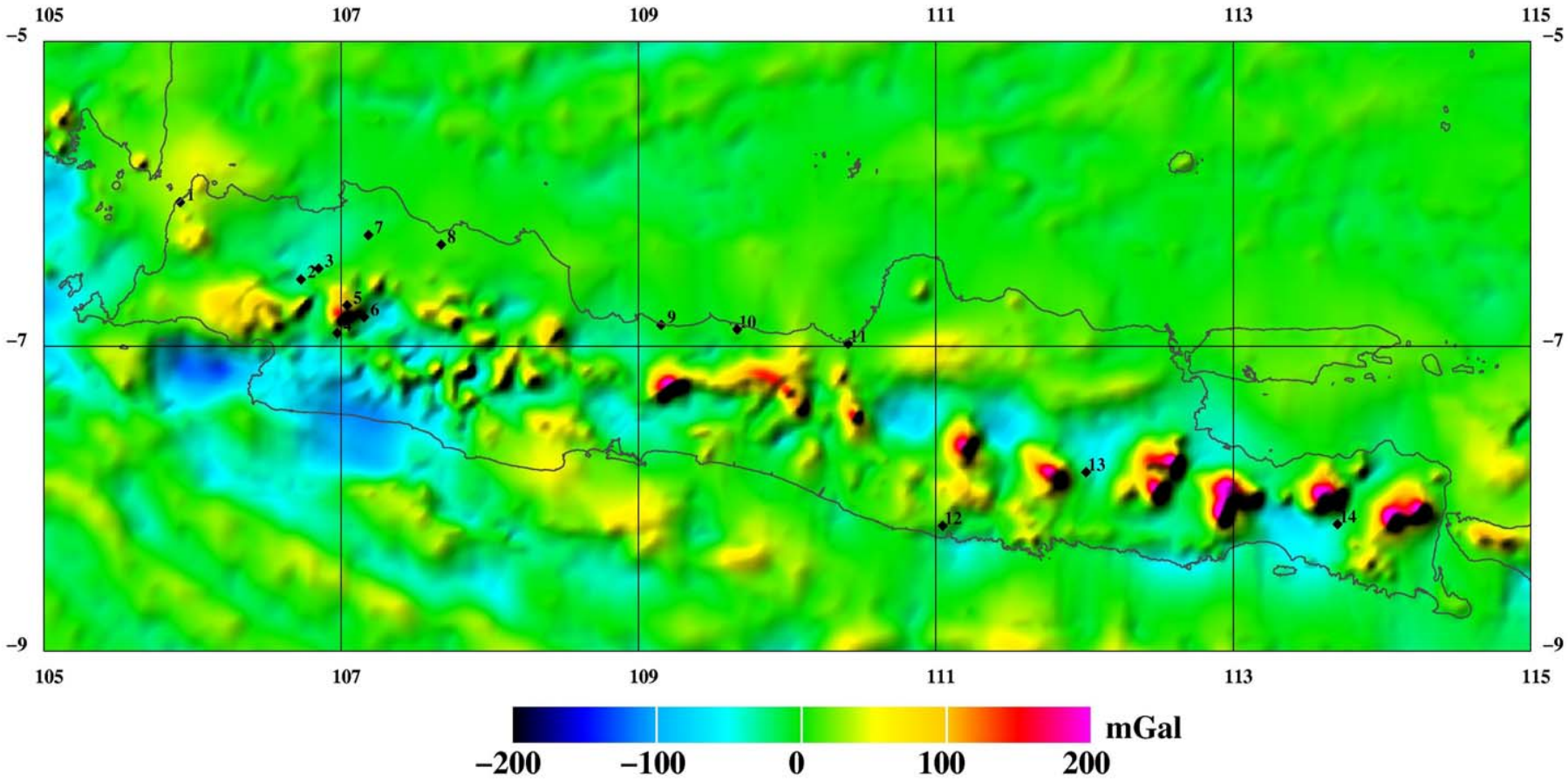

Figure 4.12 Residual free air anomalies after gridding of residual Bouguer anomalies and subsequently back substitution of Bouguer effect. This way details will be added to the gravity field in areas without gravity data. It is though an open question how well these pseudo-gravity anomalies derived from the DEM reflect the real gravity field. The marine tracks are now less visible as compared to figure 4.6 and 4.7 due to the smoothing inherent in the gridding process.

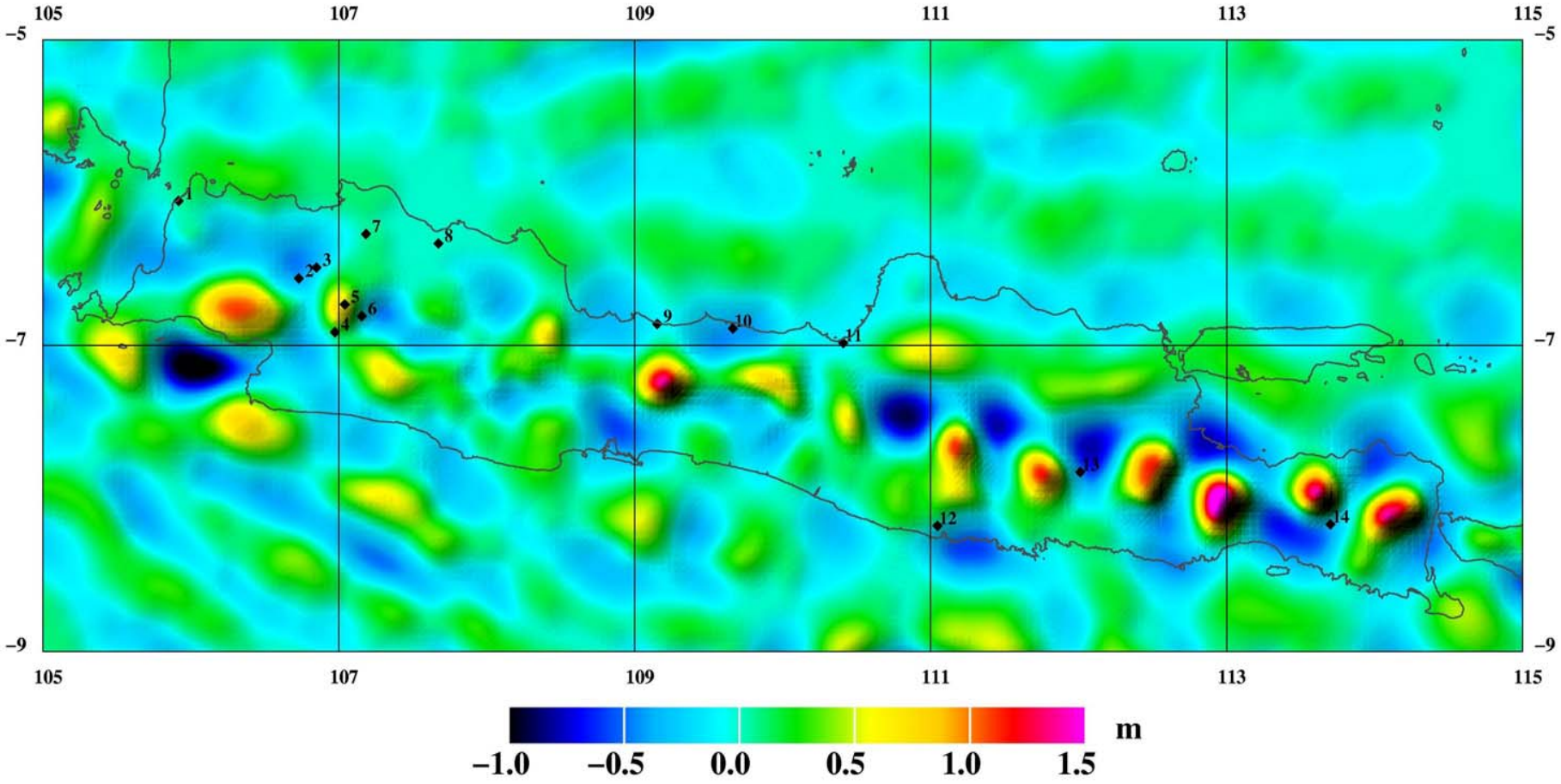

Figure 4.13 The residual geoid corresponding to the residual free air anomaly field of figure 4.13. The EGM96 geoid model to degree 360 is subsequently added to yield the geoid.

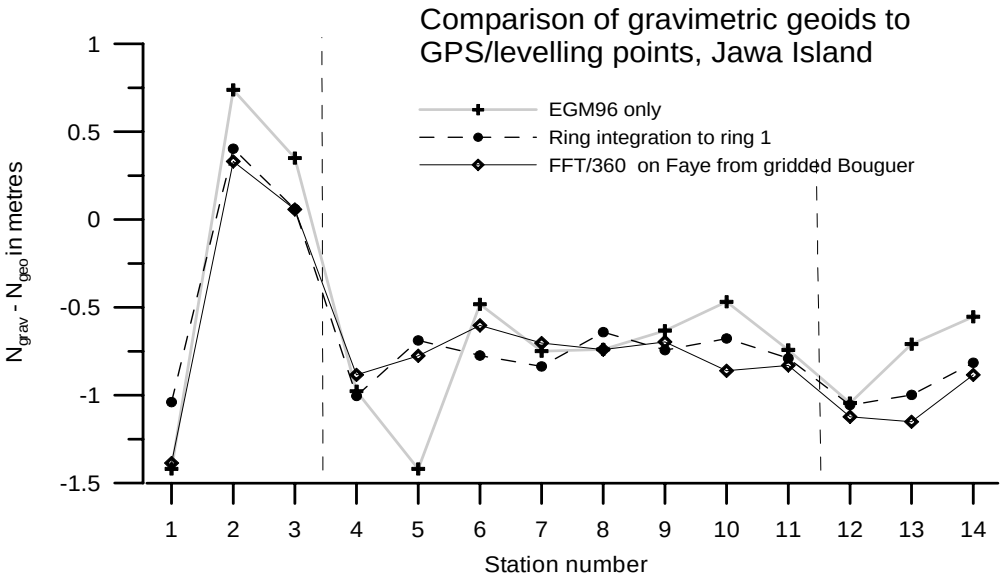

Figure 4.14. Misfit between gravimetric and geometric geoid at control points. X-axis is control point number. The control point number increases with longitude, but the points are not equidistant distributed, see also figure 4.13

Figure 4.14 shows that the three westernmost control points 1, 2 and 3 perform quite differently from the remaining points; control points 2 and 3 especially stand out. The two control points are located at rather low altitude, ranging from 17 to 200 metres see also Table 4.7, so the reason for the worse fit is not likely to be due to un-modelled topographic effects. It could of course be a problem with the geometric geoid, either in the levelling or in the GPS data. A third possible explanation could be the interpolation over areas with no gravity data. There is a data void close to control points number 2 and 3 just northwest of these, see Figure 4.7. If the real and unknown gravity field in this data void is considerable lower than the interpolated values then the computed gravimetric geoid will become too high in an area surrounding the void. It could explain the results for control points 2 and 3, since only these two control points have the data void within ring 1. The clearer picture we get when excluding these control points could also point in this direction. The argument to exclude the control points is not that we get a better fit, but that we get a more pronounced effect of e.g. changing the degree of kernel modification or of changing the capsize.

The three easternmost control points, number 12, 13 and 14, are believed to have been tied to a tide gauge on the south coast of the island, in contrast to the control

points numbered 4 through to 11, see e.g. Figure 4.13, so there is likely to be an offset in the levelling data between the set consisting of control points 4 to 11 and the set consisting of points 12 to 14. This is the reason also to include statistics only regarding the points 4 to 11 in Table 4.6.

There is no difference between the different gridding approaches at all control points, with 0.45 m misfit for each gridding of the Faye anomalies, the RTM reduced anomalies and also for when the gridding is performed on Bouguer anomalies. When restricting the misfit statistics to the control point numbered 4 through to 11, misfits become 0.14 m, 0.11 m and 0.10 m respectively. So, it appears that the inclusion of the DEM information in the gridding process improves the solution significantly. But there appears little difference as to which of the methods are used to perform the gridding, as either gridding on RTM reduced point anomalies or on bouguer point anomalies give similar results.

The misfit for the control points 4 to 11 indicates that the best fitting geoids are accurate at the 10 cm level. It should be noted that the control points 4 to 11 also include high altitude points in a mountainous terrain, the highest control point being located at 1075 meter elevation (see Table 4.7).

Table 4.7. Comparisons of geoid undulations at GPS/levelling points, unit is metre. The FFT gravimetric geoid is based on Faye anomalies derived from Bouguer anomalies.

Control point number	Lat.	Lon.	Levelled height (m)	Ellipsoid height (m)	Geom. geoid undul.	EGM96 geoid undul.	EGM96 geoid misfit	FFT geoid undul.	FFT geoid misfit
1	-6.0550	105.9174	16.979	1.681	15.298	13.879	-1.419	13.912	-1.386
2	-6.5610	106.7301	201.326	183.447	17.879	18.617	0.738	18.210	0.331
3	-6.4909	106.8500	156.834	138.180	18.654	19.004	0.350	18.712	0.058
4	-6.9143	106.9741	703.450	681.946	21.504	20.527	-0.977	20.620	-0.884
5	-6.7315	107.0412	1074.975	1053.328	21.647	20.228	-1.419	20.872	-0.775
6	-6.8085	107.1559	426.769	405.493	21.276	20.794	-0.482	20.674	-0.602
7	-6.2705	107.1838	33.700	13.675	20.025	19.276	-0.749	19.322	-0.703
8	-6.3333	107.6733	31.444	10.732	20.712	19.973	-0.739	19.972	-0.740
9	-6.8598	109.1531	27.375	4.031	23.344	22.712	-0.632	22.648	-0.696
10	-6.8894	109.6639	27.857	3.602	24.255	23.787	-0.468	23.394	-0.861
11	-6.9838	110.4095	30.605	4.563	26.042	25.300	-0.742	25.212	-0.830
12	-8.1776	111.0454	410.682	384.273	26.409	25.365	-1.044	25.287	-1.122
13	-7.8269	112.0106	93.923	66.129	27.794	27.085	-0.709	26.643	-1.151
14	-8.1682	113.7017	119.008	85.579	33.429	32.876	-0.553	32.545	-0.884

The baseline errors are given in Table 4.8 for both the EGM96 and the best fitting refined geoid, FFT360 used in combination with gridding of Bouguer anomalies. The results for the ring integration geoid are very similar. There are some quite big values in the table with baseline errors up to 1.77 metre for baselines as short as 34 km. These large values involve the more dubious control points 1 to 3. These big values blur the picture and one conclusion is clear from the table: it is mainly the shorter baselines that benefit from the geoid modelling done here. There are 22 baselines shorter than 100 km and the refined geoid performs better than the EGM96 for 20 (91 %) of these with one baseline degraded and one unchanged. For baselines longer than 100 km only 44 out of 69 (64 %) improved.

Table 4.8 Independent baseline errors in metres

Stat.	2	3	4	5	6	7	8	9	10	11	12	13	14
1	106 2.16 1.72	114 1.77 1.44	151 0.44 0.50	145 0.0 0.61	160 0.94 0.78	142 0.67 0.67	196 0.68 0.65	368 0.79 0.69	423 0.95 0.53	506 0.68 0.53	612 0.38 0.26	700 0.71 0.24	889 0.87 0.50
2		15 0.39 0.27	48 1.71 1.22	39 2.16 1.11	54 1.22 0.93	60 1.49 1.03	107 1.48 1.07	269 1.37 1.03	325 1.21 1.19	408 1.48 1.16	508 1.78 1.45	598 1.45 1.48	788 1.29 1.22
3			49 1.33 0.94	34 1.77 0.83	49 0.83 0.66	44 1.10 0.76	92 1.09 0.80	257 0.98 0.75	313 0.82 0.92	396 1.09 0.89	498 1.39 1.18	587 1.06 1.21	777 0.90 0.94
4				22 0.44 0.11	23 0.50 0.28	75 0.23 0.18	101 0.24 0.14	240 0.34 0.19	296 0.51 0.02	379 0.24 0.05	469 0.07 0.24	564 0.27 0.27	753 0.42 0.00
5					15 0.94 0.17	54 0.67 0.07	83 0.68 0.03	233 0.79 0.08	290 0.95 0.09	372 0.68 0.06	469 0.38 0.35	561 0.71 0.38	750 0.87 0.11
6						60 0.27 0.10	78 0.26 0.14	220 0.15 0.09	277 0.01 0.26	359 0.26 0.23	454 0.56 0.52	546 0.23 0.55	736 0.07 0.28
7							54 0.01 0.04	227 0.12 0.01	282 0.28 0.16	364 0.01 0.13	475 0.30 0.42	559 0.04 0.45	748 0.20 0.18
8								173 0.11 0.04	228 0.27 0.12	310 0.00 0.09	424 0.31 0.38	506 0.03 0.41	694 0.19 0.14
9									56 0.16 0.17	139 0.11 0.13	254 0.41 0.43	332 0.08 0.46	521 0.08 0.19
10										83 0.27 0.03	209 0.58 0.26	279 0.24 0.29	466 0.08 0.02
11											150 0.30 0.29	200 0.03 0.32	385 0.19 0.05
12												113 0.34 0.03	292 0.49 0.24
13													190 0.16 0.27

The 3 figures in each cell are baseline length in kilometers, EGM96 geoid misfit and FFT refined geoid misfit respectively. The FFT geoid is based on Faye anomalies derived from gridded Bouguer anomalies. Unit is metres.

The results for baselines between what is considered the most reliable control points, namely the points 4 to 11, are depicted in figure 4.15. It is seen that the refined geoid makes a much better fit than the EGM96 geoid, giving a mean error of 0.11 meter compared to 0.34 meter. A linear regression on the result for the refined geoid shows that there is hardly any correlation between baseline length and baseline error.

Both the relative improvement compared to EGM96 and the absolute numbers are quite encouraging taking into account the rather big data voids in the area. With an improved data coverage it should be possible to produce a geoid that is considerable better than 10 cm standard deviation.

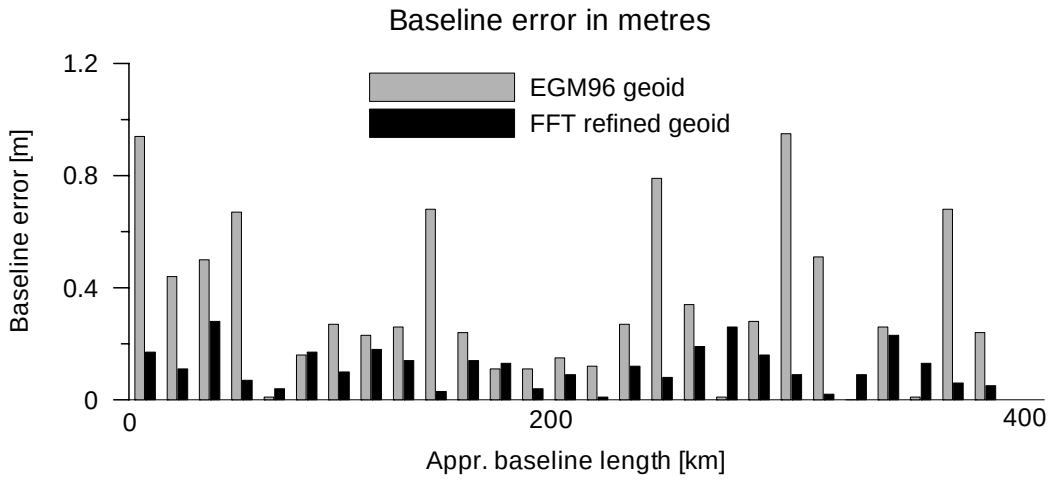

Figure 4.15 Baseline error for EGM96 and FFT gravimetric geoids as function of baseline length. Only baselines between the points 4 through to 11 are included. The mean value of the error is 0.34 m and 0.11 m for EGM96 and the FFT geoid respectively.

CHAPTER 5

ERROR PROPAGATION STUDY

This chapter is devoted to a study of the error propagation from gravity to geoid for two different scenarios. The first scenario is the existing gravity data coverage and the second scenario is a simulation of a possible future situation with airborne data covering some of the main data voids in the area. The area is shifted somewhat compared to the geoid test computation area carried out in Chapter 4. This is done in order to cover also less mountainous areas of Southeastern Sumatra, as compared to Jawa Island.

5.1 'Planar-attenuated logarithmic' covariance model

The programs GPFIT and GPCOL from the GRAVSOFT packages were used for the error propagation study. The programs feature a planar covariance function (see

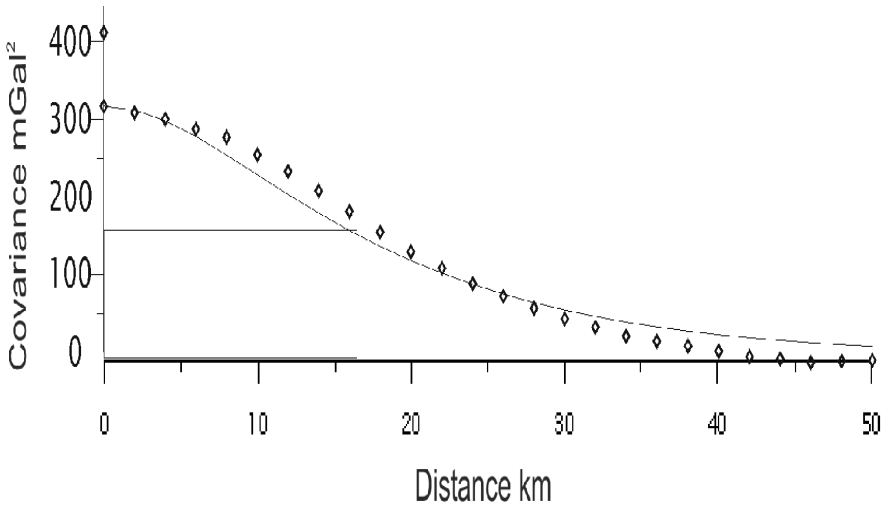

Figure 5.1 The empirical (diamonds) and the analytical covariance function. The functions are based on 21,143 gravity observations with a mean of 0.0 mGal and a covariance of 311 mGal^2. Estimated best fit parameters: D = 10 km and T = 25 km. Correlation length as derived from graph is 17 km.

Forsberg, 1987), which can be viewed as a flat earth approximation of the well - known Tscherning-Rapp spherical covariance model (Tscherning and Rapp, 1974).

This planar logarithmic covariance function is described by three parameters, the variance, C_0, and two depth parameters, D and T. The parameter D corresponds to the double Bjerhammer depth and T is a so-called compensation depth, which makes up for the inherent low frequency singularity of the planar logarithmic model.

The actual model is, for this reason, also called the 'planar-attenuated logarithmic' covariance model (see Forsberg, 1987). The reason to use the GPFIT/GPCOL programs instead of the GEOCOL program of Chapter 4 is because of the improved computational speed they offer. This advantage in speed is partly due to the simpler expressions of the planar covariance functions as compared to the spherical models – a modification which does not significantly affect the error estimates being sought.

5.2 The empirical covariance function and the actual error analysis

Figure 5.1 shows the empirical covariance function and a planar analytical approximation. The variance of the gravity field is 311 $mGal^2$, which is somewhat lower than the approximately 800 $mGal^2$ variance seen in Figure 4.3. This difference in variance is partly due to the more benign gravity field of Southeastern Sumatra as compared to the more mountainous Jawa Island and partly due to the fact that the data set used to compute the covariance in Chapter 4 has a mean value of 3.4 mGal. The mean was not removed before computing the covariance function. This will increase the computed covariance and variance (C_0) somewhat. In contrast, the data set used for the error analysis in *this* chapter has a mean value of (effectively) 0 mGal.

The optimal prediction (formulae 4.18) is not very sensitive towards the actual value of the variance (C_0) but *more dependent on how the covariance decays with distance*. This is not true for the error estimate where the result is very much dependent on the variance, see formulae 4.19. Thus, for the error analysis it is

important to consider the adopted value of the variance (C_0) together with the shape of the covariance function, in this case given by the two depth parameters. The covariance function computations were based on terrestrial free air anomalies reduced for the EGM96 reference model to degree 360. If altimetric gravity data were included in the data set used to compute the covariance function the variance would be even lower due to the more benign off-shore gravity field. The resulting error estimates would therefore also become smaller.

Apart from the variance (C_0) and the shape of the covariance function the decisive factors in the error analysis are the geometry of the gravity data coverage and the noise assigned to the gravity data. Figure 5.2 below shows the terrestrial data coverage and the altimetric gravity data when clipped at 50 km from the coastline because it was seen in Chapter 4 that the altimetric gravity data close to the coast

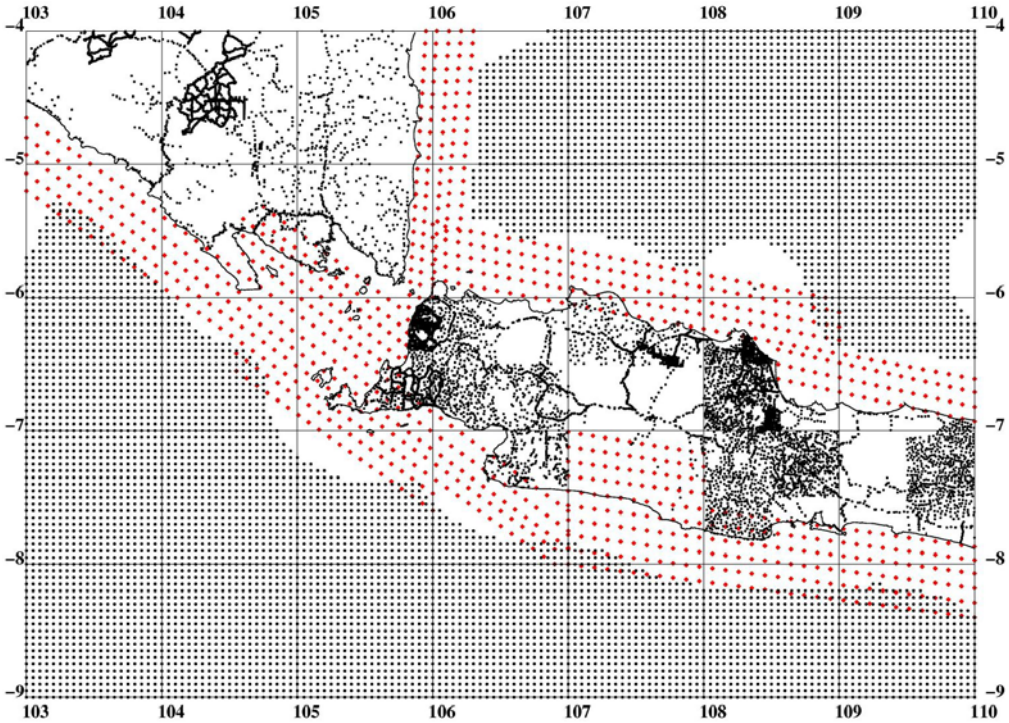

Figure 5.2. Existing gravity data coverage shown as black dots. The altimetric gravity field has been clipped at approximately 50 km from the coastline, see also the discussion in chapter 4. Shown as red dots is a possible airborne gravity coverage at 10 km line spacing. All data were assigned a 2 mGal noise in the error study.

were not reliable. A 50 km distance from the coast may even in some cases be too little in order to ensure a reliable altimetric gravity field. Marine data has not been included in this error study since there is only rather limited coverage and the accuracy of the existing marine data is not well known. As it was shown in Chapter 4 there seems to be a bias problem with some of the marine data. The inclusion of marine data will of course lower the estimated error in some areas. This is especially true for the Sunda Strait, the strait between Jawa and Sumatra Islands, where there are quite a large marine data set. The question is though, how much we should rely on these data and what noise level we should assign to them. A noise level of 2 mGal was assigned to both the altimetric and the terrestrial data, as this accords to both our theoretical expectations and the results of earlier experience.

Only gravity data observations inside the plotted area have been included in the computations, so results near the edge will be greatly influenced by the lack of data outside the plotted area, here referred to as the edge effect. Conclusions should therefore only be drawn for points well (i. e., ~ 110 km) inside the plotted area. The inner frame seen in the plots in Figures 5.3 and 5.4 indicate from where the results should be given significance.

In addition to the gravity data also one geoid observation is assumed known. The geoid observation is located at Bakosurtanal and assigned zero noise. The location is not specifically shown in the plots 5.2, 5.3 and 5.4, but can be identified as point number 3 in Figure 4.4 (see Chapter 4). This way the error study simulates the situation where a datum has been defined or the geoid model has been fitted to one known point. The estimated error field for the situation where only terrestrial and altimetric gravity data are included is shown in Figure 5.3. The upper panel shows the situation when the altimetric data is trusted for all off shore areas. The lower panel of figure 5.3 shows the error field when altimetric data has been clipped at 50 km from the coastline. The clipping of altimetric data to 50 km from the coast has not surprisingly a big impact on the error field near the coast. The estimated error increases in general from around 20 cm to 40 cm in the near coastal region when altimetric data closer than 50 km from the coast is excluded. An exception is near the

major data void in southern part of Jawa between Eastern longitude 107° and 108° where the geoid error field takes considerable higher values. It should be emphasized again that the altimetric data should ***not*** be relied on close to the coast. The data situation depicted in Figure 5.2 with a 50 km distance to the coast is the basis for the further investigations in this chapter.

Figure 5.4 shows the situation when the 50 km near coastal zone and the major terrestrial data void is covered with airborne data. The upper panel in figure 5.4 shows the resulting error field when a 20 km airborne track spacing is assumed, the lower plot corresponds to a 10 km airborne track spacing like the data distribution in figure 5.2. The inclusion of the coarse airborne gravity survey reduces the geoid error estimates to around 20 cm for the central parts of the area. Making the airborne coverage denser gives further improvement; the geoid error estimates now reduce to around 15 cm for the central parts of the area.

There are of course a lot of open questions in such an error study. For example: is the noise assigned to the gravity data reasonable; are there systematic effects like gravity datum problems not accounted for; is the 50 km coastal clipping zone too narrow or too wide? So the absolute estimated values of the geoid error field should be taken with some reservations. On the other hand the estimated geoid error field seems not to be too over-optimistic when comparing to the results of Chapter 4. Table 4.6 indicated a combined GPS/leveling and geoid error somewhere between 10 to 20 cm for the best performing geoid models (see also the discussion in Chapter 4 related to Table 4.6).

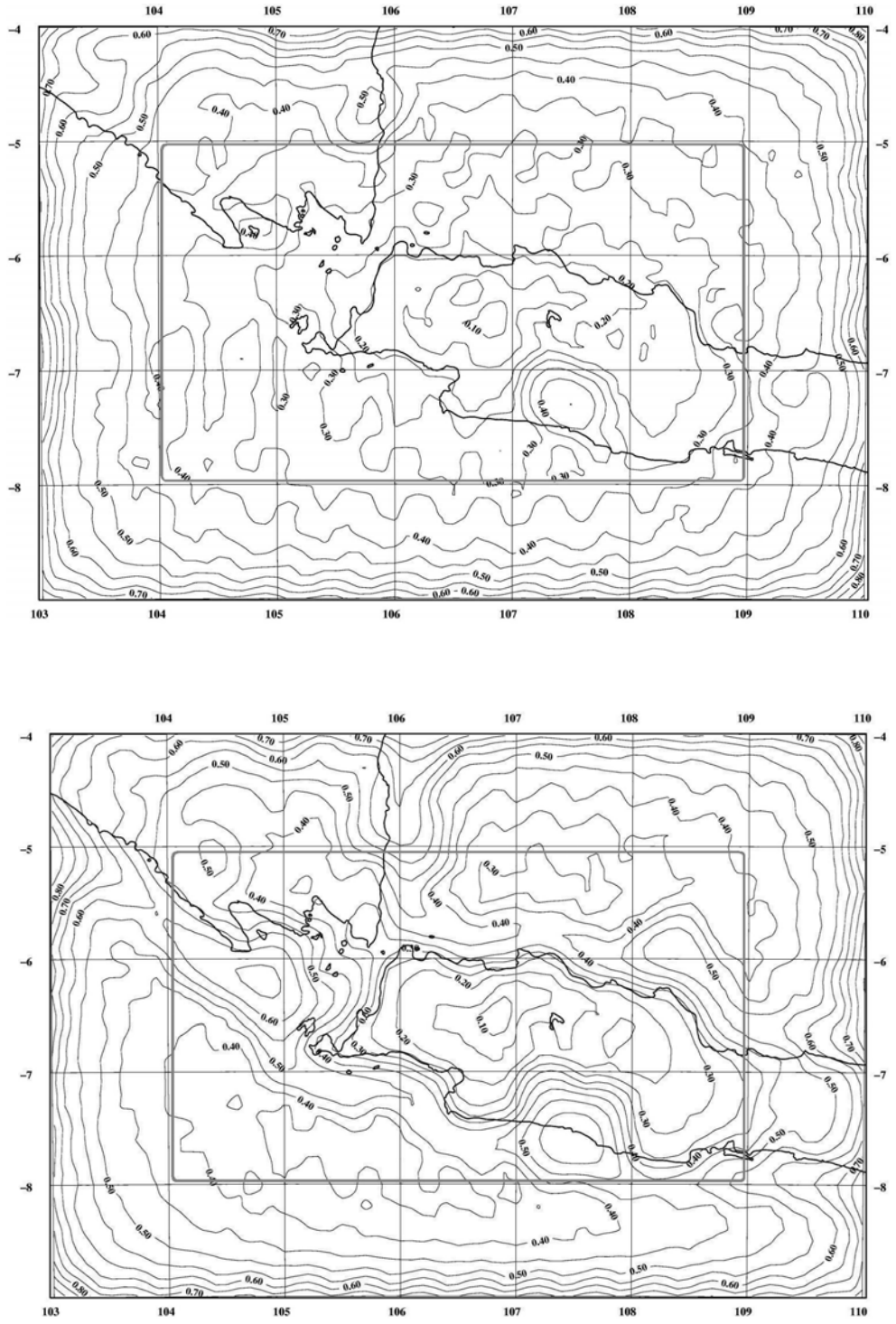

Figure. 5.3. Error propagation with terrestrial and altimetric data only. Top plot shows results with altimetric data clipped at the coastline. Altimetric data are clipped at a distance of 50 km from the coastline in the lower plot.

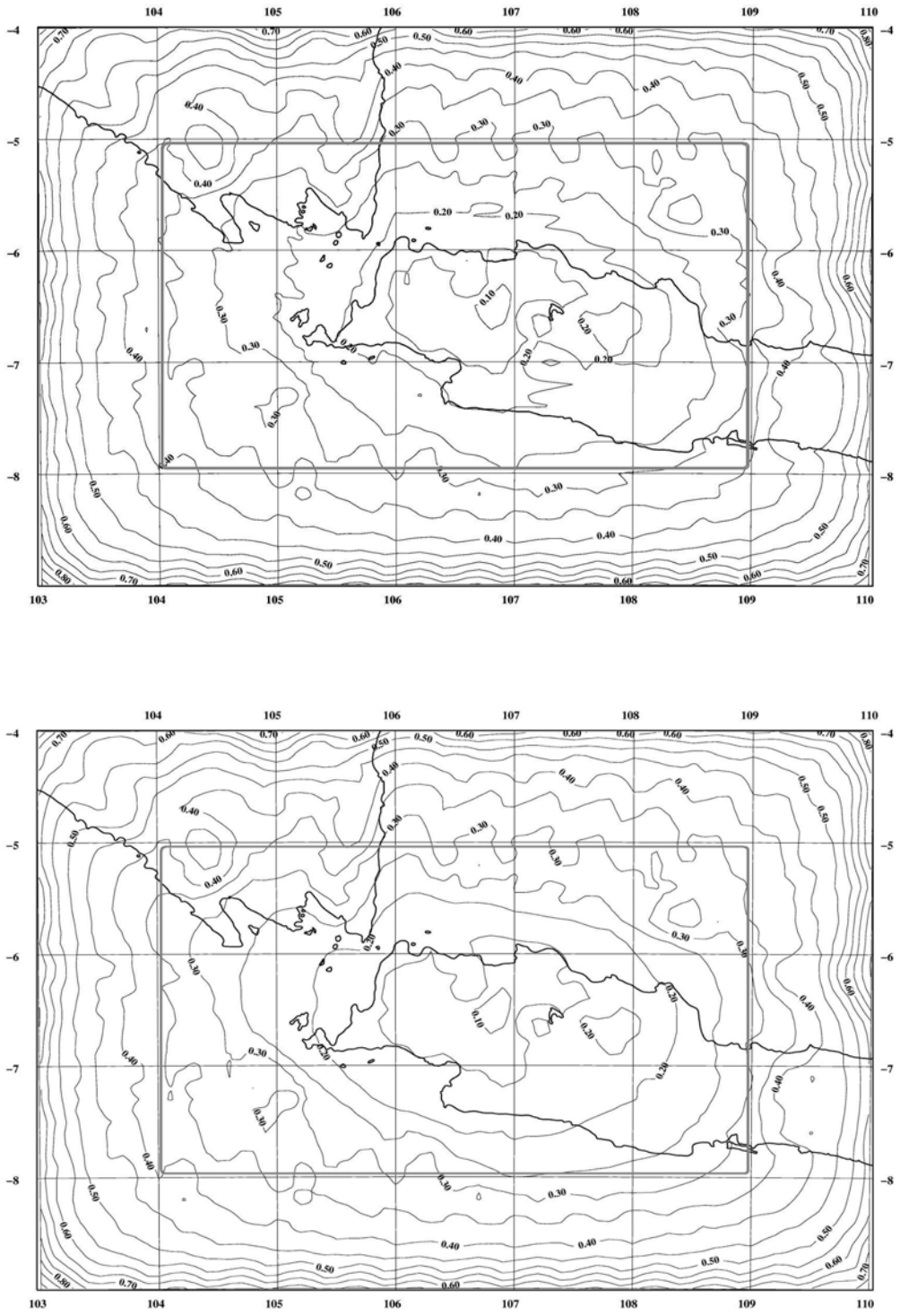

Figure 5.4 Error propagation with airborne fill-in data. Both plots have the altimetric data clipped at 50 km from the coastline. Upper plot with an airborne track spacing of 20 km, lower plot with a track spacing of 10 km as shown in Figure 5.2

CHAPTER 6

GEOID IMPROVEMENT BY SPACEBORNE DATA

Up to the present time, the Indonesian regional gravimetric geoid has suffered from the inaccuracy and poor coverage of the gravity data (see Kahar et.al, 1996 and Kasenda & Kearsley, 2002). The INDGED02 regional geoid (see Section 3.1.3) is computed from surface gravity dataset (namely INDGRAV database) which is formed in 5' grid gravity anomalies. This is the only gravity database available that extends for the whole country and is part of the SEAGP (South East Asia Gravity Project) database compiled from inhomogeneous land and marine measurements combined with gravity anomalies derived from satellite altimetry over ocean (see again Section 3.2.1). Consequently, the accuracy and reliability of the dataset to perform regional precise geoid computations for this region is dubious.

With the advent of new global geopotential models based upon satellites launched specifically for gravity field studies, the situation of the regional gravity field in this area should improve significantly, especially in the long to medium wavelengths. The first satellite dedicated to measure the earth's gravity field is CHAMP (CHAllenging Minisatellite Payload), launched in July 2000 (see website: www.gfz-potsdam.de). CHAMP will also map the earth's magnetic field and the choice of orbit is a tradeoff between lifetime, magnetic and gravity considerations. The starting orbit altitude is 454 km. The measurement principle is a combination of a 3-axis accelerometer and GPS. The satellites active lifetime is planned for 5 years.

The second mission is GRACE (Gravity Recovery And Climate Experiment), which was launched in March 2002. GRACE is a tandem mission consisting of two almost identical satellites sharing the same orbit but separated 220 km along the flight path. A very precise microwave ranging system tracks the distance between the two satellites. This highly precise tracking system in combination with accelerometers and GPS positioning constitutes the gravity measuring system. The starting altitude for GRACE is 500 km (see also website: www.csr.utexas.edu/grace/). The duration of the

GRACE mission is stated to be five years. The emphasis in the design of GRACE was put on the recovery of temporal variations in the gravity field more than on a high spatial resolution.

Figure 6.1 The GOCE gradiometer consist of 3 pairs of accelerometers mounted in a 3 axis configuration. Each accelerometer pair is separated by a distance of 50 cm. The measurement accuracy of each accelerometer is about 10^{-12} ms^{-2} or 1 part in 10,000,000,000,000 of the earth's gravity field (Illustration from www.esa.int/esaLP

GRACE is able to map gravity variations on a monthly scale and thus be able to track masses moving around on the earth's surface and in its interior with a high temporal resolution. It was hoped that the mission will yield new insight into dynamics of the earth's interior, processes involving ice sheets and glaciers and processes involving ground water.

A third dedicated gravity mission is GOCE (Gravity Field and Steady-State Ocean Circulation Explorer). GOCE is launched recently (March 2009) after been scheduled for launched in late 2007. Over its life of about 20 months, GOCE will map the variation of the gravity field at the highest possible spatial resolution.

The ultimate goal is to map the gravity field with a 1 mGal accuracy at 100 km resolution. The geoid should be determined with an accuracy of 1 to 2 cm at the same resolution. To achieve such a high resolution the starting altitude is as low as 250 km. Due to the harsh environment at low orbit the planned lifetime of the satellite is only 20 months. There will be two active mission periods of 6 months each with a hibernation period in between. The main instrument is a 3-axis gravity gradiometer, which measures gravity variations over a distance of 50 cm with an accuracy of 3 mE (milliEotvos, 10^{-12} s^{-2}), see also Figure 6.1.

The mission will in combination with satellite altimetry allow an accurate global mapping of ocean dynamic topography and hence of ocean currents. The GOCE mission is the first of a series of missions in the European Space Agency's Living Planet Program (see also *www.esa.int/esaLP/LPGoce.html*).

With the purpose of testing these expected improvements in the gravity data situation as well as geoid models for Indonesian region, I analyzed the gravity features and the gravimetric geoid from the newly released global coefficient potential models derived from the gravimetric satellites CHAMP and GRACE.

6.1 The gravity anomalies from Satellite Gravimetry

The gravity anomalies are computed from geopotential coefficients models from CHAMP and GRACE satellites by using the formula given in Heiskanen and Moritz, (1967) and rewriting the equation (4.10) as,

$$\Delta g(\theta,\lambda) = \gamma \sum_{l=2}^{L} (l-1) \sum_{m=0}^{l} \mathrm{P}_{lm}(\sin\theta)\left[C_{lm}\cos m\lambda + S_{lm}\sin m\lambda\right] \tag{6.1}$$

where γ is the mean gravity, C_{lm} and S_{lm} are the series of the geopotential coefficients models and P_{lm} is the Legendre function of degree l and order m.

6.1.1 The Free-air anomaly from CHAMP

The preliminary geopotential coefficients model C_{lm} and S_{lm} derived from CHAMP satellite gravimetry called EIGEN-2b was used to calculate the free-air gravity anomaly for the Indonesian region. The calculation was carried out at grid intervals of 6' using formula (6.1). The spherical harmonics expansion was taken up to degree and order 120. Despite the low and high anomalies shown around Banda Sea and north of Sulawesi (see Figure 6.2a top), the anomaly features in general appear less dynamic than would be expected from a medium wavelength model whose formal resolution is about 3 degrees. The magnitude varies from approximately -80 mGal around Banda Sea to about +90 mGal north of Sulawesi.

The EIGEN-2b geopotential model is derived from CHAMP GPS satellite-to-satellite and accelerometer data over only the period of six months measured in 2000 and 2001. Even though higher-degree/order terms are solved in EIGEN-2b, the preliminary solution has full power only up to about degree/order 40 due to signal attenuation at the satellite's altitude.

6.1.2 The Free-air anomaly from GRACE

The first GRACE product was made available to the public in July 2003. The geopotential coefficients model is presented in two forms namely the GGM01S and the GGM01C. The GGM01S model is the satellite only solution estimated from 111 days of K-band range-rate, attitude and accelerometer data collected from April to November 2002. The model was provided up to degree and order 120. The GGM01C model, on the other hand, was estimated based on the GGM01S in combination with the TEG4 model, incorporating other satellite information (multi-tracking data), surface gravity data and altimetric sea surface heights. This model was provided up to degree and order 200.

The second GRACE gravity model (GGM02) was released in October 2004 and is available in two forms namely the GGM02S and the GGM02C. The model is based on the analysis of 363 days of GRACE in-flight data, spread between April 4, 2002 and Dec 31, 2003. The GGM02S coefficients model is purely derived from satellite data and was provided up to harmonics degree 160, while the GGM02C model was constrained with terrestrial gravity information and was provided up to degree 200.

In order to examine the improvement by using the satellite gravimetry data only, the free-air anomalies were computed from both the GGM01S and the GGM02S models applying formula (6.1) up to degree 120. Compared to the free-air gravity anomaly features computed from the Eigen-2b model, the anomaly features computed from the GRACE models show a more disturbed gravity field (see Figure 6.2a). The high negative anomalies mirror the complex tectonic features such as the subduction zone in the Indian Ocean that expands from south west of Sumatera Island to south of Java, while the high negative anomalies around Banda Sea correlate with the presence of deep trenches. The high positive anomalies over land areas associate with the presence of high mountains. Despite the fact that the trend of both gravity features from GGM01S and GGM02S appears similar, the fluctuations or variations are slightly different. The gravity anomalies computed from GGM01S model vary from

about -192 to 175 mGal over the region while the anomalies computed from GGM02S model vary from approximately -182 mGal to 173 mGal.

6.2 Comparison to EGM96 and "terrestrial gravity data"

To evaluate the gravity situation derived from satellite measurements the gravity anomalies are compared to those derived from the EGM96 model and from the "existing terrestrial data".

In order to assess the differences between the EGM96 gravity model and the satellite gravity models, the computation of the free-air anomalies were carried out up to degree and order 120 for all geopotential models. Figure 6.2b shows the differences between EGM96 gravity anomaly and the satellite gravity anomalies. The difference between EIGEN-2b and EGM96 shows more discrepancies than the differences between EGM96 and GGMM01S and GGMM02S.

It is clear that the GRACE models more or less converge toward the EGM96 model, showing the recent model GGM02S has a good agreement with the EGM96 model up to degree 120.

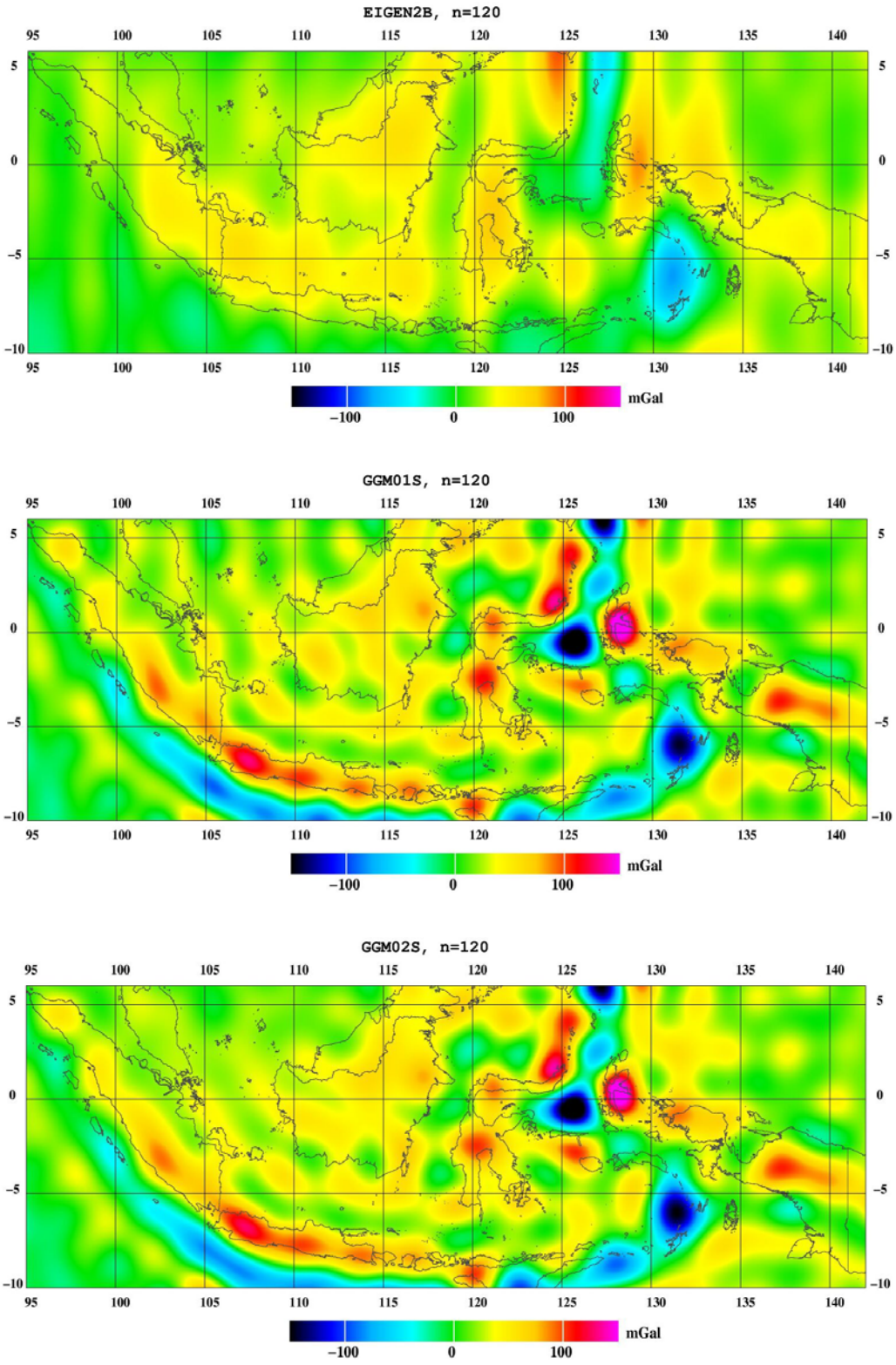

Figure 6.2a. The anomalous gravity field over Indonesia from different satellite-only based geopotential models. From top: the EIGEN2B, the GGM01S and the GGM02S model, all to degree and order 120.

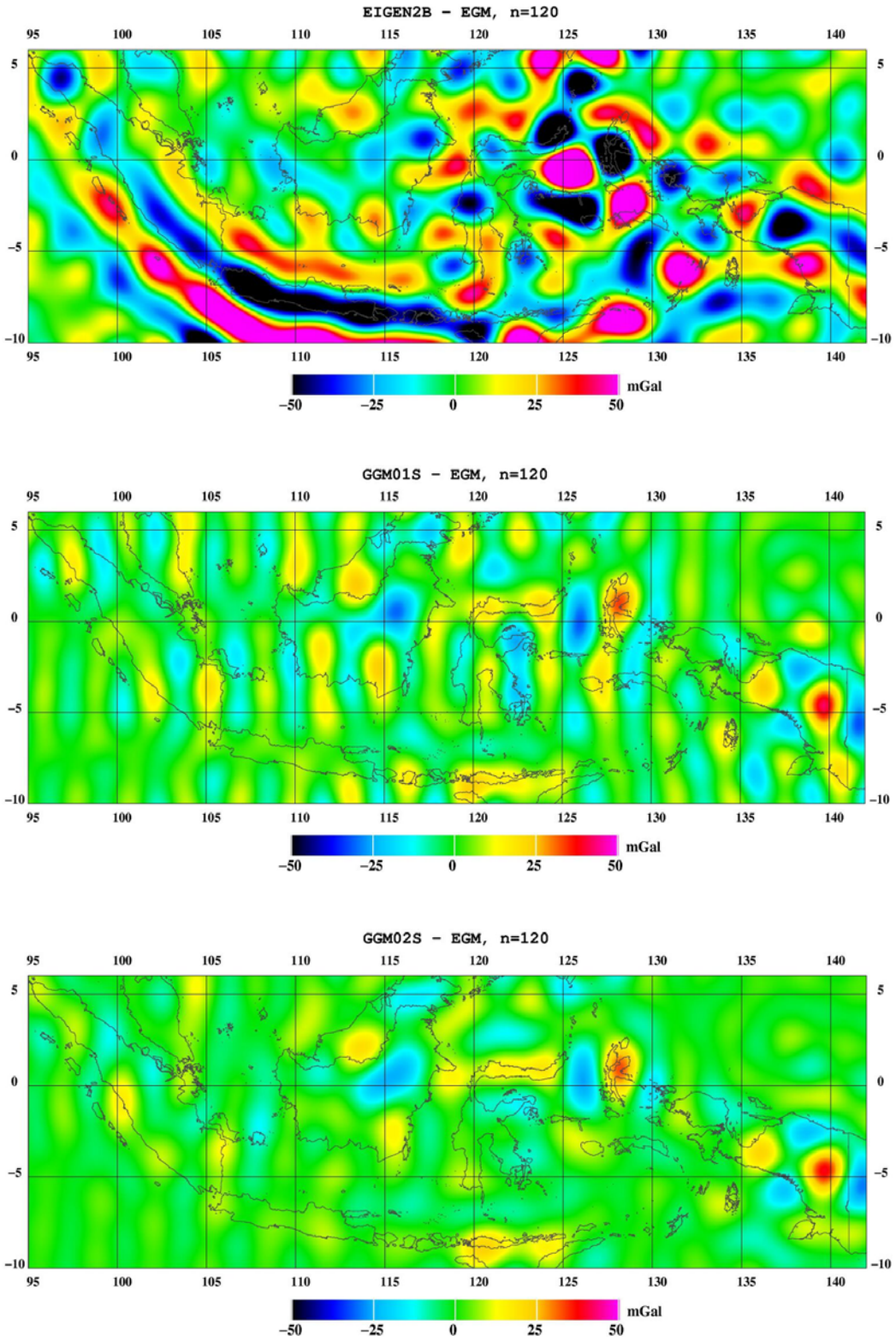

Figure 6.2b. Differences between satellite-only based geopotential models and the EGM96 model. From top: the EIGEN2B minus EGM96, the GGM01S and the GGM02S model, all to degree 120, minus EGM96 to degree 120.

The existing regional "terrestrial gravity data" (INDGRAV) used in the comparison for this region consists of a 'homogeneous' dataset of 5' grid interval. It is made up of a combination of land and marine gravity observations as well as satellite altimetry derived gravity anomalies over the open ocean areas. The distribution of the observations data is uneven, and big data gaps occur in some parts of the major islands i.e., Kalimantan, Sulawesi and Irianjaya. The "terrestrial" free-air anomaly feature based on INDGRAV data is shown in Figure 6.3, where areas lacking data are indicated by a grey color. The gravity field across the country is quite dynamic, and ranges from a minimum of -295 mGal to a maximum of 366 mGal

Numerical comparisons between INDGRAV free-air anomalies and those computed from geopotential models (EIGEN-2b, EGM96 and GGM02S) are performed at the INDGRAV grid points and the residual anomalies are presented in Figure 6.4. The EIGEN-2b residuals appear to be quite disturbed, ranging from -288.61 to 327.66 mGal. Given the weaknesses of the CHAMP satellite to pick up the short wavelength gravity signal, especially for dynamic areas with prominent deep trenches and high mountains like the Indonesian territory, significant biases arise in areas characterized by deep trenches or high mountains. The RMS of the Eigen-2 residual anomalies is 46.8 mGal compared to 53.5 mGal for the INDGRAV data (see Table 6.1).

The EGM96 residual field is much smoother than that for Eigen-2b, having an RMS of 38.3 mGal. The residual anomalies from the recent GRACE model GGM02S appear to be comparable to those for EGM96 having an RMS of 38.5 mGal (see also Figure 6.4).

Table 6.1. ***Statistics of the INDGRAV database and GM residual anomalies (unit in mGal)***

Grav. Anom.	Mean	Std.Dev.	Minimum	Maximum
INDGRAV data	21.22	53.5	-295.2	366.9
Eigen2b residual	-0.64	46.8	-288.6	327.7
EGM96 residual	-0.24	38.3	-211.6	335.4
GGMM02S residual	-0.52	38.5	-201.4	315.5

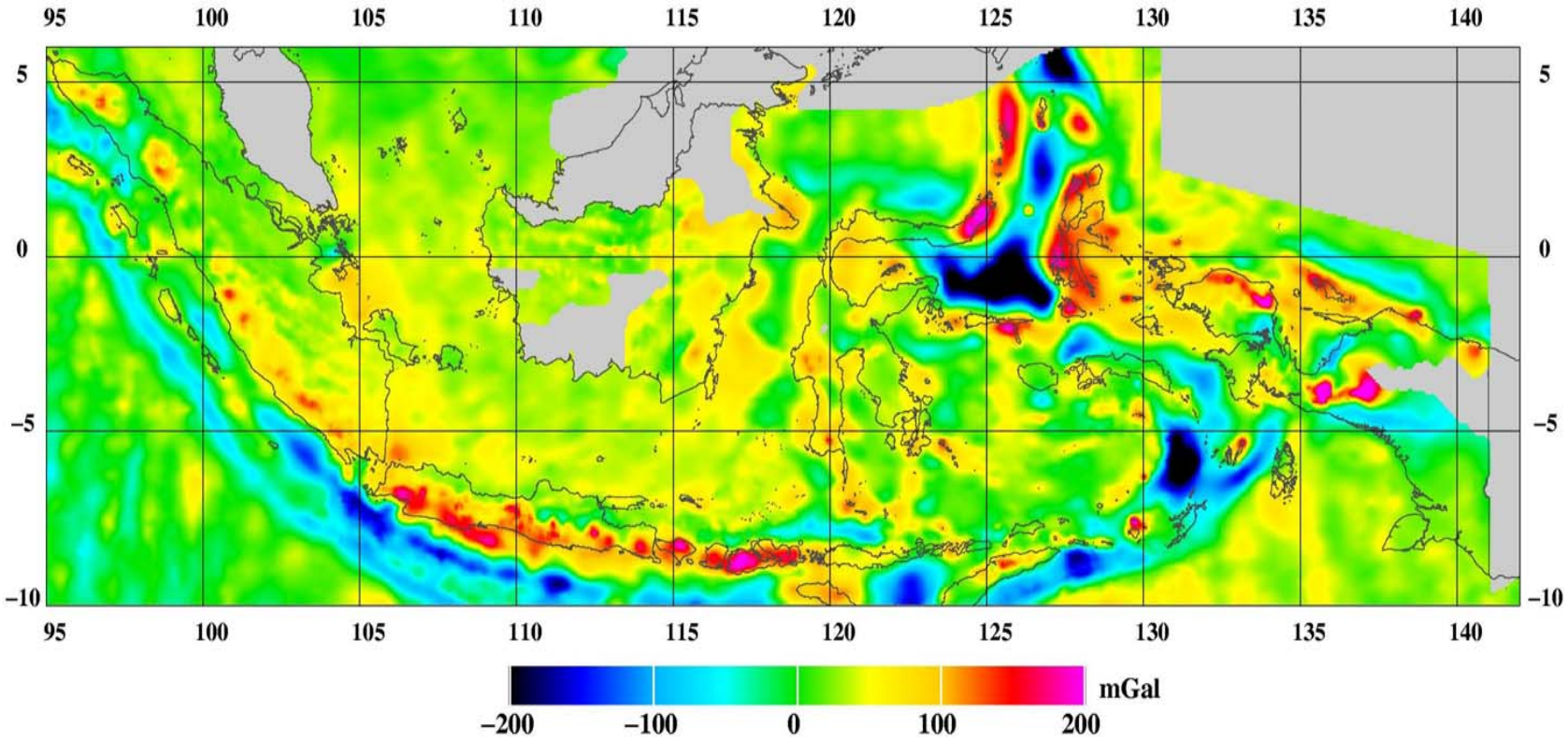

Figure 6.3. Free air anomalies based on the INDGRAV database.

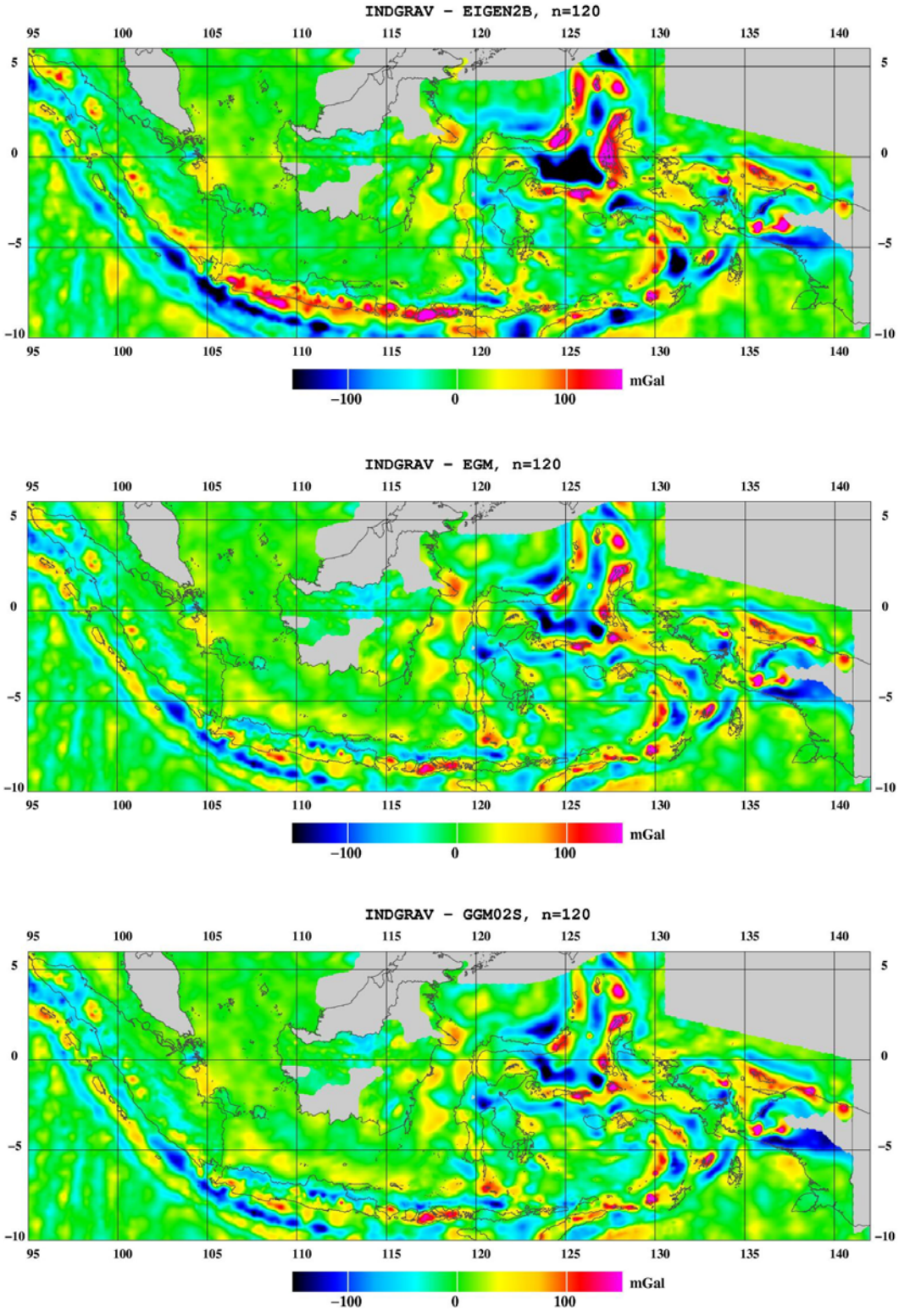

Figure 6.4. The Free-air Residual Anomalies (INDGRAV minus global models). From top EIGEN2B, EGM96 and GGM02S.

6.3 The Geoid height from CHAMP and GRACE

The gravimetric geoid heights are computed from the EIGEN-2b, EGM96 and GGM02 coefficients by using equation (4.9). The formula can be re-written as,

$$N(\theta,\lambda) = R\sum_{l=2}^{L}\sum_{m=0}^{l} P_{lm}(\sin\theta)\left[C_{lm}\cos m\lambda + S_{lm}\sin m\lambda\right], \tag{6.2}$$

where R is the earth's mean radius. The N values are calculated at grid points with interval of 0.1˚ over the region. In order to obtain the optimum N values from EIGEN-2b the computation was carried out with harmonics expansion up to degree 120, while the computation using EGM96 was done up to degree 360. The GRACE models used in the computations are the satellite only model GGM02S up to degree 120 and the combination with terrestrial model GGM02C up to degree 160. The processing is carried out using the GRAVSOFT software package and also RINT software package as an independent check of the computation.

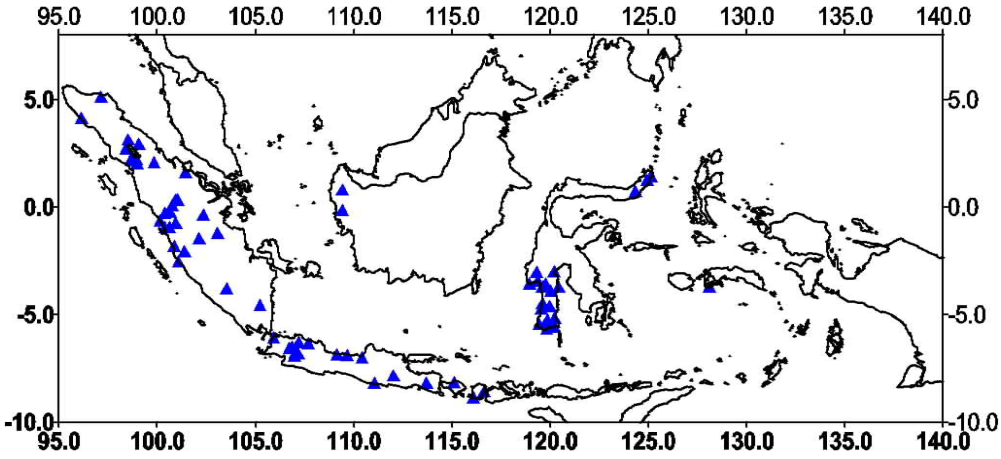

Figure 6.5 Distribution of Control Points (Δ).

Within the region there are 74 GPS points that coincide with the leveling benchmarks scattered in four main islands, i.e., 34 points in Sumatera, 14 in Jawa, 2 in Kalimantan and 17 in Sulawesi. The N values at these respective points are then interpolated from the geoid computed at grid points mentioned above. The distribution of the control points can be seen in Figure 6.5.

6.4 The Geoid height comparison

To evaluate the accuracy of the gravimetric geoid height, the gravimetric geoid (N^{grav}) values are compared with the geometric geoid height (N^{geo}) at GPS/Leveling common points. The geometric geoid height is obtained by subtracting the GPS ellipsoidal height with the orthometric height from leveling measurements at respective points. The mean differences of the geoid height ($\overline{\Delta N}$) and the standard deviation (σ) of the comparisons are written as,

$$\overline{\Delta N} = \frac{1}{n}\sum_{k=1}^{n} N_k^{geo} - N_k^{grav}$$

and

$$\sigma = \frac{1}{n}\left[\sum_{k=1}^{n}\left\{\left(N_k^{geo} - N_k^{grav}\right) - \overline{\Delta N}\right\}^2\right]^{1/2} \qquad (6.3)$$

where n is numbers of control points.

The comparison results presented in Table 6.2 shows a poor fit between the EIGEN-2b geoid and the geometric geoid. In addition to a bias of 2.3 m, a significant misfit of more than 7 m occurs at three control points in western Java and three in northern Sulawesi Island. This large misfit is most likely due to the poor resolution of the gravity field in the Eigen-2 model as a result of signal attenuation at the satellites altitude.

The GRACE geoid fits the geometric geoid better than does CHAMP's. The mean and standard deviation of the GGM02S's geoid misfit are 1.54 m and 1.48 m respectively. The same numbers for GGM02C are 1.18 m and 1.08 m. Unsurprisingly, the EGM96 geoid has the best fit with the geometric geoid. The difference has mean value of 0.77 m with a standard deviation of 0.85 m.

Table 6.2 ***The Statistics of the Geoid Comparison at 74 points (unit is meter).***

ΔN	Mean	Std.Dev.	Minimum	Maximum
$N^{geo} - N^{EIGEN\text{-}2b}$	2.30	2.61	2.73	9.09
$\mathbf{N}^{geo} - N^{EGM96}$	0.77	0.85	-1.44	2.42
$\mathbf{N}^{geo} - N^{GGM02S\ *)}$	1.54	1.48	-1.69	5.96
$\mathbf{N}^{geo} - N^{GGM02C**)}$	1.18	1.08	-0.89	3.87
*) The geo-potential model used is the GGMM02S computed up to degree/order 120 **) The geo-potential model used is the GGMM02C computed up to degree/order 160				

6.4.1 Comparison per-island partition

Most of the 74 control points mentioned above are located in four main islands such as Sumatera 34 points, Jawa 14 points, Kalimantan 2 points and Sulawesi 17 points. The leveling networks between those islands are not connected. Consequently there is datum bias as the orthometric heights are not tied to the same tide gauge station. Therefore, direct comparison using 74 points as performed in the previous section is considered rather coarse and inconsistent. In order to use consistent geometric geoid height, comparison per-island partition is carried out. Since only two points are located in Kalimantan, the comparisons are made merely for Sumatera, Jawa and Sulawesi islands.

In view of the fact that the EGM96 and GGM02 geoid models are better than the EIGEN2b and GGM01, the comparison includes only the EGM96 and the two most recent GRACE models. The results are given in Table 6.3a,b,c below. The standard deviation of the comparison shows that the EGM96 geoid gives better comparison

than the GGM02S and GGM02C geoids in Jawa, Sumatera and Sulawesi islands. The GGM02C geoid in most cases is better than the GGM02S geoid, slightly comparable with EGM96. This indicates that the better satellite gravity solution combined with the surface data will certainly improve the gravimetric geoid.

Table 6.3a The Statistic of the Geoid Comparison at 14 points in Jawa (unit is meter).

ΔN	Mean	Std.Dev.	Minimum	Maximum
$\mathbf{N}^{geo} - N^{EGM96}$	1.18	0.59	-0.18	2.05
$\mathbf{N}^{geo} - N^{GGM02S}$	0.59	1.77	-1.69	3.96
$\mathbf{N}^{geo} - N^{GGM02C}$	0.48	1.05	-0.99	2.12

Table 6.3b The Statistic of the Geoid Comparison at 34 points in Sumatera (unit is meter).

ΔN	Mean	Std.Dev.	Minimum	Maximum
$\mathbf{N}^{geo} - N^{EGM96}$	0.38	0.85	-1.44	2.42
$\mathbf{N}^{geo} - N^{GGM02S}$	1.40	1.08	-0.32	2.99
$\mathbf{N}^{geo} - N^{GGM02C}$	1.15	1.02	-0.69	2.76

Table 6.3c The Statistic of the Geoid Comparison at 17 points in Sulawesi (unit is meter).

ΔN	Mean	Std.Dev.	Minimum	Maximum
$\mathbf{N}^{geo} - N^{EGM96}$	0.98	0.80	-0.13	2.14
$\mathbf{N}^{geo} - N^{GGM02S}$	1.55	1.02	-0.02	3.65
$\mathbf{N}^{geo} - N^{GGM02C}$	1.36	1.14	-0.32	3.87

6.5 Will the new satellite missions meet the requirements for high precision geoid models?

As the previous chapters showed the satellite gravity and geoid models are improving and now give unprecedented accuracies especially for the longer wavelengths. They will therefore provide a very good basis for solving the problem about inter-island datum biases. But will they provide the needed geoid accuracy in order to be used for e.g. GPS leveling? As Table 6.3 shows the accuracy is at the meter level for the satellite models so there is still a long way to go before they will meet the typical requirement for leveling work say 5 cm or better.

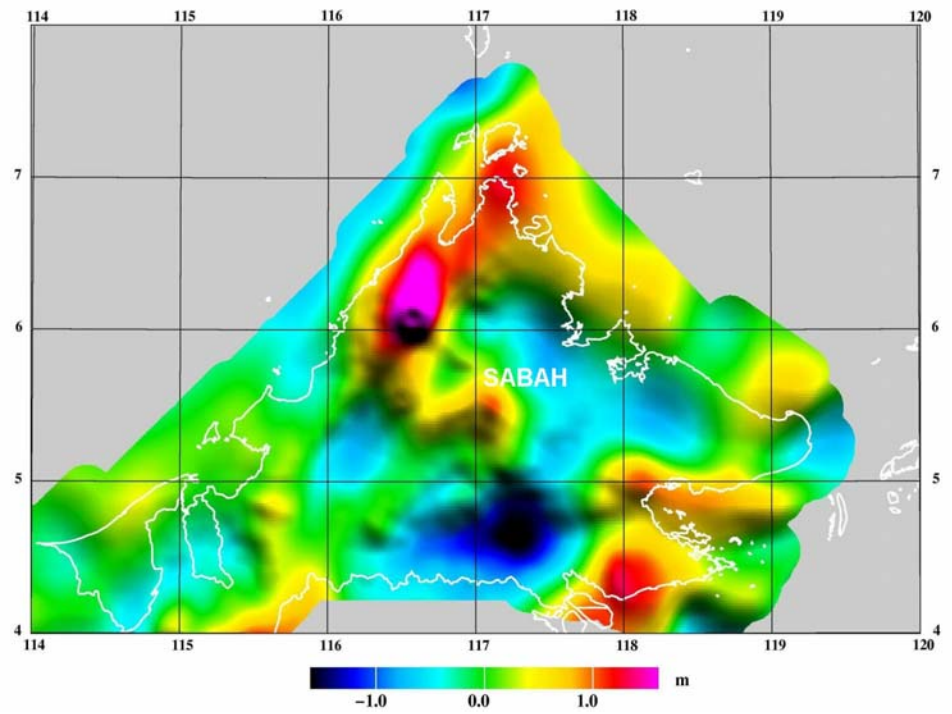

Figure 6.6. Sabah airborne geoid high-pass filtered to GOCE resolution (Olesen, A.V. personal communication)

The upcoming GOCE gravity satellite product will improve the situation somewhat but far from enough as the following will show. The Danish National Space Center did detailed airborne gravity work in neighboring Malaysia with a flight line spacing of 5 km. The aim of this survey was to come up with the best possible high resolution geoid model for the area. Figure 6.6 shows the Malaysian geoid for part of Borneo (Sabah region just north of Kalimantan) based on the airborne data and high-pass filtered to the claimed resolution (i.e. 100km) of the GOCE satellite mission (A.V. Olesen, pers. comm.). The area is characterized by a rough terrain with a high mount (up to 4000 meter above sea level). Figure 6.6 and Table 6.4 are that way an example of how much the actual geoid signal will suffer from omission errors in the future GOCE geoid models. From Table 6.4 below it is seen that one should not expect a GOCE geoid much better than around 60 cm for an area like this.

Table 6.4 Sabah high resolution airborne geoid model

Model	Standard deviation
Sabah geoid high pass filtered to GOCE resolution	0.57 m
Sabah geoid minus EGM96 to degree 360	1.08 m

6.6 The unification of datums in Indonesia using a global geoid as reference

Efforts to unify the local vertical datums of Indonesia's three major islands - Jawa, Sumatra and Sulawesi were carried out using various global geoids based both on GRACE (GGM02S, GGM02C) and the EGM96 geopotential coefficients model. The relationship between the local height datum and the global height datum is examined through equation (3.1) given in chapter 3 and distortions between local height datums in different islands are computed using equation (3.2). The mean deviation between leveling heights from its GPS/geoid heights at control points located in each of the three islands is considered by analysing the offsets between the local and global datum.

In addition to the three above-mentioned geopotential models, the new earth gravitational potential model EGM08 - which was officially released by the US National Geospatial-Intelligence Agency (Pavlis et al, 2008) - was also used as the global reference surface for height at common GPS/leveling points. Offsets between the local and global height datum is re-determined using the same approach described in the above section.

Table 6.5a Datum offset in Jawa Island (units in meter)

Global Datum	μ	σ	Min.	Max.	Range
EGM96	1.18	0.59	- 0.18	2.05	2.23
GGM02S	0.59	1.77	- 1.69	3.96	4.65
GGM02C	0.48	1.05	-0.99	2.12	3.11
EGM08	-0.65	0.45	-1.32	0.31	1.63

Table 6.5b Datum offset in Sumatra Island (units in meter)

Global Datum	μ	σ	Min.	Max.	Range
EGM96	0.38	0.85	-1.44	2.42	3.86
GGM02S	1.40	1.08	-0.32	2.99	3.31
GGM02C	1.15	1.02	-0.69	2.76	3.45
EGM08	-0.26	0.37	-1.47	0.70	2.17

Table 6.5c Datum offset in Sulawesi Island (units in meter)

Global Datum	μ	σ	Min.	Max.	Range
EGM96	0.98	0.80	-0.13	2.14	2.27
GGM02S	1.55	1.02	-0.02	3.65	3.67
GGM02C	1.36	1.14	-0.32	3.87	4.19
EGM08	-0.25	0.42	-1.17	-0.86	2.03

Tables 6.5a, 6.5b and 6.5c above give various results of local datum offsets from different global datum (geoid models) at the three separate islands. The results show that the local height datum of Jawa Island differs by 1.18 meter from the global datum of EGM96 geoid, while in Sumatra and Sulawesi Islands the differences are 0.38 meter and 0.98 meter. When using the EGM08 geoid as the global datum, the offsets are relatively smaller at each island. In Jawa Island the offset is reduced to 0.65 meter, whilst in Sumatra and Sulawesi Islands the offsets are further reduced to 0.26 and 0.25 m respectively.

The results also show that the GRACE model of GGM02C gives smaller datum offsets in all three islands and better standard deviation in both Jawa and Sumatera islands than its GGM02S model, suggesting the GGM02C provides better geoid than the GGM02S model for this area. This probably due to the fact that the GGM02S model was based only on GRACE satellite gravity and was estimated to degree and order 160 without any surface gravity data applied in generating the model. On the other hand, the GGM02C is a higher resolution global gravity model to degree and order 200 and it is a combination of the GGM02S with terrestrial gravity and mean sea surface (Tapley, et al., 2005).

The range between minimum and maximum values of datum offset at each island given by GRACE models are slightly higher than those given by the EGM models. This is also reflected in the higher standard deviations (greater than 1 meter for both GRACE models in all islands). Despite the fact that the GRACE GGM02C is better modeled in lower degrees than the EGM96, the better standard deviations showed by

using EGM96 geoid as global datum indicates that the EGM96 geoid is more reliable than the GRACE GGM02C geoid for the area.

When using the EGM08 geoid model as the global height datum, the offset gives even better and more consistent standard deviations (i.e., 0.45 meter in Jawa, 0.37 meter in Sumatra and 0.42 meter in Sulawesi) compares to other models. This shows that the EGM08 model provides better geoid for Indonesia than the EGM96 model. Also, compare to the regional geoid INDGED02 (i.e., based on EGM96 and local gravity data, see Section 3.2.2), the EGM08 model gives better standard deviations of datum comparisons in Jawa and Sumatera islands (see again Table 3.5). This implies that the EGM08 model alone provide even better geoid than the detailed one where surface gravity data of the subset area (see Section 3.2.1) was included. Nevertheless, a higher precision geoid is still needed in order to meet the requirements for precise GPS leveling.

The *mean* offsets between the local datum and the global height datum varies between the islands (see Tables 6.5a, 6.5b, 6.5c). This indicates the inconsistencies between the local datums, and thus points to the presence of distortions between local height datum in Jawa, Sumatra and Sulawesi. Table 6.6 below shows the size of the local height distortions between the three islands. The magnitude of the distortions given in this table is rather speculative since systematic errors in leveling and GPS measurements - as well as errors in the global geoid - are not taken into account.

The improved standard deviations in the datum comparisons (see Tables 6.5a, 6.5b, 6.5c) given by the EGM08 global geoid implies the superiority of this model compared to the GRACE and the EGM96 models. For this reason, it is preferable to use the EGM08 geoid as the global datum to further examine the distortions of the local height datum in Indonesia. As is shown in Table 6.6 below, a distortion of 48 cm occurs between local height datums in Jawa and Sumatra. Also, distortion of 43 cm is observed between local height datum in Jawa and Sulawesi whereas the estimated distortion between Sumatra and Sulawesi is only 5 cm.

Table 6.6 Local height datums distortion (units in meter)

Global Reference	Jawa – Sumatra	Jawa – Sulawesi	Sumatra - Sulawesi
EGM96	0.80	0.22	-0.58
GGM02S	-0.81	-0.96	-0.15
GGM02C	-0.67	-0.88	-0.21
EGM08	0.48	0.43	-0.05

Processes in the ocean such as currents, temperature differences, varying salinity and prevailing wind systems will produce the observed distortions of local datum as the spirit leveling is tied and adjusted to tide gauges. Figure 6.6 depicts the difference between mean sea surface height and the EGM08 geoid (DNSC08 model, Andersen, 2008). This difference which is also known as the Mean Dynamic Topography (MDT) shows many small scale features which may not necessarily reflect reality but should rather be considered noise. Features near the coast especially should be considered with some suspicion as the quality of satellite altimetry is questionable here.

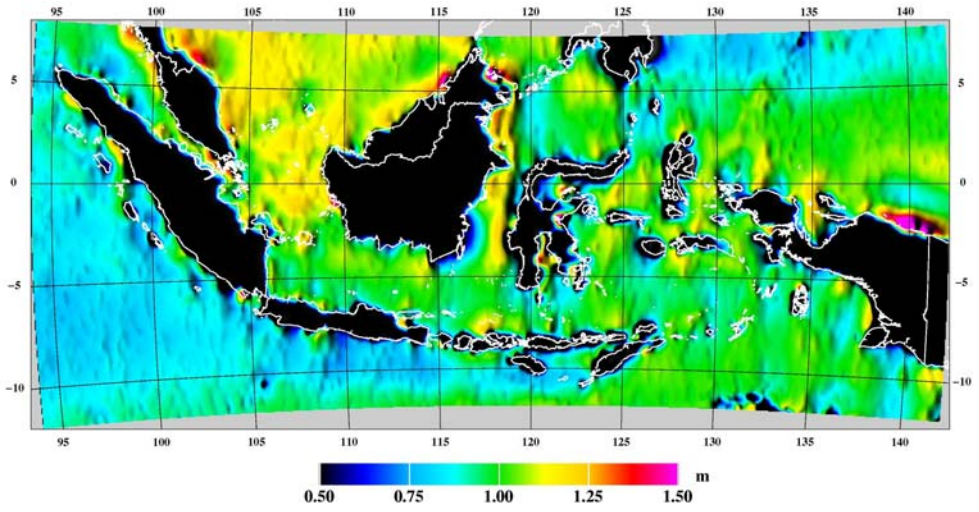

Figure 6.6 Deviation of Mean Sea Surface from the EGM08 geoid across Indonesian waters (DNSC08 model, Andersen 2008)

Also some larger scale features are seen along the coast, e.g. SE corner of Kalimantan and north of Papua. These features could indicate errors in the EGM08 geoid as the features are not easy to interpret as ocean processes (Andersen, O.B., personal comm.). Nevertheless some larger trends are clear, first of all the difference in MDT between the Indian Ocean and the South China Sea (and Banda Sea). The difference amounts to approximately 40 cm and are thus at the same scale as the observed distortions in the local height datum.

A further analysis of the impact of MDT on tide gauge observations and thereby on local height distortion is complicated to pursue as satellite altimetry doesn't have the required precision near the coast. An alternative could be airborne altimetry that would connect the local sea level near tide gauge stations to the open sea.

6.7 The EGM08

The EGM08 model, the successor of the EGM96, improves the situation in many areas in the world, especially where new surface gravity data has been included (Pavlis, et al., 2008). The long wavelength part of the EGM08 is defined by the GRACE gravity satellite mission data, which is more accurate, so the medium to long wavelength errors present in EGM96 were reduced. In addition to more new surface data included in the development of the model, the high resolution digital elevation model from the Shuttle Radar Topographic Mission (the SRTM) was also used as the source for filling -in those areas lacking in gravity (Kenyon, et al., 2007) This very high degree spherical harmonic model to 2160 degrees expansion offers high resolution (5'x5') of global gravity field information with a geoid accuracy of 15 cm RMS worldwide. But those areas lacking in surface gravity data will still have problems in producing geoid with the stated accuracy specified by the EGM08. This lack is certainly the case in many parts of Indonesia.

The near coastal zone poses a special problem. This is an area where one may want the most precise geoid due to the high population and infrastructure density in these regions. Importantly, natural hazard management like flood control and tsunami

warning systems require a good coastal geoid determination in order to make use of fast and cheap GPS leveling instead of tedious and costly spirit leveling. Unfortunately there is currently a pronounced lack of data in this zone as is shown in this study. There is only little marine data available - partly due to shallow water that does not allow for ship-borne measurements - and satellite altimetry derived models are in general not reliable near the coast (Andersen and Knudsen, 1998).

6.8 The impact on the local height datum offset of changing W_0

The global vertical datum is defined as the equipotential surface of the earth gravity field potential. The constant gravity potential of the geoid (W_0) can be determined from satellite altimetry data on the basis of a global geopotential model (GGM). A new W_0 constant value has been suggested by the IAG ICP1.2 Working Group at the IAG-IUGG joint meeting in Perugia, August 2007. This new W_0 value ($62\ 636\ 856.0 \pm 0.5\ m^2s^{-2}$) was proposed to be adopted as a fundamental constant, as it can now be determined directly and accurately from observations (Bursa et al., 2006). The conventional value ($62\ 636\ 860.850\ m^2s^{-2}$) is related to Somigliana-Pizetti normal gravity field generated by GRS'80 ellipsoid. The impact of using the new W_0 value to find out the offset between the local and the global height datums gives *direct* and *indirect* effects (Kearsley, 2007). The direct effect $\Delta_{(\phi,\lambda)}$, i.e., the separation between the global physical and the model reference surfaces at any point on the globe, is computed by

$$\Delta_{(\phi,\lambda)} = \Delta W_0 / \gamma_{(\phi),} \qquad (6.4)$$

where the ΔW_0 is the difference between the proposed and the current W_0 values and the $\gamma_{(\phi)}$ is the computed normal gravity at the respective points (for e.g., tide gauges or any vertical control points). The indirect effects are corrections to the *local* geoid

resulting from this change in W_0. It can be evaluated by computing the bias in the height as

$$B_{(\phi,\lambda)} = (h - N)_{(\phi,\lambda)} - H_{(\phi,\lambda)}, \qquad (6.5)$$

It bias is then mapped into the free air anomaly systematically by $\Delta N_S = B*0.3086$. Its impact upon the local geoid is computed using ring integration with an optimum cap size radius of approximately 25 km. This scheme has been used to find the relationship between the fundamental reference surface and the Australian Height Datum (Kearsley, ibid). To examine the impact of using the Bursa $\boldsymbol{W_0}$ value in the unification of Indonesian height datum, a similar procedure (after Kearsley, ibid) is applied to compute the impact of changing the $\boldsymbol{W_0}$ upon the N value. The geoid is computed based on the geopotential model EGM08, with no local surface gravity measurements included in the geoid computation. The correction which results from changing the fundamental constant ($\Delta W_0 = 4.85\ m^2s^{-2}$) is applied. The effect ($\Delta_{(\phi,\lambda)}$) of this change is obtained by dividing the ΔW_0 value by normal gravity (see eq.6.4) at each vertical control points and the result is given in Table 6.7 below.

Table 6.7 Corrections applied in changing the W_0

Control points	ϕ	λ	h GPS (meter)	H Leveling (meter)	N (EGM08) (meter)	$\gamma_{(\phi)}$	$\Delta_{(\phi,\lambda)}$ (meter)
1	4.15300	96.13190	-27.72	2.744	-31.107	978059.76	0.49588
2	5.12070	97.13190	-21.22	3.689	-26.008	978073.81	0.49587
3	2.73160	98.39170	1007.47	1021.840	-14.583	978044.40	0.49589
4	2.74250	98.39900	1007.47	1021.840	-14.503	978044.50	0.49589
5	2.76220	98.45930	1379.21	1392.890	-13.928	978044.67	0.49589
6	3.14520	98.50750	1291.05	1305.160	-14.365	978048.22	0.49588
7	2.19230	98.64180	1301.49	1314.910	-12.827	978040.23	0.49588
8	2.22470	98.65630	1408.67	1421.010	-12.528	978040.46	0.49588
9	2.25220	98.67780	1464.54	1476.590	-12.218	978040.65	0.49589
10	2.25680	98.71170	1392.90	1404.730	-11.919	978040.68	0.49589
11	2.26240	98.85930	1401.70	1412.740	-11.156	978040.72	0.49589
12	2.24850	98.90210	1393.59	1404.510	-10.946	978040.62	0.49589
13	2.22500	98.93930	1308.86	1319.370	-10.791	978040.46	0.49588
14	2.02060	98.96230	944.53	955.499	-11.174	978039.10	0.49589
15	2.93580	99.04780	422.00	434.271	-12.574	978046.22	0.49588

16	2.09520	99.83390	28.47	36.790	-8.795	978039.58	0.49588
17	-0.62030	100.12040	-4.10	3.573	-8.266	978033.28	0.49589
18	-0.94390	100.36920	0.80	5.703	-6.368	978034.08	0.49589
19	-0.27160	100.36930	909.88	913.516	-3.846	978032.79	0.49589
20	-0.94350	100.62210	996.70	998.765	-2.159	978034.08	0.49589
21	-0.22390	100.63340	510.38	512.467	-2.277	978032.76	0.49589
22	0.09660	100.74720	88.43	90.571	-2.388	978032.69	0.49589
23	-1.80900	100.85550	34.40	37.086	-3.220	978037.82	0.49589
24	0.33160	100.89210	49.20	52.598	-2.703	978032.85	0.49589
25	-0.72770	100.94450	179.41	180.034	-0.715	978033.51	0.49589
26	0.34660	101.02520	34.52	36.616	-2.407	978032.87	0.49589
27	-2.51400	101.06870	-1.35	3.551	-5.425	978042.61	0.49588
28	-2.05440	101.39050	807.96	805.159	2.690	978039.31	0.49589
29	1.61920	101.43590	15.17	17.075	-2.092	978036.80	0.49589
30	-1.46290	102.12350	53.98	49.421	4.209	978036.04	0.49589
31	-0.34920	102.33390	25.08	21.466	3.474	978032.87	0.49589
32	-1.20550	103.06580	39.99	32.044	7.632	978034.96	0.49589
33	-3.78570	103.53320	122.62	112.536	9.858	978055.18	0.49588
34	-4.55320	105.22130	37.75	22.226	15.272	978065.22	0.49587
35	-6.05500	105.91740	16.98	1.681	14.289	978090.13	0.49586
36	-6.56100	106.73010	201.33	183.447	18.190	978100.09	0.49585
37	-6.49090	106.85000	156.83	138.180	18.415	978098.66	0.49586
38	-6.91430	106.97410	703.45	681.946	20.343	978107.51	0.49585
39	-6.73150	107.04120	1074.97	1053.328	20.460	978103.62	0.49585
40	-6.80850	107.15590	426.77	405.493	20.398	978105.25	0.49585
41	-6.27050	107.18380	33.70	13.675	18.701	978094.27	0.49586
42	-6.33330	107.67330	31.44	10.732	19.880	978095.51	0.49586
43	-6.85980	109.15310	27.38	4.031	22.651	978106.34	0.49586
47	-6.98380	110.40950	30.61	4.563	25.542	978109.01	0.49585
48	-8.17760	111.04540	410.68	384.273	25.909	978137.15	0.49584
49	-7.82690	112.01060	93.92	66.129	27.365	978128.44	0.49584
50	-8.16820	113.70170	119.01	85.579	32.949	978136.91	0.49584
51	-8.14760	115.10560	178.40	142.699	35.052	978136.39	0.49584
52	-8.86850	116.08650	39.15	4.205	34.365	978155.40	0.49583
53	-8.55210	116.63170	58.55	20.718	38.030	978146.87	0.49583
54	-3.56970	118.93650	54.70	1.804	52.612	978052.69	0.49588
55	-3.02340	119.30500	1040.54	979.464	60.926	978047.04	0.49588
56	-3.43510	119.35000	60.50	2.342	57.693	978051.21	0.49588
57	-5.43380	119.43750	55.48	3.251	52.063	978078.98	0.49587
58	-4.70860	119.54670	57.02	2.116	54.776	978067.47	0.49587
59	-3.69610	119.59880	71.65	14.153	57.092	978054.13	0.49588
60	-4.47400	119.60900	150.09	95.578	55.369	978064.10	0.49587
61	-3.55520	119.77340	116.29	57.310	58.548	978052.53	0.49588
62	-5.63550	119.81690	101.56	49.217	52.048	978082.47	0.49587
63	-5.24800	119.85520	1094.17	1038.827	55.407	978075.87	0.49587
64	-4.60500	119.97690	163.03	106.703	55.861	978065.96	0.49587
65	-5.57290	120.03230	55.70	2.239	53.062	978081.37	0.49587
66	-3.90260	120.03390	76.77	19.774	56.304	978056.59	0.49588
67	-2.99490	120.19310	65.00	3.454	61.197	978046.77	0.49588
68	-5.55060	120.20130	54.90	1.543	53.058	978080.98	0.49587
69	-5.15080	120.21970	165.73	110.832	54.453	978074.29	0.49587
70	-3.70550	120.41970	60.07	1.586	57.316	978054.24	0.49588
71	0.73710	124.33090	384.94	316.745	68.707	978033.53	0.49589
72	1.25750	124.93190	758.91	687.882	70.921	978035.16	0.49589

Even though the variation of the effect at all vertical control point is very small (less than 1 millimeter) - because of the change in normal gravity is insignificant, the impact upon a geoid height themselves of using the proposed new W_0 is significant (in the order of 49.6 centimeter). Biases relating to the *short* wavelength geoid components also need to be considered when using surface free air gravity anomalies in the detailed geoid computation where the height used to compute the gravity anomaly is referred to the *local* datum (cf. the geoid). The impact is then added to the N values and the global heights (which refer to the EGM08 geoid using new W_0) are obtained by subtracting the ellipsoidal height with the amended N values at control points. The local height datum offset by changing W_0 is then assessed by comparing them to the 'corrected' global height at all control points. The impact of new W_0 upon N and offsets of local height datums (dH) at all control points is shown in Table 6.8 below.

Table 6.8 The impact of new W_0 upon N

Control points	ϕ	λ	h GPS (m)	H Leveling (m)	N (EGM08) (m)	Amended N (m)	dH (m)
1	4.15300	96.13190	-27.72	2.744	-31.107	-30.611	0.147
2	5.12070	97.13190	-21.22	3.689	-26.008	-25.512	0.603
3	2.73160	98.39170	1007.47	1021.840	-14.583	-14.087	-0.283
4	2.74250	98.39900	1007.47	1021.840	-14.503	-14.007	-0.363
5	2.76220	98.45930	1379.21	1392.890	-13.928	-13.432	-0.248
6	3.14520	98.50750	1291.05	1305.160	-14.365	-13.869	-0.241
7	2.19230	98.64180	1301.49	1314.910	-12.827	-12.331	-1.089
8	2.22470	98.65630	1408.67	1421.010	-12.528	-12.032	-0.308
9	2.25220	98.67780	1464.54	1476.590	-12.218	-11.722	-0.328
10	2.25680	98.71170	1392.90	1404.730	-11.919	-11.423	-0.407
11	2.26240	98.85930	1401.70	1412.740	-11.156	-11.652	0.612
12	2.24850	98.90210	1393.59	1404.510	-10.946	-10.450	-0.470
13	2.22500	98.93930	1308.86	1319.370	-10.791	-10.295	-0.215
14	2.02060	98.96230	944.53	955.499	-11.174	-10.678	-0.291
15	2.93580	99.04780	422.00	434.271	-12.574	-12.078	-0.193
16	2.09520	99.83390	28.47	36.790	-8.795	-8.299	-0.021
17	-0.62030	100.12040	-4.10	3.573	-8.266	-7.770	0.097
18	-0.94390	100.36920	0.80	5.703	-6.368	-5.872	0.969
19	-0.27160	100.36930	909.88	913.516	-3.846	-3.350	-0.286
20	-0.94350	100.62210	996.70	998.765	-2.159	-1.663	-0.402
21	-0.22390	100.63340	510.38	512.467	-2.277	-1.781	-0.306
22	0.09660	100.74720	88.43	90.571	-2.388	-1.892	-0.249
23	-1.80900	100.85550	34.40	37.086	-3.220	-2.724	0.038

24	0.33160	100.89210	49.20	52.598	-2.703	-2.207	-1.191
25	-0.72770	100.94450	179.41	180.034	-0.715	-0.219	-0.405
26	0.34660	101.02520	34.52	36.616	-2.407	-1.911	-0.185
27	-2.51400	101.06870	-1.35	3.551	-5.425	-4.929	0.028
28	-2.05440	101.39050	807.96	805.159	2.690	3.186	-0.385
29	1.61920	101.43590	15.17	17.075	-2.092	-1.596	-0.309
30	-1.46290	102.12350	53.98	49.421	4.209	4.705	-0.146
31	-0.34920	102.33390	25.08	21.466	3.474	3.970	-0.356
32	-1.20550	103.06580	39.99	32.044	7.632	8.128	-0.182
33	-3.78570	103.53320	122.62	112.536	9.858	10.354	-0.270
34	-4.55320	105.22130	37.75	22.226	15.272	15.768	-0.244
35	-6.05500	105.91740	16.98	1.681	14.289	14.785	0.514
36	-6.56100	106.73010	201.33	183.447	18.190	18.686	-0.803
37	-6.49090	106.85000	156.83	138.180	18.415	18.911	-0.261
38	-6.91430	106.97410	703.45	681.946	20.343	20.839	0.665
39	-6.73150	107.04120	1074.97	1053.328	20.460	20.956	0.686
40	-6.80850	107.15590	426.77	405.493	20.398	20.894	0.383
41	-6.27050	107.18380	33.70	13.675	18.701	19.197	0.828
42	-6.33330	107.67330	31.44	10.732	19.880	20.376	0.332
43	-6.85980	109.15310	27.38	4.031	22.651	23.147	0.202
47	-6.98380	110.40950	30.61	4.563	25.542	26.038	0.009
48	-8.17760	111.04540	410.68	384.273	25.909	26.405	0.002
49	-7.82690	112.01060	93.92	66.129	27.365	27.861	-0.070
50	-8.16820	113.70170	119.01	85.579	32.949	33.445	-0.014
51	-8.14760	115.10560	178.40	142.699	35.052	35.548	0.153
52	-8.86850	116.08650	39.15	4.205	34.365	34.861	0.084
53	-8.55210	116.63170	58.55	20.718	38.030	38.526	-0.694
54	-3.56970	118.93650	54.70	1.804	52.612	53.108	-0.212
55	-3.02340	119.30500	1040.54	979.464	60.926	61.422	-0.346
56	-3.43510	119.35000	60.50	2.342	57.693	58.189	-0.031
57	-5.43380	119.43750	55.48	3.251	52.063	52.559	-0.330
58	-4.70860	119.54670	57.02	2.116	54.776	55.272	-0.368
59	-3.69610	119.59880	71.65	14.153	57.092	57.588	-0.091
60	-4.47400	119.60900	150.09	95.578	55.369	55.865	-1.353
61	-3.55520	119.77340	116.29	57.310	58.548	59.044	-0.064
62	-5.63550	119.81690	101.56	49.217	52.048	52.544	-0.201
63	-5.24800	119.85520	1094.17	1038.827	55.407	55.903	-0.560
64	-4.60500	119.97690	163.03	106.703	55.861	56.357	-0.030
65	-5.57290	120.03230	55.70	2.239	53.062	53.558	-0.097
66	-3.90260	120.03390	76.77	19.774	56.304	56.799	0.197
67	-2.99490	120.19310	65.00	3.454	61.197	61.693	-0.147
68	-5.55060	120.20130	54.90	1.543	53.058	53.554	-0.197
69	-5.15080	120.21970	165.73	110.832	54.453	54.949	-0.051
70	-3.70550	120.41970	60.07	1.586	57.316	57.812	0.672
71	0.73710	124.33090	384.94	316.745	68.707	69.203	-1.008
72	1.25750	124.93190	758.91	687.882	70.921	71.417	-0.389

The mean offsets between local and global datums with new $\boldsymbol{W_0}$ value at each island are computed by (eq. 3.1) and the local height datum distortion between separated islands is estimated by analyzing the datum offsets. The offset between local and global datum defined by this new $\boldsymbol{W_0}$ value at each islands is given in Table 6.9.

The offset defined by the new W_0 is slightly change compared to the offsets using the old W_0 (0.5 centimeter in Jawa, 6 centimeter in Sumatera and 0.8 centimeter in Sulawesi). The standard deviations of the comparisons are more or less the same, but the range of the offset with respect to the new W_0 in Sumatera and Sulawesi islands are slightly smaller than their previous values (see Table 6.9, Tables 6.5a, 6.5b and 6.5c). Therefore, it may be desirable to use the new value as it reflects the actual ocean mean surface more effectively than the old GRS80 based one.

Table 6.9 Offsets between local and global datums with new W_0 value (units in m)

Location/island	μ	σ	Min.	Max.	Range
Jawa	- 0.655	0.45	- 0.803	0.828	1.631
Sumatra	- 0.202	0.39	- 1.191	0.969	2.160
Sulawesi	- 0.242	0.42	- 1.353	0.672	2.025

Figure 6.7 below shows the local datum offsets at individual control points in Sumatera, Jawa and Sulawesi islands (as given in Table 6.8). In Sumatera, the relatively small offset occurs at control points along the west coast and increases in the mid land towards the east coast. The trend indicates a good agreement along the west coast, where most of the tide gauges station are located, however it is difficult to identify which control points refer to which tide gauge as documentation for the adjustment of the leveling networks is not available. The bigger offset in middle part of the island towards the east coast is likely due to a different MDT between the west and east coast of Sumatera (see Figure 6.6). The mountain range that exists along the middle part of the island could also contribute to error in the geoid if the signal is not present in the EGM08 model. The spatial distribution of datum offset in Jawa shows a tendency to clustering, i.e., higher in the western part than the eastern part. This pattern seems to agree with the MDT figure in the northwest and southeast coast of Jawa. The more complex pattern in Sulawesi is due to incomplete leveling networks, which are concentrated only in the southern part of the island with a small loop in the north. The complex coastline and the influence of the Indonesian throughflow along the west coast of the island could result from the inaccuracy in the mean sea level

determination at the tide gauges stations to which the local heights have been referred.

As a general observation, these results also show the danger in assuming a single constant offset between the datum for an island and the global geoid. The picture is likely to be much more complicated if the height datum is defined by more than one tide gauge, due to distortions in the definition of Mean Sea Level between the different tide gauges.

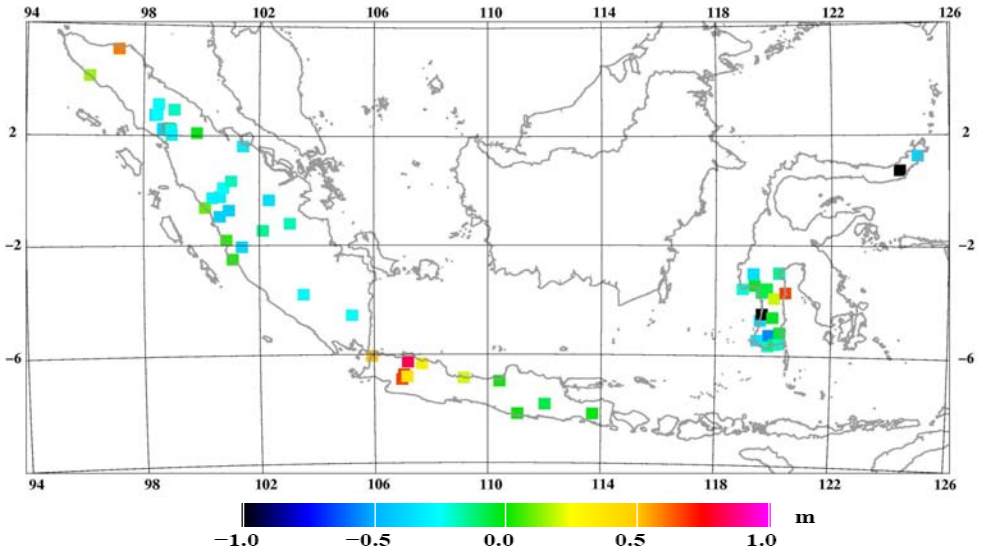

Figure 6.7 Offset between local and global (EGM08) datums with new W_0 value.

CHAPTER 7

CONCLUSION

The current height reference system in Indonesia was established by using a classical spirit leveling measurements. This technique is a well known approach that has been used in most countries for more than a century. Despite being an accurate method for determining height differences, spirit leveling is costly and difficult to undertake in remote areas. The Indonesian mapping authority has started its vertical reference network using precise spirit leveling measurements since the early eighties, however up to present time less than 25 % of the land area has been covered. Lack of infrastructure such as road access, which is required for terrestrial observations, is one of the impediments in completing the job. As a result, the height datum is not available in most part of the country such as in two major islands of Kalimantan or Irianjaya (west Papua). This will slow down the development of the two potential natural resource rich areas.

A modern society requires the ability to measure elevations relative to mean sea level easily, accurately and at the lowest possible cost. The alternative approach to the classical terrestrial technique is the spaceborne technique. A combination of ellipsoidal height measurements derived from satellite (GPS, GLONASS or GALILEO) together with a precise geoid model could give orthometric height with accuracies comparable to precise leveling measurements. If the two components were errorless, they would produce the same results. The GNSS (Global Navigation Satellite System) surveying technique, i.e. to determine height derived from GPS, GLONASS or GALILEO satellites will speed up the tedious leveling work. It provides a more consistent height datum, faster and cheaper than the traditional technique.

The consistent height datum is not only required in mapping and cadastral surveys, but is also needed for navigation and resources management, construction works and mineral exploration, coastal boundary definition, assessment of potential

flooding areas as well as monitoring sea level rise. The classical height system measured by spirit leveling has been inconsistent between different islands. The conventional height system, which is referred to the mean sea level deviates from the modern GPS based height system, which is referred to the geoid. This is due to the fact that the mean sea level, which is determined by tide gauge observations along the coast, is dynamic and does not necessarily co-inside with the geoid.

7.1 Major Conclusions

The deviation known as the offset between the local and the global or regional height datum in different major islands in Indonesia has been investigated by means of different geoid models. The Indonesian geoid (INDGED02) has been used as the regional height datum to examine the offset between the local and global height datums in two separated islands of Jawa and Sumatra undertaken in Chapter 3. The investigation has been limited to these two major islands in western part of the archipelago due to the availability of the surface gravity anomaly data coverage (see Section 3.2.1). The result from the analysis carried out in Chapter 3 suggests that local height distortion of about 78 cm appears in the inter-island datum comparisons between Sumatra and Jawa. The computation result shows large standard deviation of the misfit between the local datum and the global datum comparisons (see in Table 3.5) which can be partly explained by the small sample size (numbers of control points located in Jawa island), but also indicates problem with the underlying gravity data and so the INDGED02 geoid (see the gravimetric geoid in Section 3.2.1b). The accuracy of the 5’ grid gravity dataset used in the gravimetric geoid computation is uncertain due to lack of measured data in the land areas (especially in the mountains) and in the coastal regions (see Figure 3.2).

The launch of satellite gravity GRACE product and the release of the new earth gravitational potential EGM08 has provided a valuable data for performing better nationwide geoid for Indonesia. The GGM02S, GGM02C and EGM08 models have been used in the geoid computation based on global geopotential models only. These geoids then serve as global height datum to re-examine the inter-island datum comparisons in three major islands. The result of the analysis which was undertaken

in Section 6.6 shows different offsets between local and global height datums in each island of Jawa, Sumatra and Sulawesi. The offsets and standard deviations of the datum comparisons are also depend on the geopotential model used for the geoid modeling. The much better standard deviation given by using EGM08 geoid as global datum in the datums comparison make it superior among other models (see again Tables 6.5a, Table 6.5b, and Table 6.5c in Chapter 6). Based on the results it is concluded that the EGM08 geoid best suits as national geoid for Indonesia at present time until a better geoid for this area can be realized.

Having analyzed the datum offsets in each island using the EGM08 geoid as global datum computed in Section 6.6, the intra-island datum comparison shows distortion of 48 centimeter occurs between local height datum in Jawa and Sumatra. Distortion of 43 centimeter is observed between local height datum in Jawa and Sulawesi whereas the estimated distortion between Sumatra and Sulawesi datums is only 5 cm (see Table 6.6). These observed distortions are in line with the feature of the mean dynamic topography (MDT) between the Indian Ocean and the South China Sea (and Banda Sea) which shows the difference of approximately 40 centimeter (see Figure 6.6).

The datum offsets defined by adopting ***new*** $\boldsymbol{W_0}$ are slightly change and the standard deviations of the comparisons are more or less the same compared to the offsets using the ***old*** $\boldsymbol{W_0}$ (see Table 6.9), however the range of the offset with respect to the *new* $\boldsymbol{W_0}$ in Sumatera and Sulawesi islands are slightly smaller than their previous values given in Tables 6.5a, 6.5b and 6.5c.

Since the high precision gravimetric geoid plays a key role in datum unification and in establishing a consistent GPS based height system, there is a demand for more gravity data in this region even after the EGM08 has became available. The recently launched GOCE gravity satellite hopefully will improve the situation even further and will contribute to a better determination of inter-island height datum offsets in this region.

The examination of geoid computation techniques carried out in Chapter 4 showed that a 10 cm geoid was already achievable in major parts of Jawa island. Each of the Ring integration, Collocation and FFT techniques were examined together with various reduction schemes for the gravity data. The main obstacle to achieve a better precision was identified as the lack of gravity data over larger areas. The error propagation study presented in Chapter 5 indicates that further improvement could be reached by gathering more gravity data over inland data voids (mountainous areas) and by covering the near coastal zone with reliable gravity data.

The simulation study indicated 20 cm error with 20 km spaced 'fill-in airborne data' and approximately 15 cm with 10 km spaced data. The results seem to be rather pessimistic when compared to the results obtained in Chapter 4. If the Chapter 5 results are scaled to the Chapter 4 results, the error estimates will approximately drop to half their value, i.e. 10 cm error with 20 km spaced fill-in data and 7 cm error for 10 km fill-in. The latter numbers are believed to be a more realistic assessment of the error field than the un-scaled numbers presented in Chapter 5. Also the inclusion of new higher quality and higher resolution elevation models will further improve the situation as compared to the assumptions for the error study and to the data situation in Chapter 4.

The dedicated satellite gravity missions CHAMP and GRACE improved the medium to long wavelength gravity field across the archipelago with seamless data coverage. However, differences reaching several hundreds mGal were seen in the south of Jawa, in the northern part of Sulawesi and north of Banda Sea when compared with the existing data (see Table 6.1 and Figure 6.4). These significant differences arise in areas characterized by deep trenches and high mountains. The upcoming GOCE gravity satellite product will improve the gravity data situation, but it will be far from precise enough in order to meet the requirement for GPS/levelling (see Section 6.5.). The GOCE geoid is not likely to be better than 50 to 60 cm in an area with such a disturbed gravity field like Indonesia.

In order to implement a modern GPS based height system for Indonesia in the near future, a higher precision geoid model is required. A five cm or better geoid would be desirable. The EGM08 model together with GOCE and new high resolution topography models (e.g. SRTM 3 arc second) will provide a good backbone for such models, but more gravity data are required in most places. Airborne gravimetry offers a fast and relatively cheap way to collect these data. But even with airborne gravimetry it will still be a challenge to reach a 5 cm or better geoid nationwide. Maybe we would be better off by relaxing the general requirement to say a 5 to 10 cm geoid for the nationwide coverage and then in turn focus our effort in areas where we need a higher precision geoid, say 2 to 5 cm precision. Regions where the high precision is needed will typically be in areas that are more densely populated and where there is high economic interest related to infrastructure development. This will often coincide with the coastal regions where there also will be an interest in a high precision geoid to support coastal management and flood control.

As the conclusion, the realization of a new national vertical datum for Indonesia by *geoid modeling* rather than by *geodetic leveling* is strongly proposed. It will enable measurements of elevations with respect to a consistent vertical datum everywhere across the country using the Global Positioning System (GPS) and emerging Global Navigation satellite System (GNSS) technologies. To achieve that, it requires a strategic planning and implementation as well as improvement of the geoid model.

7.2 Recommendation and future works

My recommendations for future work in order to improve the gravity/geoid situation in Indonesia will therefore be a two-step approach: first a nationwide or near nationwide coverage with airborne gravimetry that in combination with global geopotential models will provide a 5 to 10 cm geoid nationwide. A 5 to 20 km line spacing should be sufficient. The airborne coverage must include the near coastal offshore zone (out to approximately 50 km from the coastline) where altimetric gravity models are weak. Then as second step, a densification of the gravity coverage over areas where a higher precision geoid is needed. This densification could be done

by airborne as well as by traditional terrestrial gravimetry. In some areas, like parts of Jawa island, the dense coverage is already there. Although some of the existing data may have to be validated.

Thus, as the first step, the (near) nationwide airborne gravity measurements is urgent for future work in all major islands in the region, where data voids are huge such as in Kalimantan, Sulawesi and Irianjaya islands. Whilst in Sumatra and Jawa islands measurements are needed to improve the situation of the existing surface data.

Following are the proposed airborne gravity surveys plan for:

1. Kalimantan island

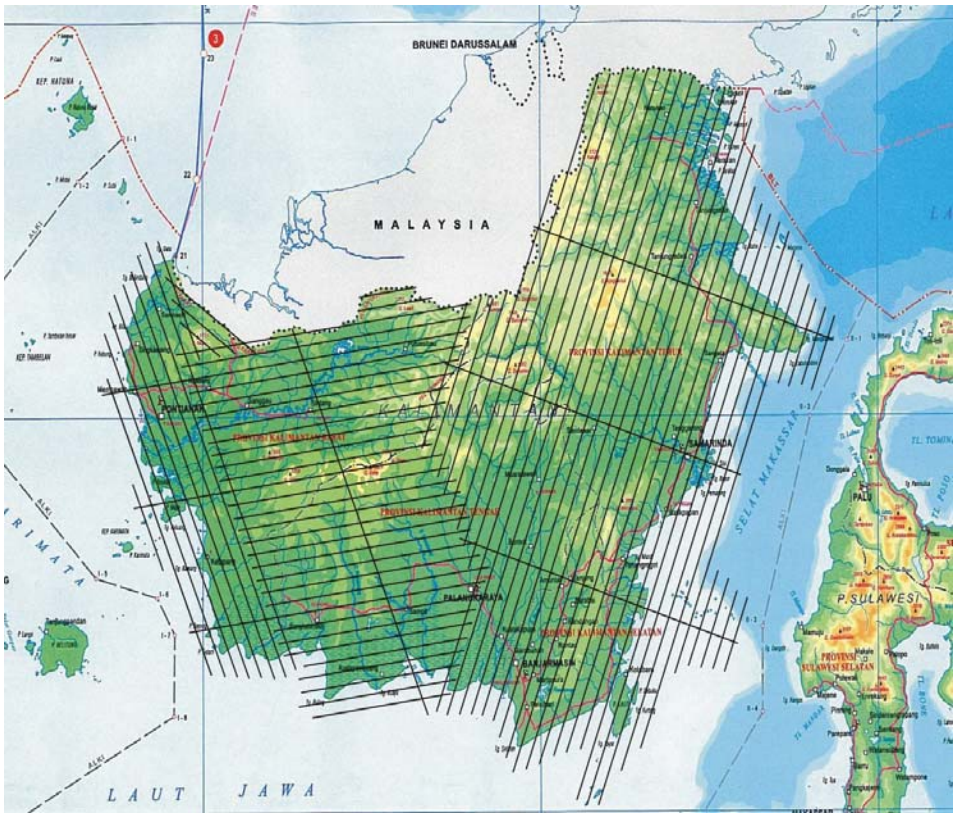

Figure 7.1 Draft survey layout for airborne gravity over Kalimantan. Total flight volume is approximately 400 hours airborne.

2. Sulawesi island

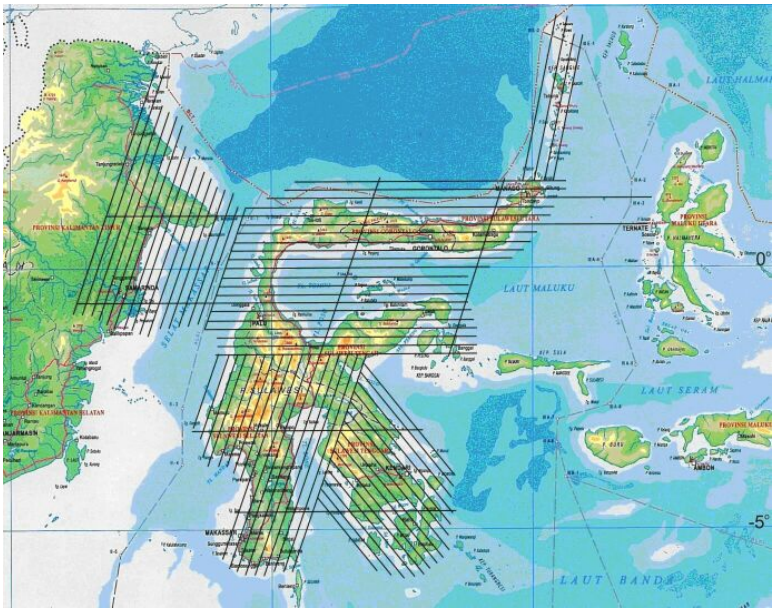

Figure 7.2 Draft survey layout for airborne gravity measurements over Sulawesi. Total flight volume is approximately 170 hours airborne.

3. Irianjaya island

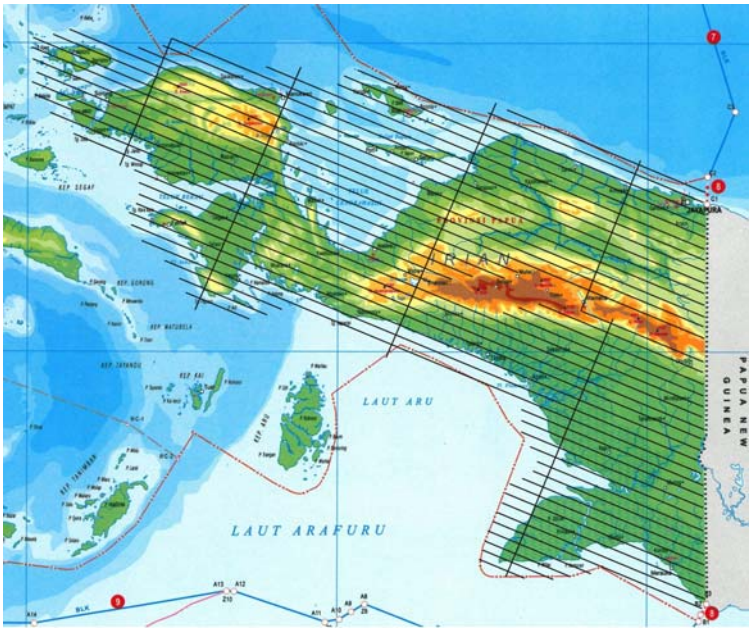

Figure 7.3 Draft survey layout for airborne gravity measurements over Irianjaya. Total flight volume is approximately 400 hours airborne.

4. Sumatra island

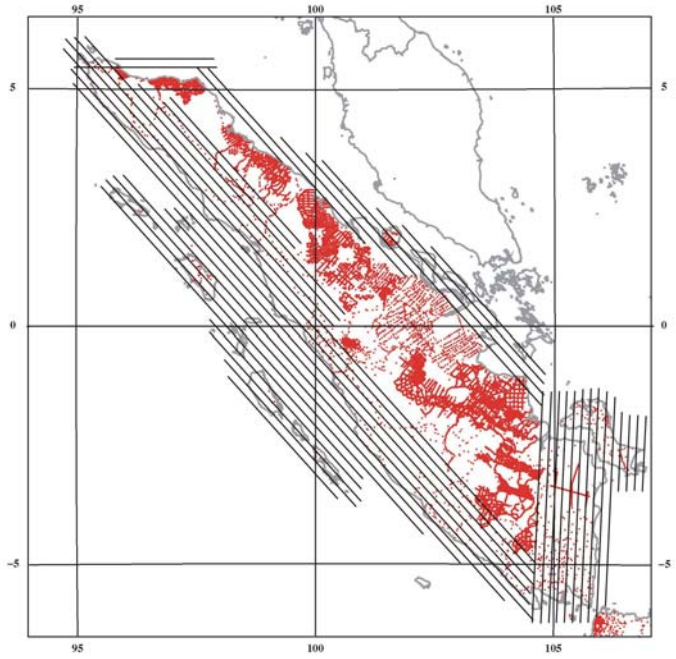

Figure 7.4 Draft survey layout for airborne gravity measurements over Sumatra. Total flight volume is approximately 160 hours airborne. Existing surface data are plotted in red dot.

5. Jawa island.

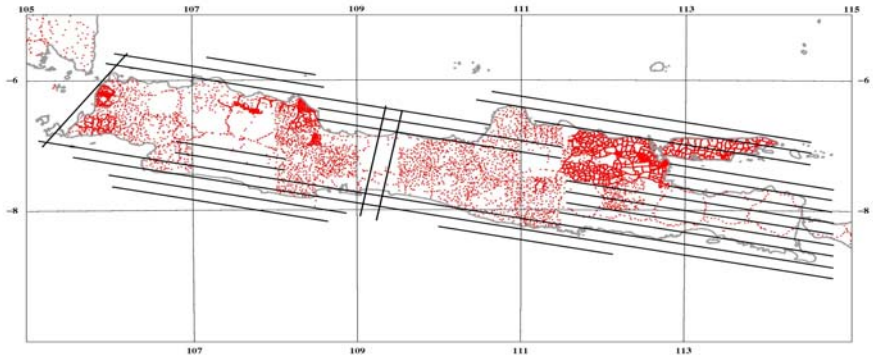

Figure 7.5 Draft survey layout for airborne gravity measurements over Jawa Island. Total flight volume is approximately 120 hours airborne.

REFERENCES

Amos, M. J., Featherstone, W. E., 2002. Development of a Gravimetric Geoid for New Zealand and a Single National Vertical Datum. Proceedings of Third Meeting of the International Gravity and Geoid Commission, Thessaloniki, Greece, August 26-30, 2002.

Andersen, O.B., Woodworth, P.L., and Flather, R.A., 1995. Intercomparison of recent ocean tide models. J. Geophysics. Res., 100, 25, 261 – 25,282.

Andersen O. B. and Knudsen, P., 1998. Global Marine Gravity Field from the ERS-1 and GEOSAT Geodetic Mission Altimetry, J. Geophys. Res., 103(C4), pp. 8129-8137, 1998.

Andersen, O. B., and Knudsen, P., 2000. The role of satellite altimetry in Gravity field modeling in Coastal areas, Phys. chem. Earth (A), **25**,1,17-24, 2000

Andersen, O.B., Knudsen, P., 2008. The DNSC08MDT Mean Dynamic Topography. Presented at EGU meeting, Vienna, Austria, April 2008.

Ardalan, A., Grafarend, E. and Kakkuri, J., 1997. National height datum, the Gauss-Listing geoid level value W_o and its time variations (Baltic Sea Level Project :Epoch 1990.8, 1993.8, 1997.4) – draft.

Balasubramania, N., 1994. Definition and realization of a global vertical datum, Report No. 427, Dept. Geodetic Science and Surveying, The Ohio State University, Colombus.

Becker,M., Angermann, D., Nordin, S., Reigberg, R., Reinhart, E., 2000. Das Geschwindigkeitsfeld in Suedostasien aus einer kombinierten GPS Loesung der drei GEODYSSEA Kampagnen von 1994 bis 1998, ZfV, Heft 3/2000, Witter.

Beutler, G., et.al., 2002. Earth Gravity Field from Space – from Sensors to earth Sciences. In Space Sciences Series of ISSI. Kluwer Academic Publishers, 2003. Netherlands.

Bursa, M., et.al, 1999. Geoidal Geopotential and World Height System. Studia Geophysica et. Geodesy 43 : 327 – 337.

Bursa, M., Kenyon, S., Kouba, J., Radej, K., Vatrt, V., Vojtiskova, M., and Simek, J., 2002. World height system specified by geopotential at tide gauge stations. Proceedings of IAG Symposium, Vertical Reference System, 20-23 February 2001, Cartagena, Columbia, pp. 291-296, Springer Verlag, Berlin.

Bursa, M., et.al, 2006. Twelve years of developments : Geoidal geopotential W_o for the establishment of a world height system - present state and future. Proceedings of the 1st International Symposium of the Int. Gravity Field service, Istanbul, Turkey, 28 August – 1 September, 2006.

Bursa, M., et.al, 2007. The geopotential value W_o for specifying the relativistic atomic time scale and a global vertyical reference system. Journal of Geodesy, vol. 81, No. 2/February, 2007.

Colombo, O.L., 1980. A world vertical network. Report 296, Dept. Geodetic Science, The Ohio State University, Colombus, Ohio.

Colombo, O. L., 1980. Transoceanic vertical datum connections. Proc. 2nd International Symposium on problems related to the redefinition of North American Vertical Geodetic Networks, The Canadian Inst. Of Surveying, Ottawa.

Ekman, M., and Mäkinen, J., 1991. The deviation of mean sea level from the mean geoid in the Baltic sea. Bulletin Geodesique, 65, 83 – 91.

Ekman, M., 1994. Deviation of mean sea level from the mean geoid in the transition area between the North sea and the Baltic sea. Marine Geodesy, 17, 161 – 168.

Emery, K., and Aubrey, D., 1991. Sea levels, Land levels, and tide gauges. Springer – Verlag, Berlin.

Farelly, B., 1991. The Geodetic Approximations in the conversion of geoid height to gravity anomaly by Fourier Transform. Bull. Geodesique, 65, 92 – 101.

Featherstone, W. E., Olliver, J. G., 1997. A method to validate gravimetric geoid computation software based on Stokes's formula. Journal of Geodesy, vol. 71, 571-576.

Featherstone, W.E., Stewart, M.P., 1998. Possible Evidences for Distortions in the Australian Height Datum in Western Australia. Geomatics Research Australasia, No. 68, June, 1998, pp. 1-12.

Featherstone, W.E., Kirby, J.F., 1998. Estimates of the Separation between the Geoid and the Quasigeoid over Australia. Geomatics Research Australasia, No. 68, June, 1998, pp. 79-90.

Featherstone, W.E., 2002. Prospects for the Australian Height Datum and geoid model. Proceedings of IAG Symposium, vol. 125, Vistas for Geodesy in the New Millennium, 2-7 September 2001, Budapest, Hungary, pp.96-101, Springer Verlag, Berlin

Forsberg, R. and Tscherning, C.C. 1981. The use of height data in gravity field approximation by collocation. Journal of Geophysical Research, 86 (B9): 7843-7854.

Forsberg, R., 1987. A new covariance model for inertial gravimetry and gradiometry. Journal Geoph. Res., vol. 92, B2, pp. 1305 – 1310.

Forsberg, R., and Sideris, M.G., 1993. Geoid computations by multi-band spherical FFT approach. Manuscripta Geodetica, 18, 2, 82 – 90.

GETECH, 1995. The South East Asia Gravity Project – Indonesia, Technical Report, University of Leeds, UK, June, 1995.

GLOBE Task Team and others (Hastings, David A., Paula K. Dunbar, Gerald M. Elphingstone, Mark Bootz, Hiroshi Murakami, Hiroshi Maruyama, Hiroshi Masaharu, Peter Holland, John Payne, Nevin A. Bryant, Thomas L. Logan, J.-P. Muller, Gunter Schreier, and John S. MacDonald), eds., 1999. The Global Land One-kilometer Base Elevation (GLOBE) Digital Elevation Model, Version 1.0. National Oceanic and Atmospheric Administration, National Geophysical Data bbCenter, 325 Broadway, Boulder, Colorado 80303, U.S.A.

Haagmans, R., De Min, E., and Von Gelderen, M., 1993. Fast evaluation of convolution integrals on the sphere using 1D FFT, and a comparison with existing methods for Stokes's integral. *Man. Geod.* 18, 227-241, 1993

Hamon, B., and Godfrey, J., 1980. Mean Sea Level and its interpretation. Marine Geodesy, 4(4), 315 – 329.

Heck, B., 1990. An evaluation of some systematic error sources affecting terrestrial gravity anomalies. Bulletin Geodesique, vol. 64, 88 – 108.

Heiskanen, W., and Moritz, H., 1967. Physical Geodesy, W.H. Freeman and Co., San Fransisco.

Hipkin, R., 2002. Defining the geoid by $W=W_o=U_o$: Theory and practice of a modern height system. Proc. 3rd Meeting of the International Gravity and Geoid Commission (IGGC), pp. 367-377, Tessaloniki, Greece, August 2002.

Hofman-Wellendof, B., Leichtenegger, H. And Collins, J., 1994. GPS Theory and Practice. Third Edition, Springer-Verlag, NY, 355 pp.

Jekeli, C., 2000. Heights, the Geopotential and Vertical Datum. Final Technical Report, Ohio Sea Grant Development Program. NOAA Grant No.NA86R60053.

Kahar, J., 1981. Analysis of geoid in Indonesian region. Ph.D thesis. Jurusan Tehnik Geodesi, ITB, ID Publ. JBPTITBPP. Bandung, Indonesia

Kahar, J., Kasenda, A., Prijatna, K., 1996. The Indonesian geoid model 1996, Proc. Int. Symp. Gravity, Geoid and Marine Geodesy. Sept. 30- Oct. 5, 1996, Tokyo, Japan.

Kasenda, A., Kearsley, A.H.W, 2001. Towards The Establishment of the Indonesian unified vertical datum. Proceedings IAG Symposia, International Association of Geodesy Symposia (in Drewes at al . Eds.) Vertical Reference Systems, 20-23 February 2001, Cartagena, Columbia, Springer Verlag, Berlin.

Kasenda, A., Kearsley, A.H.W, 2002. Offsets between some local height datums in the South East Asia region. Proceedings of Third Meeting of the International Gravity and Geoid Commission, Thessaloniki, Greece, August 26-30, 2002.

Kasenda, A., Kearsley, A.H.W, 2006. The Indonesian Geoid and Height System. Presented at the IAG Workshop – Height Systems, Geoid and Gravity of Asia – Pacific, Ulaanbaatar, Mongolia, June 6-8, 2006, unpublished.

Kasenda, A., et.al, 2008. A unified Vertical Datum for the Indonesian Archipelago. Poster presentation, The Symposium on Gravity, Geoid and Earth Observation, Chania**,** Greece, 23-27 June 2008.

Kaula, W.M., 1966. Theory of Satellite Geodesy. Waltham, Blaisdel.

Kearsley, A.H.W., 1977. The computation of deflections of the vertical from gravity anomalies. Ph.D Thesis. University of New South Wales. Sydney, Australia.

Kearsley, A.H.W., 1985. Towards the Optimum Evaluation of the Inner Zone Contribution to Geoidal Heights. Australian J. Geod. Photo. Surv. No. 42, June 1985, pp. 75-98.

Kearsley, A.H.W., 1986. Data requirements for determining precise relative geoid heights from Gravimetry. Journal of Geophysical Research, Vol. 91, B9, pp. 9193-9201, August 10, 1986.

Kearsley, A.H.W., 1999. The Unification of Vertical Datums. Paper presented in the General Assembly, IUGG Symposium, Birmingham, July 18-30.1999.

Kearsley, A.H.W., Govind, R., and lutton, G., 2007. The distortion of the Australian Height Datum with respect to a Global Geoid. Presented at the IAG General Assembly at IUGG XXIV 2007, Perugia, Italia, July 2-13, 2007.

Kenyon, S., Factor, J., Pavlis, N. and Holmes, S., 2007. Towards the next earth gravitational model. Paper presented at the Society of Exploration Geophysicists 77th Annual Meeting, San Antonio, Texas, USA, September 23-28, 2007.

Khafid, K.H. Ilk, Rummel, R., Kasenda, A. and Prijanto, A., 1994. The connection of local height systems: A case study in Indonesia, Proc. Int. Symp. On Marine Positioning (INSMAP), Sept. 19-23,1994, Hannover, Germany.

Khafid, 1998. On the unification of Indonesian local height systems, DGK Reihe C, Heft Nr. 488.

Knudsen, P., 1987. Estimation and modeling of the local empirical covariance function using gravimetry and satellite altimetry data, Bulletin Geodesique, 61, 145-160.

Lambert, W.D. and Darling, F.W. 1936. Tables for determining the form of the geoid and its indirect effect on gravity. US-Coast and Geodtic Survey, Spec. Publ. No.199

Lemoine, F.G., Kenyon, S. C., Factor, J.K, Trimmer, R.G, Pavlis, N.K., Chinn, D.S., Cox, C.M., Kloslko, S.M., Luthcke, S.B., Torrence, M.H., Wang, Y.M., Williamson, R.G., Pavlis, E.C., Rapp, R.H., Olson, T.R., 1998. The Development of the Joint NASA GSFC and the National Imagery and Mapping Agency (NIMA) Geopotential Model EGM96, NASA Goddard Space Flight Center, NASA/TP –1998 – 206861, Greenbelt.

Martin, D., Chapin, J., and maul, G., 1996. State-of-the-art sea level monitoring. Marine Geodesy, 19, 105 – 114.

Mather, R.S., Rizos, C., Morrison, T. On the Unification of geodetic Levelling Datum using Satellite Altimetry. Nasa/GSFC Report. 1978.

Meyer, T.H., Roman, D.R., and Zilkoski, B., 2006. What does height realy mean ? Part III: Height Systems. Surveying and Land Information Science, vol. 66, No.2, 2006.

Morgan, P., 1992. An Analysis of the Australian Height Datum : 1971, The Australian Surveyor, March 1992, Vol. 37, No.1.

Moritz, H., 1980. Advanced Physical Geodesy, Herbert Weichmann Verlag, Karlsruhe, Germany, 1980.

Nahavandchi, H., and Sjöberg, L.E., 1998. Unification of Vertical datums by GPS and Gravimetric Geoid Models using Modified Stokes Formula, Marine Geodesy, 21 : 261 – 273.

Omang, O.L.D., Forsberg, R., 2002. The Northern European Geoid : a case study on long-wavelength geoid errors. Jornal of Geodesy, 2002, Vol. 76, pp. 369-380.

Pan, M. and Sjöberg, 1998. Unification of Vertical Datums by GPS and Gravimetric Geoid Models with Application to Fennoscandia, J. Geod., 72 : 64 – 70.

Pavlis, N.K., Holmes, S.A., Kenyon, S.C., Schmidt, D., and Trimmer, R., 2005. A Preliminary Gravitational Model to Degree 2160. Proceedings Gravity, Geoid and Space Missions, IAG International Symposium, Porto, Portugal, August 30 – September 3, 2004.

Pavlis, N.K., and Saleh, J., 2005. Error propagation with geographic specificity for very high degree Geopotential Models. Proceedings Gravity, Geoid and Space Missions, IAG International Symposium, Porto, Portugal, August 30 – September 3, 2004.

Pavlis, N.K., Holmes, S.A., Kenyon, S.C., and Factor, J.K., 2008. An Earth Gravitational Model to degree 2160: EGM08. Presented at the 2008 General Assembly of the European Geosciences Union, Vienna, Austria, April 12 – 18, 2008.

Prijatna, K., 1998. A strategy for geoid determination in the Indonesian archipelago, DEOS Progress Letter 98.1, pp.101-122, Delft University Press, Netherlands.

Rapp, R.H., and Balasubramania, N., 1992. A conceptual formulation of a world height system, Report 421, Dept. f Geodetic Science and Surveying, The Ohio State University, Columbus.

Rapp, R.H., 1994. Separation between reference surfaces of selected vertical datums, Bull. Geod., 69, pp.26-31.

Rapp, R.H., 1995. A world vertical datum proposal, Allgemeine Vermessungs-Nachrichten, Wichmann, Heft 8-9/95, pp.297-304.

Rapp, R.H., 1997. Use of potential coefficient model for geoid undulation determinations using a spherical harmonic representation for the height anomaly/geoid undulation difference. Journal of Geodesy, 71, 282-289.

Rothacher, M., 2001. Estimation of Station heights with GPS. Proc. Vertical Reference Systems, IAG Symposia, Vol. 124, pp. 82-90, Cartagena, Colombia, February 20-23, 2001

Roelse, A., Granger, H.W., and Graham, J.W., 1971. The adjustment of the Australian levelling survey 1970-1971, Technical Report 12, Division of National Mapping, Canberra, Australia.

Rummel, R., and Teunissen, P., 1988. Height datum definition, height datum connection and the role of the geodetic boundary value problem, Bull. Geod., Vol. 62, No.4,pp.477-498.

Rummel, R., and Ilk, K. H., 1995. Height datum connection – the ocean part., Allgemeine Vermessungs-Nachrichten, Wichmann, Heft 8-9/95, pp.321-329.

Rummel, R., 2000. Global Unification of Heights Systems and GOCE. Proc. Gravity, Geoid and Geodynamics 2000, IAG Symposia, Vol. 123, pp. 13-20, Banff, Alberta, Canada, July 31-Ausgust 4, 2000.

Rummel, R., Balmino, G., Johannessen, J., Viser, P., Woodwaorth, P., 2002. Dedicated gravity field missions – principles and aims, Journal of Geodynamics, 33, pp. 3 – 30, 2002.

Rummel, R., 2003. How to climb the Gravity wall. Space Sciences Reviews, Vol. 108, pp. 1-14, 2003. Kluwer Academic Publisher, Netherlands.

Sandwell, D.T., and Smith, W.H.F., 1997. Marine gravity anomaly from GEOSAT and ERS-1 satellite altimetry. J. Geophysics Res., 102, 10,039 – 10,054.

Sideris, M.G., 1994. Geoid determination by FFT techniques. Lecture notes, International School for the determination and use of the geoid, DIIAR, Politecnico di Milano, October, 1994.

Smith, J.R., 1997. Introduction to Geodesy : The History and Concepts of Modern Geodesy. John Wiley & Sons, Inc., USA.

Smith, B., and Sandwell, D. 2003. Accuracy and resolution of Shuttle Radar Topography Mission data. Geophysical Research Letters, vol. 30, No. 9, 1467.

Strang van Hees. 1990. Stokes' formula using Fast Fourier Technique. Manuscr. Geod., 15, 235-239. 1990.

Sutisna, S. 2001. Vertical control network in Indonesia. Prosiding Laporan Tahunan KGN 2001, Komite gayaberat Nasional, Bandung, Indonesia.

Tapley, B., Ries, J., Bettadpur, S., Chambers, D., Cheng, M., Condi, F., Gunter, B., Kang, Z., Nagel, P., Pastor, R., Pekker, T., Poole, S., and Wang, F., 2005. GGM02 An improved Earth gravity field model from GRACE. Journal of Geodesy, 79/(8):467–478. 2005

Tscherning, C.C. and Rapp, R.H., 1974. Closed covariance expressions for gravity anomalies, geoid undulations and deflections of the vertical implied by anomaly degree variance model. Ohio State University, Dept. of Geodetic Sciences, Colombus, Ohio, vol.208.

Tscherning, C.C., Forsberg, R., and Knudsen, P. The GRAVSOFT package for geoid determination. Proc.1. Continental Workshop on the Geoid in Europe, Prague, May 1992, pp. 327-334, Research Institute of Geodesy, Topography and Cartography, Prague, 1992.

Vanicek, P., Christou, N.T. ,eds., 1994. Geoid and Its Geophysical Interpretations. CRC Press, Inc., Boca Raton, USA.

Van Onselen, K., 1997. Quality investigation of vertical datum connection, DEOS Report No. 97.3, Delft University of Technology, Netherlands.

Wong, L., Gore, R., 1969. Accuracy of geoid heights from modified Stokes kernels. Geophys J Royal Astr. Soc. 18, 81-91, 1969

www.gfz-potsdam.de, The Satellite System: The CHAMP Satellite.

www.csr.utexas.edu/grace/, The GRACE Satellite Tandem: High Precision Earth Monitoring for a better understanding of climate.

www.esa.int/esaLP, Esa the Living Planet Program, Scientists view GOCE satellite.

Xu, P., and Rummel, R., 1991. A quality investigation of global vertical datum connection. Technical Report 34, Netherlands Geodetic Commission.

Zilkoski, D.B., Richards, J.H., and Young, G.M. (1992). Results of the general adjustment of the North American Vertical Datum of 1988. Surveying and Land Information Systems, **52**(3), 133-149.